COMPUTATIONALLY EFFICIENT ALGORITHMS FOR RESOURCE ALLOCATION IN COGNITIVE RADIO AND GREEN COMMUNICATION SYSTEMS

by

Muhammad Naeem
M.Sc., University of Engineering and Technology, Taxila, 2005
B.Sc., University of Engineering and Technology, Taxila, 2000

THESIS SUBMITTED IN PARTIAL FULFILLMENT OF
THE REQUIREMENTS FOR THE DEGREE OF

DOCTOR OF PHILOSOPHY

in the

School of Engineering Science

SIMON FRASER UNIVERSITY

Summer 2011

APPROVAL

Name: **Muhammad Naeem**

Degree: **Doctor of Philosophy**

Title of Thesis: **Computationally Efficient Algorithms for Resource Allocation in Cognitive Radio and Green Communication Systems**

Examining Committee:

Chair: **Dr. Shawn P. Stapleton**
Professor, School of Engineering Science

_____

Dr. Daniel C. Lee
Senior Supervisor
Associate Professor, School of Engineering Science

_____

Dr. Paul Ho
Supervisor
Professor, School of Engineering Science

_____

Dr. Ivan V. Bajić
Supervisor
Assistant Professor, School of Engineering Science

_____

Dr. Jie Liang
Internal Examiner
Associate Professor, School of Engineering Science

_____

Dr. Alagan Anpalagan
External Examiner
Professor, Ryerson University, Toronto, Canada

Date Defended/Approved: 11 May 2011

Partial Copyright Licence

ABSTRACT

Cognitive radio is an interesting concept for solving the problem of spectrum availability by allowing non-licensed users to exploit underutilized licensed frequency bands. We note that a combination of the cognitive radio with cooperative communication and/or MIMO technology can possibly enhance the system performance significantly. In this research, a number of resource allocation problems are examined for cognitive radio systems (CRS) that have relaying and/or MIMO capabilities, and computationally efficient resource allocation schemes are proposed. The general objective is to devise resource allocation schemes in the cognitive radio that maximize the resource utilization under the constraint of acceptable interference to the primary (licensed) users. In particular, in this thesis we present efficient schemes for jointly deciding the assignment of multiple relays to users and their power levels. Fairness is also considered in assigning multiple relays to multiple secondary users. We also propose low-complexity distributed schemes for joint subcarrier and relay assignment in cooperative multi-carrier multi-cast CRS. Another class of resource allocation problems addressed this thesis regards selecting and scheduling users in multiuser systems. In multiuser cognitive MIMO systems, user selection and scheduling significantly affects the system performance. This thesis addresses joint user scheduling and power allocation in the CRS equipped with multiple antennas. Optimization of such user scheduling and power allocation has combinatorial aspects, and the exhaustive search for an exactly optimal solution is impractical due to its computational complexity. This thesis presents low-complexity suboptimal algorithms to maximize the sum-rate capacity of the uplink communication in cognitive MIMO systems under the constraint that the interference to the primary users is below a specified level.

Keywords: Relay assignment, Cognitive radio, Cooperative communication, MIMO, User selection, Subcarrier allocation

DEDICATION

To my family

ACKNOWLEDGEMENTS

First and foremost, all praises are due to Allah, who has given me strength, knowledge and patience to accomplish this work. Without His Blessings, Mercy and Grace, this dissertation would not have been possible.

I would like to thank my supervisor Professor Daniel C. Lee for his guidance and support over the past years. His expertise, understanding, and patience added considerably to my graduate experience. Through constant encouragement and invaluable advices, he helped me to develop as a researcher and an independent thinker.

I am grateful for the support and help of faculty, staff and graduate students of the mobile communication lab. Special thanks to Udit, Saad, Munsub, Maryam, Jane, Song, Ajit and Mehdi. I would like to thank the Natural Science and Engineering Council of Canada (NSERC) for providing me the financial support of this work.

My deepest appreciations go out to my family members to whom I owe so much. I would like to thank my parents for the sacrifices they have made and for the inspiration and support, they have provided throughout my life. I am blessed with my lovely wife, Rukhsana, whose love, patience, understanding and support made my doctoral journey come to this end. Finally, I would like to thank someone very special: my daughter Ayesha and son Muhammad Usman, for being the constant source of joy and happiness.

TABLE OF CONTENTS

Approval ..... **ii**
Abstract ..... **iii**
Dedication ..... **iv**
Acknowledgements ..... **v**
Table of Contents ..... **vi**
List of Figures ..... **ix**
List of Tables ..... **xiii**
List of Abbreviations ..... **xv**
Chapter 1: Introduction **1**
1.1 Research Motivation 1
1.2 Background 2
1.2.1 Cognitive Radio System 2
1.2.1.1 Spectrum sensing 3
1.2.1.2 Dynamic Spectrum Access 4
1.2.2 Cooperative Communication 6
1.2.3 Green Communication 8
1.3 Thesis Overview 10
1.3.1 Relay assignment 10
1.3.2 Subcarrier assignment 11
1.3.3 User scheduling 11
1.4 Literature Review 12
1.4.1 Relay assignment and power allocation 12
1.4.1.1 RAS without CR capability 14
1.4.1.2 RAS with CR capability 16
1.4.2 Subcarrier assignment and power allocation 16
1.4.3 User scheduling 19
1.5 Summary of Contributions 21
1.6 Organization of Thesis 22
1.7 Chapter References 23
PART 1: RELAY ASSIGNMENT **33**
Chapter 2: Relay Assignment and Power Allocation for CRS **34**
2.1 Problem Formulation 36
2.1.1 Decoupling of source power 40
2.2 Algorithm for Relay Assignment with Continuous Power 44

2.2.1 Phase 1: Relay assignment 44
2.2.2 Optimization of Relay Transmission Power for a Given Relay Assignment 45
2.2.3 Phase 2: Power Allocation 46
2.2.4 Complexity Analysis 50
2.2.5 Performance Results with Continuous Power 50
2.3 Algorithm for Relay Assignment with Discrete Power Allocation 54
2.3.1 IAGA for Discrete Power Allocation 55
2.3.2 Fairness aware IAGA 62
2.3.3 Complexity Analysis 63
2.3.4 Relay Assignment Results with Discrete Power Levels 64
2.4 Summary 72
2.5 Chapter References 72

Chapter 3: Green Resource allocation 74

3.1 Multi-objective Optimization 76
3.2 Green Relay Assignment for GCCRN 77
3.3 Hybrid EDA for GCCRN MOO Problem 79
3.3.1 Modified EDA 82
3.3.2 Iterative Greedy Algorithm 86
3.3.2.1 Step 1: Relay Assignment without Interference Constraint 86
3.3.2.2 Step 2: Final Relay Assignment with Interference Constraint 87
3.3.3 Numerical Results 89
3.4 Summary 94
3.5 Chapter References 94

PART 2: SUBCARRIER ASSIGNMENT 97

Chapter 4: Resource allocation In Cooperative Multicast CRS 98

4.1 Subcarrier Assignment for Sum-rate maximization 98
4.1.1 System Model 98
4.1.2 Dual Decomposition Algorithm 103
4.1.3 Computational complexity of dual decomposition algorithm 106
4.1.4 Iterative Algorithm for JPSARA 106
4.1.5 Numerical Results 109
4.2 Max-Min Resource Allocation in Multicast CRS 113
4.2.1 Proposed Algorithm and Complexity Analysis 114
4.2.2 Numerical Results 118
4.3 Summary 122
4.4 Chapter References 122

PART 3: USER SCHEDULING 124

Chapter 5: User scheduling and Power allocation in CRS 125

5.1 System Model 127
5.2 Proposed algorithms 131
5.2.1 Estimation-of-distribution Algorithm 131
5.2.1.1 Method of Applying Threshold 135
5.2.2 Interference Aware capacity maximization algorithm 137

5.2.3 Iterative User scheduling with interference minimization 138
5.3 Complexity Analysis 141
5.3.1 Complexity of IACMA and IUSIM 142
5.3.2 Exhaustive Search Algorithm 142
5.4 Numerical results 143
5.5 Summary 152
5.6 Chapter References 152
Chapter 6: Contributions and Future work 155
6.1 Contributions 155
6.1.1 Relay Assignment 155
6.1.2 Joint subcarrier allocation and relay assignment 156
6.1.3 User scheduling 156
6.2 Future work 156
6.2.1 Resource allocation in multi-hop CRS 157
6.2.2 Resource allocation in cooperative CRS with imperfect CSI 157
6.2.3 Green communication with adaptive weights 157
Appendices 158
Appendix A 158
Appendix B 160
Appendix C 161
Appendix D 163
Appendix E 165

LIST OF FIGURES

Fig. 1.1 Dynamic spectrum access strategies. 4

Fig. 1.2 Overlay spectrum access. 5

Fig. 1.3 Underlay spectrum access. 5

Fig. 1.4 Joint overlay and underlay spectrum access. 5

Fig. 1.5 Multiuser cooperative communication system. 8

Fig. 1.6 Estimated distribution of global CO_2 emissions from ICTs. 9

Fig. 1.7 Organization of thesis. 23

Fig. 2.1 Relay Assisted Cognitive Radio Network. 35

Fig. 2.2 Upper Bound on the AF channel capacity 51

Fig. 2.3 Sum-rate capacity vs. Interference comparison. The parameters are *L* = *7, K* = 3,*M* = 1, $p_s = 10\text{w}, p_l = \{10\text{w}, 1\text{w}\}$ 53

Fig. 2.4 Sum-rate capacity vs. Interference comparison. The parameters are *K* = 3, $p_s = 10\text{w}$, *L* = {6,3}, *M* = {1,3} 53

Fig. 2.5 Sum-rate capacity vs. number of primary user's comparison. The parameters are *L = 5, K* = 3, $I_{m,k}^{\max} = \{10mw, 1mw\}$ 54

Fig. 2.6 Sum-capacity vs. maximum interference threshold to primary users with *L*=6, *K*= 4, *M= 4,* $\lambda = 1$, P_s^{max} *=10w* and $p_l^{max} = P_s^{max}/10$, $p_l \in \{0, p_l^{max}\}\ \forall l$ 65

Fig. 2.7 Sum-capacity vs. maximum interference threshold to primary users with *L*=5, *K*=3, *M= 4,* $\lambda = 2$, P_s^{max} *=10w*, $p_l^{max} = P_s^{max}/10$, $p_l \in \{0, p_l^{max}/2, p_l^{max}\}$ 66

Fig. 2.8 Sum-capacity vs. number of relays with K = 4, M= 1, $\lambda = 1$, P_s^{max} =10w, $p_l^{max} = P_s^{max}/10$, $p_l \in P_L = \{0, p_l^{max}\}\ \forall l$ and $I_{m,k}^{max}$ = 10mw $\forall m$ 66

Fig. 2.9 Sum-capacity vs. number of relays with K = 2, M= 2, $\lambda = 2$, P_s^{max} =10watt, $p_l^{max} = P_s^{max}/10$, $p_l \in \left\{0, p_l^{max}/2, p_l^{max}\right\} \forall l$ and $I_{m,k}^{max}$ = 1mw $\forall m$ 67

Fig. 2.10 Sum-capacity vs. number of primary users with K = 2, L= 5, $\lambda = 1$, P_s^{max} =10watt, $p_l^{max} = P_s^{max}/10$, $p_l \in \left\{0, p_l^{max}\right\} \forall l$, and $I_{m,k}^{max}$ = 1mw $\forall m$ 67

Fig. 2.11 User's individual capacities vs. user index with K = 10, M= 10, $\lambda = 2$, P_s^{max} =10w, $p_l^{max} = P_s^{max}/10$, and $I_{m,k}^{max}$ = 10mw for $\forall m$ 69

Fig. 2.12 User's individual capacities vs. user index with K = 10, M= 10, $\lambda = 4$ P_s^{max} =5w, $p_l^{max} = P_s^{max}/10$, and $I_{m,k}^{max}$ = 1mw for $\forall m$ 69

Fig. 2.13 Percentage IAGA performance to ESA-Discrete for different $I_{m,k}^{\max}$ 71

Fig. 2.14 Percentage IAGA performance to ESA-Discrete for different $I_{m,k}^{\max}$ 71

Fig. 3.1 CO_2 emission estimate by GeSI in Mega Tones/Year 75

Fig. 3.2 Flow diagram for continuous EDA 83

Fig. 3.3 Continuous EDA with threshold 84

Fig. 3.4 Power and sum-capacity trade-off plot with K = 10, L = 10, $I_m^{\max} = 10m\text{w}$ 91

Fig. 3.5 Power and sum-capacity trade-off plot with K = 20, L = 10, $I_m^{\max} = 10m\text{w}$ 91

Fig. 3.6 Power and sum-capacity trade-off plot with (K,L, $I_m^{\max}$) = (10/20,10/20,10mw/1mw) 92

Fig. 3.7 Iterations vs. Fitness plot for different (L,K) configuration. The parameters are (M, p_l^{max}, I_m^{max} ,w1,w2)=(1,10w,10mw,0.5,0.5) 92

Fig. 3.8 Iterations vs. Fitness plot for different (L,K) configuration. The parameters are (M, p_l^{max}, I_m^{max} ,w1,w2)=(1,10w,1w,0.5,0.5) 93

Fig. 3.9 Iterations vs. Fitness plot for different number of relays. The parameters are (M, p_l^{max}, I_m^{max} ,K ,w1,w2)=(1,10w,1w,20, 0.5 0.5 93

Fig. 3.10 Iterations vs. Fitness plot for different number of relays. The parameters are (M, p_l^{max}, I_m^{max} ,L ,w1,w2)=(1,10w,1w,20, 0.5 0.5) 94

Fig. 4.1 Cooperative MMCRS..... 99

Fig. 4.2 Lower and upper limits of the primary band..... 100

Fig. 4.3 Performance of IJPSARA with $p_l^{\max} = 0.1\text{w},$, L = 2, N = 8, G = 2, $|K_g|$ =*200* , g = 1, 2,…,*G* ,*B* = 1M Hz, and T_s = 1*μ* sec 111

Fig. 4.4 Performance of IJPSARA with $p_l^{\max} = 0.1\text{w},$, L = 2, G = 4, N = 128, $|K_g|$ =*150* , g = 1, 2,…,*G* ,*B* = 1M Hz, and T_s = 1*μ* sec 111

Fig. 4.5 Performance of IJPSARA with $p_l^{\max} = 0.1\text{w},$, L = 2, G = 4, N = 64, $|K_g|$ =*100* , g = 1, 2,…,*G* ,*B* = 1M Hz, and T_s = *1μ* sec 112

Fig. 4.6 Performance of IJPSARA with $p_l^{\max} = 0.1\text{w},$, L = 2, G = 4, N = 32, $|K_g|$ =*100* , g = 1, 2,…,*G* ,*B* = 1M Hz, and T_s = 1*μ* sec 112

Fig. 4.7 Percentage IJPSARA performance to the Dual algorithm 113

Fig. 4.8 Performance comparison of the multiuser multicast relay network with, $p_l^{\max} = 5\text{w},$, L = 3, N = 10, B = 1M Hz, and T_s = 1*μ* sec 119

Fig. 4.9 Effect of greediness control factor on the performance of proposed algorithm with $p_l^{\max} = 5\text{w},$ L = 3, N = 16, G = 8, B = 1M Hz, and T_s = 1*μ* sec 120

Fig. 4.10 Effect of greediness control factor on the performance of proposed algorithm with $p_l^{\max} = 5\text{w},$ L = 3, N = 16, G = 8, B = 1M Hz, and T_s = 1*μ* sec 120

Fig. 4.11 Minimum group capacity vs. the number of primary users with $p_l^{\max} = 5\text{w},$, L = 3, N = 10, G = 4, K = *3,B* = 1M Hz, and T_s = 1*μ* sec. 121

Fig. 5.1 EDA Flow Diagram 134

Fig. 5.2 Biased Random Population 134

Fig. 5.3 Sum-rate capacity comparison. The parameters are $\left[K, K_s, N_T, N_R, \lambda, I_m^{\max}\right]$ = [8, 3, 2, 6, 8, 1mw]. 146

Fig. 5.4 Sum-rate capacity comparison .The parameters are $\left[K, K_s, N_T, N_R, \lambda, I_m^{\max}\right]$ = [12, 3, 2, 6, 8, 1mw]. 147

Fig. 5.5 Sum-rate capacity comparison .The parameters are $\left[K, K_s, N_T, N_R, \lambda, M\right]$ = [8, 3, 2, 6, 8, 4]..... 147

Fig. 5.6 Sum-rate capacity comparison .The parameters are $\left[K, K_s, N_T, N_R, \lambda, M\right]$ = [12, 3, 2, 6, 8, 4]..... 148

Fig. 5.7 Sum-rate capacity comparison for different power levels .The parameters are $\left[K, K_s, N_T, N_R, SNR, M\right]$ = [8, 3, 2, 6, 8dB, 4]. 148

Fig. 5.8 Sum-rate capacity comparison for different power levels .The parameters are $\left[K, K_s, N_T, N_R, SNR, M\right]$ = [12, 3, 2, 6, 16dB, 4]. 149

Fig. 5.9 Sum-rate capacity vs. number of primary users. The parameters are $\left[K, K_s, N_T, N_R, SNR\right]$ = [8, 3, 2, 6, 8dB]. 149

Fig. 5.10 Sum-rate capacity vs. number of primary users. The parameters are $\left[K, K_s, N_T, N_R, I_m^{\max}\right]$ = [8, 3, 2, 6, 10mw]. 150

Fig. 5.11 Sum-rate capacity vs. number of secondary users. The parameters are $\left[K_s, N_T, N_R, I_m^{\max}, M\right]$ = [3, 2, 6, 1mw, 4]..... 150

Fig. 5.12 Sum-rate capacity vs. number of secondary users. The parameters are $\left[K_s, N_T, N_R, SNR, M\right]$ = [3, 2, 6, 8dB, 4]. 151

Fig. 5.13 Effect of threshold on the performance of EDA. $\left[K, K_s, N_T, N_R, SNR, M\right]$ = [12, 3, 2, 6, 8dB, 1]. 151

Fig. D.1 Stage 1 of IAGA..... 163

Fig. D.2 Stage 2 of IAGA..... 164

LIST OF TABLES

Table 1.1 IEEE 802.22 system parameters. 3
Table 1.2 Cooperative communication protocol..... 7
Table 1.3 Relay Assignment. 15
Table 1.4 Subcarrier Assignment With power allocation. 18
Table 1.5 User scheduling in Multi Access MIMO System. 21
Table 2.1 Notations used in chapter 2. 36
Table 2.2 Iterative Joint Relay Assignment and Power Allocation (IJRAPA) 49
Table 2.3 Power Allocation Routine..... 49
Table 2.4 IAGA 60
Table 2.5 Example of IAGA 61
Table 2.6 Percentage IAGA performance to ESA-Discrete for different $I_{m,k}^{\max}$ 70
Table 2.7 Percentage IAGA performance to ESA-Discrete for different *L* 70
Table 2.8 Number of flops required by ESA, IAGA and IJRAPA 70
Table 3.1 Parameters and notations of CEDA..... 80
Table 3.2 Iterative greedy relay assignment for each EDA individual..... 85
Table 3.3 Explanation of abbreviations used in simulation results..... 89
Table 4.1 Dual Decomposition Algorithm. 105
Table 4.2 Iterative greedy algorithm for JPSARA sum-rate maximization 109
Table 4.3 Percentage IJPSARA performance to Dual algorithm 113
Table 4.4 IJPSARA for MMCRS 117
Table 4.5 Number of flops required by ESA, Dual and IJPSARA 121
Table 5.1 Notations 127
Table 5.2 IACMA 139
Table 5.3 Example..... 140
Table 5.4 IUSIM..... 141

Table 5.5 Number of flops required by ESA, EDA, IACMA and IUSIM..... 152

LIST OF ABBREVIATIONS

APF	Access Proportional Fairness
AF	Amplify-And-Forward
CCS	Cooperative Communication System
CRS	Cognitive Radio System
DPA	Discrete Power Allocation
DSA	Dynamic Spectrum Access
EA	Evolutionary Algorithms
ESA	Exhaustive Search Algorithm
EDA	Estimation-of-distribution Algorithm
ESA-UB	Exhaustive Search With Upper Bound
FCC	Federal Communications Commission
GeSI	Global e-Sustainability Initiative
GCCRN	Green Cooperative Cognitive Radio Network
IUSIM	Iterative User Scheduling With Interference Minimization
IACMA	Interference Aware Capacity Maximization Algorithm
IAGA	Interference Aware Greedy Assignment
IEA	International Energy Agency
ITU	International Telecommunication Union
ICT	Information And Communication Technologies
JSUS-QPC	Joint Secondary User Selection/Scheduling And Quantized Power Control
JPSARA	Joint Power, Subcarrier Allocation And Relay Assignment
MMCRS	Multiuser Multicast CRS
MOO	Multi-Objective Optimization
MEDA	Modified EDA
PU	Primary User
RPF	Rate Proportional Fairness
SU	Secondary User
WEO	World Energy Outlook
WRAN	Wireless Regional Area Network

CHAPTER 1: INTRODUCTION

1.1 Research Motivation

The increasing service demand poses new challenges in future wireless communication. One of the most prominent challenges in meeting the demand is the scarcity of radio resources. In the past decade, a number of techniques have been proposed in the literature for efficiently utilizing the radio resources (e.g. cognitive radio [1] [2] [3], multiple-input multiple-output (MIMO) communication, cooperative communication systems (CCS) etc). Cognitive radio is an emerging technology intended to enhance the utilization of the radio frequency spectrum. Multi-input multi-output (MIMO) system and cooperative communication systems (CCS), with the same total power and bandwidth of legacy wireless communication systems, can increase the data rate of the future wireless communication systems.

A combination of cognitive radio with CCS and MIMO can further improve the future wireless systems performance. However, the combination of these techniques raises new issues in the wireless systems that need to be addressed. One of the important issues is the complexity of resource allocation schemes in the combined system. This thesis focuses on designing computationally efficient algorithms for resource allocation in multiuser cognitive radio system (CRS) with relaying and/or MIMO capabilities. In particular, in this thesis, a number of low-complexity algorithms are proposed for power allocation, subcarrier assignment, relay assignment and user scheduling in multiuser CRS with relaying and MIMO capability.

1.2 Background

In this section, we provide a brief overview of the cognitive radio system, cooperative communication, and green communication.

1.2.1 Cognitive Radio System

Formally, a cognitive radio is defined as [4]

"*A radio that changes its transmitter parameters based on the interaction with its environment*"

The cognitive radio has been mainly proposed to improve the spectrum utilization by allowing unlicensed (secondary) users to use underutilized licensed frequency bands [1] [2] [3]. In reality, unlicensed wireless devices (e.g., automatic garage doors, microwaves, cordless phones, TV remote controls etc.) are already in the market [5] [6]. The IEEE 802.22 standard for Wireless Regional Area Network (WRAN) addresses the cognitive radio technology to access white spaces in the licensed TV band. In North America, the frequency range for the IEEE 802.22 standard will be 54–862 MHz, while the 41–910MHz band will be used in the international standard [2]. Table 1.1 shows the IEEE 802.22 system parameters, e.g., frequency range, bandwidth, modulation types, maximum transmit power ratings, multiple access schemes, etc. [7].

In the context of cognitive radio, the Federal Communications Commission (FCC) recommended two schemes to prevent interference to the television operations due to the secondary (unlicensed) users. These are listen-before-talk and geo-location/database schemes [5] [6]. In the listen-before-talk scheme, the secondary/unlicensed device senses the presence of TV signals in order to select the TV channels that are not in use. In geo-location/database scheme, the licensed/unlicensed users have a location-sensing device (e.g., GPS receiver etc.) The locations of primary and secondary users are stored in a central database. The central controller (also known as spectrum manager) of the secondary/unlicensed users has the access to the location database.

Table 1.1 IEEE 802.22 system parameters.

Parameters	Specification	Remarks
Frequency range	54-862 MHz	TV band
Bandwidth	6 MHz, 7 MHz, 8 MHz	
Modulation	QPSK, 16-QAM, 64-QAM	
Transmit power	4W	For USA, may vary in other regulatory domains
Multiple access	OFDMA	

The main functions of cognitive radio to support intelligent and efficient utilization of frequency spectrum are as follows:

1.2.1.1 Spectrum sensing

Spectrum sensing determines the status of the spectrum and activity of the primary users [2] [8]. An intelligent cognitive radio transceiver senses the spectrum hole without interfering with the primary users. Spectrum holes are the frequency bands currently not used by the primary users. Spectrum sensing is implemented either in a centralized or distributed manner. The centralized spectrum sensing can reduce the complexity of the secondary user terminals, since the centralized controller performs the sensing function. In distributed spectrum sensing, each mobile device (secondary user terminal) senses the spectrum independently. Both centralized and distributed decision-making is possible in distributed spectrum sensing [2]. The central controller (spectrum manager), based on the spectrum sensing information, allocates the resources for efficient utilization of the available spectrum. One major role of the central controller is to prevent overlapped spectrum sharing between the secondary users [2] [3] [4].

1.2.1.2 Dynamic Spectrum Access

Dynamic spectrum access (DSA) is defined as real-time spectrum management in response to the time varying radio environment − e.g., change of location, addition or removal of some primary users, available channels, interference constraints etc [2] [3]. There are three DSA models in the literature, namely, exclusive-use model, common-use model and shared-use model [3]. Fig. 1.1 shows a hierarchal overview of DSA.

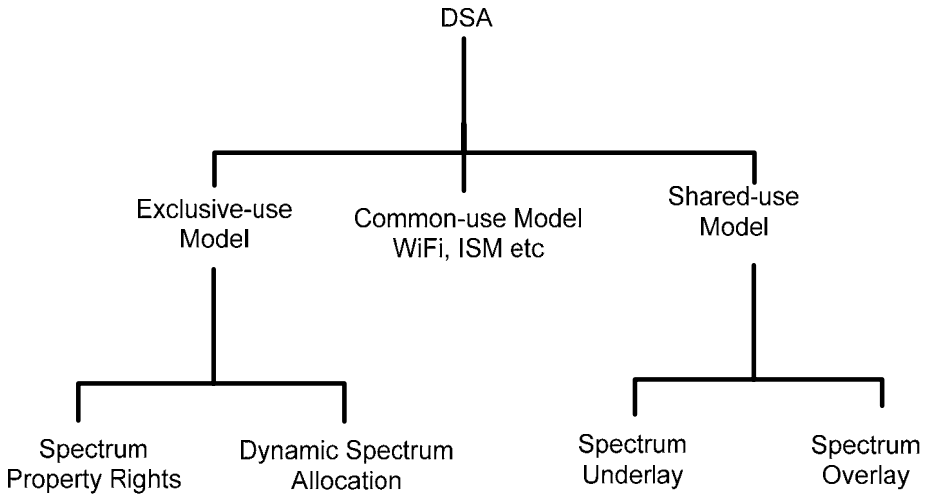

Fig. 1.1 Dynamic spectrum access strategies.

The exclusive-use model has two approaches, spectrum property rights and dynamic spectrum allocation. In spectrum property rights, owner of the spectrum can sell and trade spectrum; and is free to choose the technology of interest. Dynamic spectrum allocation improves spectrum efficiency by exploiting the spatial and temporal traffic statistics of different services [3]. The European Union funded DRiVE (Dynamic Radio for IP Services in Vehicular Environments) project is a classical example of dynamic spectrum allocation [9]. It uses cellular (e.g., GSM, GPRS, and UMTS) and broadcast technologies (e.g., Digital Video Broadcast Terrestrial, Digital Audio Broadcast) to enable spectrum efficient vehicular multimedia services.

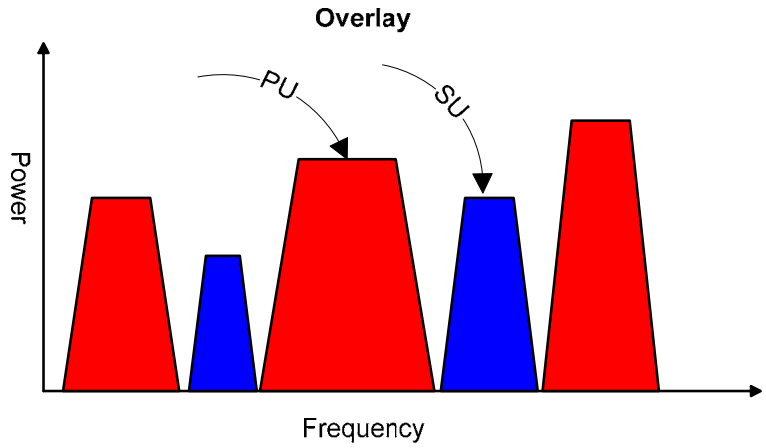

Fig. 1.2 Overlay spectrum access.

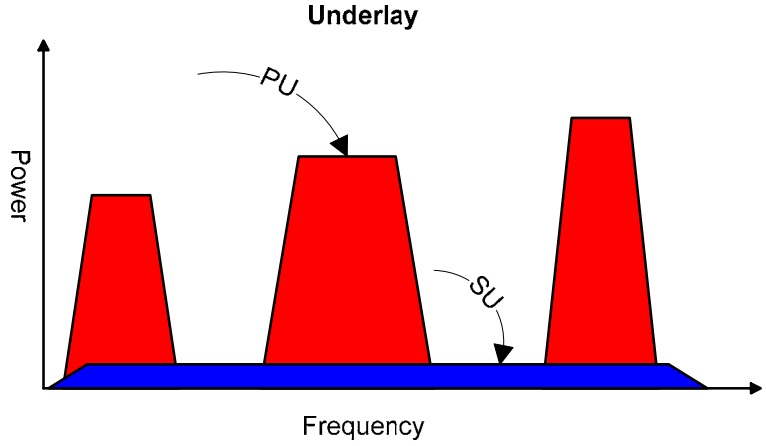

Fig. 1.3 Underlay spectrum access.

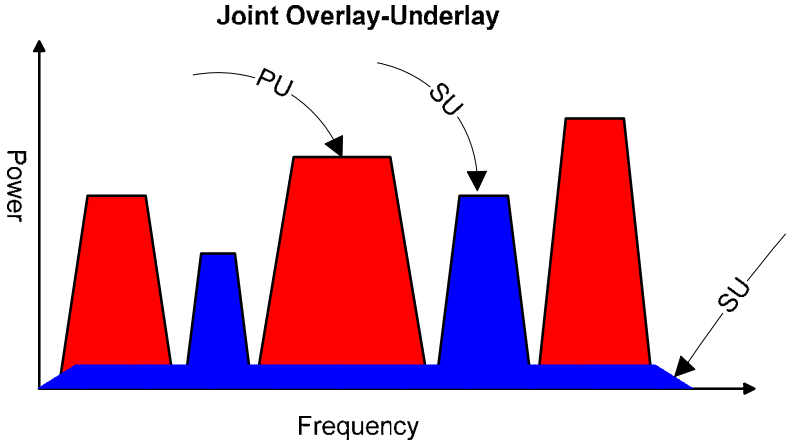

Fig. 1.4 Joint overlay and underlay spectrum access.

The common-use model is an open sharing regime in which spectrum is accessible to all users. The ISM (industrial, scientific and medical) band and Wi-Fi are examples of the commons-use model. Spectrum underlay and overlay approaches are used in the shared-use model [2] [3]. Spectrum overlay or opportunistic spectrum access is shown in Fig. 1.2. In spectrum overlay, the secondary users first sense the spectrum and find the location of a spectrum hole (vacant frequency band). After locating the vacant frequency bands, the secondary users transmit in these frequency bands. In spectrum underlay technique, the secondary users can transmit on the frequency bands used by the primary users as long as they do not cause unacceptable interference for the primary users. This approach does not require secondary users to perform spectrum sensing, however the interference caused by the secondary user's transmission must not exceed the interference threshold. Fig. 1.3 shows the spectrum underlay model.

In [10], a joint spectrum overlay and underlay method is proposed for better spectrum utilization. An illustration of joint spectrum overlay and underlay is shown in Fig. 1.4. In joint spectrum overlay and underlay approach, the secondary users with the help of spectrum sensing first try to find a spectrum hole. If there is a spectrum hole then the secondary users can use the spectrum overlay technique. If there is no spectrum hole then the secondary users will use spectrum underlay technique.

1.2.2 Cooperative Communication

Recent research in wireless communication systems shows that relaying techniques can offer significant benefits in the throughput enhancement, and range extension [12]. A number of relaying schemes −e.g., amplify-and-forward (AF) decode and forward (DF), incremental relaying etc. −for improving the performance of the wireless networks are in the literature e.g., [12] [13]. In a simple AF relaying scheme, a relay amplifies the received signal and forwards it to the destination. In decode and forward relaying scheme, a relay first decodes

the received signal and then transmits the re-encoded signal to the destination. Table 1.2 shows a simple cooperative communication protocol. In this protocol, conveyance of each symbol from the source to the destination takes place in two phases (two time slots). In the first phase, the source transmits its data symbol, and the destination and the relay(s) receive the signal carrying the symbol. In the second phase, the relay(s) forwards the data to the destination.

Table 1.2 Cooperative communication protocol.

Time T_1	**Time T_2**
S → D, S → R	
	R → D

The performance of a cooperative communication system can be improved by using multiple relays, rather than a single relay, which convey the same information to the destination. The multiple relays selection/assignment gives more freedom to select good paths between source to relay(s) and relay(s) to destination(s). Fig. 1.5 shows the multiuser cooperative communication system with multiple relays. The use of multiple relays in a network comprising single source and multiple destinations brings the issue of how to best assign the relays to the destinations. Optimization of such relay assignment and power control has combinatorial aspects, and the exhaustive search for an exactly optimal solution is impractical due to its computational complexity. There are a number of low-complexity relay selection/assignment schemes in the literature [32] – [45]. However, these relay assignment schemes are not applicable to CRS because optimal relay assignment and power allocation obtained from these schemes may generate more interference to the primary users than allowed.

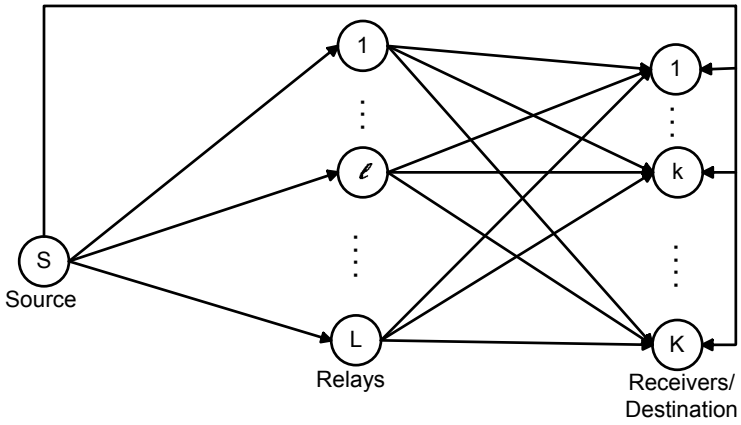

Fig. 1.5 Multiuser cooperative communication system.

1.2.3 Green Communication

Recent advances in the field of information and communication technologies (ICTs) have significant impact on the environment. The enormous growth of the telecommunication sector (especially the wireless sector) plays a significant role in global warming. Research in green technology will enable the communication system designer to develop and design the systems that will help the environment by reducing carbon dioxide (CO_2) emissions.

According to the International Telecommunication Union (ITU) report [19], primary sources of CO_2 emissions are electricity generation, transport vehicles, buildings and agricultural by-products etc. By the year 2030, World Energy Outlook (WEO) has forecasted that the demand of electricity will be twice as high as compared to the current demand, driven by the rapid growth in population and by the continuous increase in the residential and commercial electrical devices [20]. The ICTs sector is responsible for approximately five percent of global electricity demand and CO_2 emission [21] [22]. The CO_2 emission from the ICTs sector is equivalent to the airline industry [19] [22].

The electricity demand of ICTs sector is divided into four major categories as shown in Fig. 1.6. These are (1) servers (23%), (2) PCs data monitors (40%),

(3) telecommunications (31%), and miscellaneous (6%). From Fig. 1.6, we can see that the landline and mobile telecommunications contribute to approximately 77% of the total telecommunication CO_2 emissions. As the ICTs industry is growing faster than the rest of the economy, this share will likely increase over time. The number of the mobile subscribers is nearly equal to half of the global population [23]. There is a need in the design of future wireless communication systems to reduce the transmission power of mobile devices to bring down the CO_2 emissions. In the context of green communication, intelligent resource allocation schemes for CRS with relaying capability can help in reducing the CO_2 emissions.

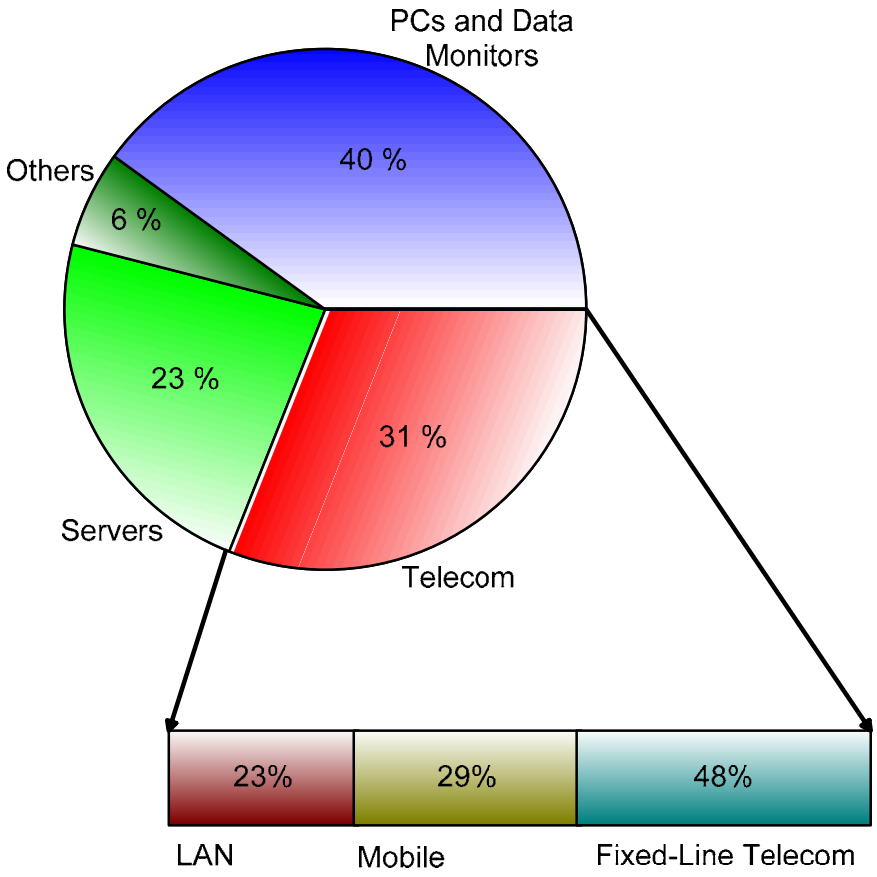

Fig. 1.6 Estimated distribution of global CO_2 emissions from ICTs.

1.3 Thesis Overview

The main objective of this thesis is to provide low-complexly algorithms for resource allocation in cognitive radio and green communication systems. In the context of resource allocation, this thesis basically discusses three problems: 1) relay assignment, 2) subcarrier assignment, and 3) user scheduling. In all three problems, we examine the effect of different system parameters (e.g., interference threshold level, the number of primary users, the number of secondary users, relay power levels, etc.) on the performance of the proposed algorithms.

1.3.1 Relay assignment

The use of multiple relays can increase the performance of a cooperative communication system. A well designed multiple relay assignment and power allocation scheme can be helpful in reducing the interference induced to the primary users in multiuser CRS. In this work, we propose a framework and low-complexity algorithm for interference aware joint power allocation and multiple relays assignment (IAJPARA) in multiuser CRS. In the proposed multiuser CRS framework, a secondary user can receive data through multiple relays. The proposed IAJPARA, when mathematically formulated, is basically a non-convex mixed integer non-linear optimization problem (NC-MINLP). The main objective of IAJPARA in our mathematical formulation is to maximize the sum-capacity by finding an optimal assignment of multiple relays to the secondary users in multiuser CRS under the constraint of acceptable interference to the primary users. The computational complexity of an obvious algorithm (exhaustive search-based), for the IAJPARA, grows exponentially with the number of relays and secondary users. We present a computationally efficient, suboptimal relay assignment and power allocation scheme for IAJPARA. For comparison, we provide an upper bound on the sum-rate capacity of IAJPARA. We examine the effect interference threshold, number of primary users, relay power levels on the

performance of the proposed scheme. We also show that with little modification of our proposed algorithm, we can include fairness in the system.

The use of relays in a CRS can also reduce the overall transmission power of the systems that can be helpful in reducing global warming by minimizing the CO_2 emissions. In this research, we present a multi-objective architecture for resource allocation in green cooperative cognitive radio network (GCCRN). The proposed multi-objective framework jointly assigns the relays to the users and allocates power to each relay in GCCRN while optimizing two conflicting objectives. The first objective is to maximize the sum-rate capacity and the second objective is to minimize the total CO_2 emissions. We apply an Estimation-of-distribution Algorithm (EDA) to the multi-objective optimization for resource allocation in GCCRN.

1.3.2 Subcarrier assignment

Orthogonal frequency division multiple access (OFDMA) is an emerging technique in multiuser multiple-access system. Multiple-access is achieved in OFDMA by allocating different subcarriers to the individual users. In this research, we propose a framework for joint power, subcarrier allocation and relay assignment (JPSARA) in multiuser multicast cognitive radio system (MMCRS). The main objective of the proposed resource allocation is to maximize the total system throughput of secondary users in MMCRS under the constraint of an acceptable interference level to the primary users. In this research, for JPSARA, we propose a low-complexity iterative algorithm based on primal dual decomposition. We also present a max-min fairness aware scheme for resource allocation in MMCRS.

1.3.3 User scheduling

Generally, in multiuser wireless systems, due to resource limitations, user scheduling is an intelligent way to achieve high throughput. User scheduling schemes select the best group of users at each time slot to maximize the sum-

rate capacity of the multiuser MIMO system. The complexity of an exhaustive search for user scheduling increases exponentially with the number of users. For example, if *K* is the total number of users, then the number of possible ways of scheduling/selecting *k* users is $\binom{K}{k}$. Enumerating all possible combinations to find the one that gives the best performance is computationally inefficient. Due to the high computational complexity of the optimal selection (e.g., Exhaustive search algorithm), a number of suboptimal solutions were proposed in the literature. These traditional user scheduling schemes in the multiuser MIMO systems are not applicable in the CRS because the selected subset of users, which maximize the sum-rate capacity in the traditional multiuser MIMO systems, may generate more interference to the primary users than desirable. In this thesis, we present low-complexity algorithms for joint user scheduling and power control in multiuser MIMO CRS to maximize the sum-rate capacity, under the constraint that the interference to the primary users is below specified levels.

1.4 Literature Review

This section contains a literature review for resource allocation strategies in wireless communication system.

1.4.1 Relay assignment and power allocation

Table 1.3 summarizes the literature review for the relay assignment strategies (RAS) in the wireless communication systems. The first column in Table 1.3 lists the objective functions as defined in the literature. The succeeding columns show the number of relays attached to any destination/user, cognitive radio capability, protocol type (e.g. centralized, distributed or decentralized) and power allocation capability respectively. There are three major classes of resource allocation in cooperative communications. The classes are, centralized resource allocation [32-35] [39] [42-43], distributed resource allocation [36] [45], and decentralized resource allocation [37] [38] [44].

In [32], joint bandwidth and power allocation strategies for a Gaussian relay network are investigated. Orthogonal and shared-band AF and DF schemes are analyzed for joint bandwidth and power allocation. The main objective of joint bandwidth and power allocation is to maximize the signal-to-noise ratio at the receiver using AF and DF schemes. The study in [33] proposes a centralized framework that selects multiple relays for transmission in a two-hop network. The aim of the multiple relay selection is to maximize the SNR at the destination using binary power allocation at the relays. An optimal relay assignment and power allocation in a cooperative cellular network is discussed in [34]. Using the sum-rate maximization as a design metric, the authors proposed a convex optimization problem that provides an upper bound on performance. A heuristic water-filling algorithm is also suggested to find a near-optimal relay assignment and power allocation. In [35], a linear-marking mechanism is investigated for relay assignment in a multi-hop network with multiple source-destination pairs. The aim of the proposed linear-marking mechanism is to maximize the worst user capacity.

A distributed nearest neighbour relay selection protocol and its outage analysis are presented in [36]. For the relay assignment in a multiuser communication system, decentralized protocols are discussed in [37] and [41]. The decentralized framework in [37] uses decode and forward relaying and assigns relays without exercising power control. In [41], decentralized amplify and forward protocol is used for joint relay assignment and power control. The scheme maximizes a harmonic mean-based approximate expression for the instantaneous received signal-to-noise ratio. The relay assignment and selection schemes described in [32] − [38] and [41] are not applicable in the CRS because the interference caused by the relays to the primary users can exceed the prescribed interference limit.

The relay selection scheme for a cognitive radio network has been considered in several recent works [39]−[45]. In [39], a mathematical formulation is proposed with the objective of minimizing the required network-wide radio spectrum resource for a set of user sessions. The proposed formulation is a

mixed-integer non-linear program. The authors proposed a lower bound for the objective by relaxing the integer variables and using a linearization technique. A near-optimal algorithm is presented that is based on a sequential fixing procedure, where the integer variables are determined iteratively via a sequence of linear programs. In [42], relay selection in multi-hop CRS with the objective of minimizing the outage probability is proposed. The power allocation problem is solved using standard convex optimization techniques for both AF and DF protocols under Rayleigh fading conditions. A joint relay selection, spectrum allocation and rate control (JRSR) scheme in CRS is proposed in [43]. A three-stage sub-optimal algorithm is proposed to address the JRSR problem. A non-cooperative game based decentralized power allocation for primary and secondary users is considered in [44]. The two kinds of links, one of which includes the primary users and their relay, the other includes the secondary users and their relay, are treated as players of the non-cooperative game. Each player competes against the other by choosing the power allocation strategy that maximizes its own rate, subject to the QoS threshold of the primary system. A relay-assisted iterative algorithm is proposed to efficiently reach the Nash equilibrium. In [45], authors proposed both centralized and distributed power allocation schemes for multi-hop wideband CRS. The main objective is to maximize the output signal-to interference plus noise ratio (SINR) at the destination node of the CRS. From the literature review, we separate the relay assignment/selection schemes into two categories,

1.4.1.1 RAS without CR capability

a) Multiple relays assignment with one source and one destination [32] [33]

b) Single relay assignment with one source and multiple destinations [34].

c) Single relay assignment with multiple source-destination pairs [35].

d) Multiple relays assignment with one source, one destination and multi-hops [38].

Table 1.3 Relay Assignment.

Objective	**Relays to one SD pair per hop**	**CR**	**Protocol Type**	**Power Control**	**Ref. [Ref Num, Name]**
Maximize the SNR of AF/DF shared bandwidth schemes	Multiple	No	Centralized	Yes	[32, I. Maric et. al]
Select the multiple relays to maximize the SNR in shared bandwidth AF scheme	Multiple	No	Centralized	Binary Power Control	[33, Y. Jing et al.]
Sum-rate maximization	Single	No	Centralized	Yes	[34, Kadloor et al.]
Maximize the minimum capacity	Single	No	Centralized	No	[35, Y. Shi et al.]
Protocols and outage analysis	Single	No	Distributed	No	[36, Sadek et al.]
Average sum-capacity	Single	No	Decentralize	No	[37, P. Zhang et al.]
Maximize the instantaneous received SNR	Single	No	Decentralize	Yes	[38, G. Farhadi et al.]
Minimize the total bandwidth	Single	Yes	Centralized	No	[39, T. Hou et al.]
Closed-form expressions of detection probability	Single	Yes	----	No	[40, J. Zhu et al.]
Cooperation between primary user and secondary user.(secondary user act as relay for primary user)	Single	Yes	----	Yes	[41, R. Manna et al.]
Minimize outage probability	Single	Yes	Centralized	Yes	[42, Jayasinghe et al.]
Maximize Average throughput	Single	Yes	Centralized	Yes	[43, H. Chun et al.]
Maximize the rate utility function	Single	Yes	Decentralize	Yes	[44, Xiaoyu et al.]
Maximize SNR of RD link	Single	Yes	Distributed	Yes	[45, Mietzner et al.]

1.4.1.2 RAS with CR capability

a) Multiple relay assignment with one source, one destination and multi-hops [39].

b) Single relay assignment with multiple source-destination pairs [44].

c) Single relay assignment with one source and multiple destinations [43].

From the literature review of relay selection/assignment strategies as summarized in Table 1.3, we can observe that the relay selection/assignment in the wireless network is an active area of research. However, there is still a need of low-complexity algorithms and protocols that can efficiently perform multiple relay assignment in a multiuser CRS.

1.4.2 Subcarrier assignment and power allocation

Table 1.4 summarizes the literature review of the subcarrier assignment (SA) and power allocation techniques in the multicarrier communication systems. In [49], a centralized subcarrier assignment scheme is proposed in a multi-cell CRS. The main objective is to maximize the weighted sum-rate of secondary users over multiple cells. An iterative water-filling algorithm is suggested to control the inter-cell interference. The study in [50] proposes a distributed subcarrier assignment algorithm to maximize the rate of each user and its perturbation analysis in the ad-hoc cognitive radio network. In particular, in [50], an upper bound on perturbation of each user's allocated power, rate, and interference caused to the primary users is investigated. In [51], a risk-return model based subcarrier assignment is studied to maximize the sum-rate of secondary users. A linear rate-loss function is introduced in the optimization. In a cognitive radio environment, loss of useful power can be represented as a rate loss whenever a primary user reoccupies the channel or when there is an error in correctly sensing the channel. Two sub-optimal subcarrier assignment schemes, step ladder and nulling, are studied to reduce the computational complexity of subcarrier assignment. In the step ladder scheme, low power is assigned to

subcarriers that are closer to the primary users bands. In the nulling method, zero power is allocated to subcarriers adjacent to a primary users' band (one nulling) or zero power to two subcarriers closest to the primary user's band on each side (two nulling). In [52], authors proposed the nulling method to maximize the downlink transmission capacity of the secondary users in an OFDM based CRS.

In [53], the authors proposed optimal power control policies for secondary users to minimize the outage probability for a given outage capacity under the primary user's outage constraint, along with the average and peak transmit power constraint of secondary users. A fairness aware joint rate and power allocation scheme with a QoS constraint for CRS is studied in [55]. The authors derived outage probabilities for secondary users and interference-constraint violation probabilities for primary users. Based on the analysis, the authors developed a framework to perform joint admission control and rate/power allocation.

A non-cooperative game based subcarrier assignment is proposed in [56]. The authors model the competitive behaviour of the secondary users as a non-cooperative game and address the existence and uniqueness of Nash equilibrium. Based on the unique equilibrium, a non-convex pricing framework for the primary service provider is discussed. A sub-optimal pricing scheme in terms of revenue maximization of the primary service provider is presented. References [57], [58] and [59] provide centralized and distributed algorithms for the subcarrier assignment in multi-cast CRS.

In [59], authors introduce a general rate-loss function, which gives a reduction in the attainable throughput whenever primary users reoccupy the temporarily accessible sub-channels. The main objective is to maximize the expected sum-rate of secondary users in multicast groups. A dual decomposition based iterative algorithm is presented for joint subcarrier and power-allocation. In [60], a decentralized fairness aware subcarrier assignment framework is proposed for relay-assisted downlink cellular CRS.

Table 1.4 Subcarrier Assignment With power allocation.

Objective	**Relays**	**CR**	**Protocol Type**	**Power Control**	**Ref. [Ref Num, Name]**
Sum-rate maximization	No	Yes	Centralized	Yes	[49, Y.Ma et. al]
Maximize the rate of each user and user perturbation analysis	No	Yes	Distributed	Yes	[50,H. Keshavar et. al]
Sum-rate maximization with loss function	No	Yes	Centralized	Yes	[51, Z.Hasan et. al]
Sum-rate maximization	No	Yes	Centralized	Yes	[52, G. Bansal et. al]
Minimize the outage probability	No	Yes	Centralized	Yes	[53, X. Kang et. al]
Sum-rate maximization with rate loss constraint	No	Yes	Distributed	Yes	[54, X. Kang et. al]
Sum-rate maximization	No	Yes	Centralized	Yes	[55, D. I.Kim et. al]
Maximize the total revenue	No	Yes	Decentralize	Yes	[56, Z. Li et. al]
Minimize the expected energy (*for Multicast*)	No	Yes	Centralized	Yes	[57, W. Ren et. al]
Sum-rate Maximization of Multicast groups	No	Yes	Centralized	Yes	[58, D. Ngo et. al]
Sum-rate Maximization of Multicast groups with rate loss function	No	Yes	Distributed	Yes	[59, D. Ngo et. al]
Average weighted goodput (utility maximization)	Yes	Yes	Distributed	Yes	[60, R.Wang et. al]
Maximize the worst user capacity	Yes	Yes	Centralized	Yes	[61, J. Guo et. al]
BER analysis	Yes	No	Centralized	Yes	[62, M. Adnan et. al]
1-Maximize the minimum rate 2- Maximize the rate with proportional fairness	No	Yes	Centralized	Yes	[63, L. B. Le et. al]
Sum-rate maximization	No	Yes	Centralized	Yes	[64, K. Hamdi et. al]
Maximize the Ergodic capacity	No	Yes	Centralized	Yes	[65, R. Zhang et. al]
Maximize total transmission rate	No	Yes	Centralized	Yes	[66, A. T. Hoan et. al]

Objective	Relays	CR	Protocol Type	Power Control	Ref. [Ref Num, Name]
Sum-rate maximization	Yes	No	Centralized	No	[67, H. Rasouli et. al]
BER analysis	Yes	No	Centralized	Yes	[68, S. Senthuran et. al]
Weighted sum-rate maximization	No	Yes	Centralized	Yes	[69, L. zhang et. al]
Maximize average system utility	No	Yes	Distributed	Yes	[70, R. Zhang et. al]
Maximize system goodput	Yes	No	Distributed	Yes	[71, Y. Cui et. al]
Minimize energy per bit	No	Yes	Distributed	Yes	[72, S. Gao et. al]
Survey of resource allocation in OFDM	——	———	—————	———	[73, S. Sdr et. al]

In [61], max-min capacity based centralized relay assignment scheme is proposed for multi-hop cognitive radio network. In [63]-[66] and [69], a number of centralized sub-optimal sub-carrier assignment algorithms are proposed for sum-rate maximization in CRS. A time division protocol based downlink subcarrier allocation in a cooperative multiuser OFDM system is proposed in [67]. In [68], joint Subcarrier and power allocation schemes are proposed and analyzed for a two-hop orthogonal frequency and code division multiplexing (OFCDM). Distributed subcarrier assignment is investigated in [70]-[72]. Reference [73] provides a survey of the downlink subcarrier assignment and power allocation in multiuser wireless system.

1.4.3 User scheduling

Table 1.5 summarizes the literature review of user scheduling in multiple-access MIMO systems. The main motivation of user scheduling is to improve the system performance in terms of either sum-rate capacity or bit error rate. Due to the high computational complexity of the optimal selection (e.g., ESA), a number of suboptimal solutions were proposed in the literature [74] − [90]. In [74], [76]

and [77], authors propose centralized iterative schemes for user scheduling without power control for the multiuser MIMO system. The main objective of these schemes was to maximize the sum-rate capacity. In [74], authors proposed a centralized user selection framework for the uplink multiuser MIMO system. A centralized downlink multiuser scheduling with power allocation for multiuser MIMO systems is presented in [75] − [80] and [84]. In [82] [83] [88] and [90], authors propose a centralized approach for user scheduling in the cognitive MIMO system. A distributed user-scheduling scheme in a cognitive SISO system is proposed in [81]. In [85] and [87], the authors presented decentralized user scheduling schemes for SISO and MIMO cognitive radio systems respectively. From the literature review of user scheduling in Table 1.5, it can be observed that little work has been done on the uplink user scheduling and power allocation in multiuser MIMO CRS. There is a need to develop low-complexity algorithms for user scheduling in uplink multiuser MIMO CRS.

Table 1.5 User scheduling in Multi Access MIMO System.

Objective	Uplink /Downlink	MIMO/ SISO/MISO	CR	Protocol Type	Power Control	Ref.
Maximize sum-rate	Uplink	MIMO	No	Centralized	No	[74, Y. Zhang et. al]
Maximize sum-rate	Downlink	MIMO	No	Centralized	Yes	[75, Z. Shen et. al]
Maximize sum-rate	Downlink	MIMO	No	Centralized	No	[76, R. Elliott et. al]
Maximize sum-rate	Downlink	MIMO	No	Centralized	No	[77, X . Zhang et. al]
Maximize sum-rate	Downlink	MIMO	No	Centralized	Yes	[78, Z. Min et. al]
Jointly maximize each user's SNR	Downlink	MIMO	No	Centralized	Yes	[79, X. Zhang et. al]
Maximize sum-rate	Downlink	MIMO	No	Centralized	Yes	[80, B.C. Lim et. al]
Maximize the time average rate	———	SISO	Yes	Distributed	No	[81,Urgaonka et. al]
Maximize sum-rate	Downlink	MIMO	Yes	Centralized	Yes	[82, W. Zong et. al]
Maximize Fairness aware sum-rate	Downlink	MIMO	Yes	Centralized	Yes	[83, Q. Meng et. al]
Maximize sum-rate	Downlink	MIMO	No	Centralized	Yes	[84, A. Bayesteh et. Al]
Maximize sum-rate utility	———	SISO	Yes	Decentralized	Yes	[85, A. Khisti et. al]
Maximize sum-rate	———	MISO	Yes	Decentralized	Yes	[86, Jorswiek et. al]
Maximize sum-rate	Uplink /Downlink	SISO	Yes	Centralized/ Decentralized	Binary	[87, B. Zayen et. al]
Maximize sum-rate	Downlink	MIMO	Yes	Centralized	Yes	[88, J. Wang et. al]
Maximize sum-rate	Uplink	SISO	Yes	Centralized	Yes	[89, K. Hamdi et. al]
Max. sum-rate	Downlink	MIMO	Yes	Centralized	Yes	[90,C. Lv et. al]

1.5 Summary of Contributions

This thesis solves resource allocation problems by proposing low-complexity algorithms for cognitive radio with MIMO and relaying capabilities. All the proposed algorithms in this thesis have polynomial-time complexity.

First, we present a joint multiple relay assignment with discrete and continuous power allocation, which is formulated as a non-convex mixed integer non-linear programming problem. The complexity of the proposed easily conceivable optimization of the relay assignment shows exponential growth with the number of secondary users and number of relays. We propose an iterative greedy algorithm that has very low complexity and its performance is near the exhaustive search algorithm. This algorithm also shows some fairness in assigning relays to the secondary users.

Second, a multi-objective framework is proposed for green resource allocation in CRS. One of the objectives of green resource allocation is to reduce CO_2 emissions. We propose a hybrid estimation-of-distribution algorithm for green resource allocation in CRS.

Third, we presented a low-complexity distributed algorithm for joint subcarrier, relay assignment and power allocation in multicast CRS. A primal-dual decomposition approach is used for distributed resource allocation. The proposed algorithm has a polynomial-time complexity. We also present a max-min fairness-based resource allocation framework for joint subcarrier and relay assignment in multicast CRS.

In the last part of this thesis, three different algorithms are proposed for joint user scheduling and power control in multiuser MIMO CRS.

1.6 Organization of Thesis

Fig. 1.7 shows the hierarchal overview of the thesis. Chapter 2 describes different relay assignment schemes for relay assisted CRS. Green communication is presented in Chapter 3. Chapter 4 contains the framework and algorithms for subcarrier assignment in cooperative multicast CRS. User scheduling is presented in Chapter 5.

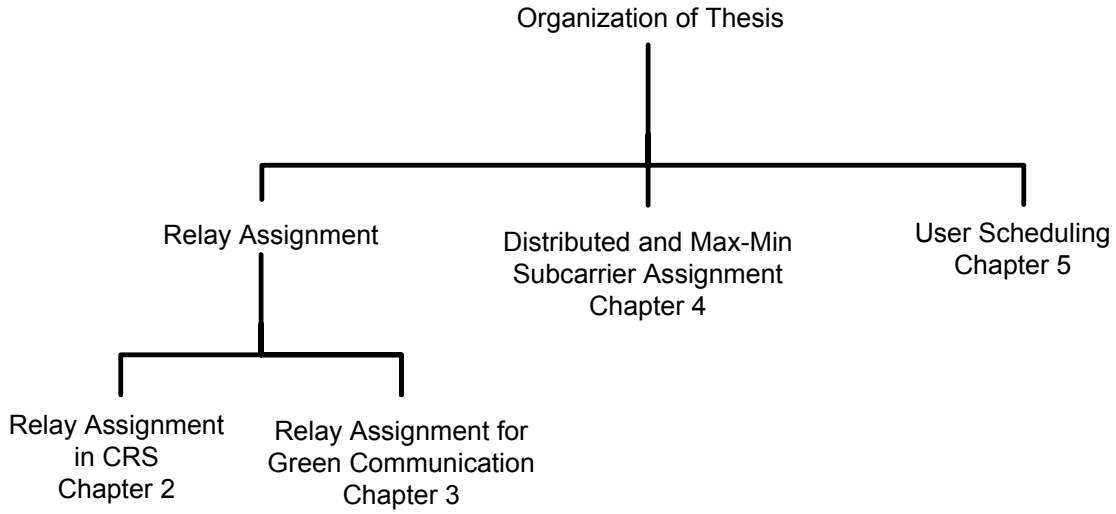

Fig. 1.7 Organization of thesis.

1.7 Chapter References

[1] Federal Communications Commission, Spectrum Policy Task Force Report, FCC 02-135, 2002.

[2] E. Hossain, D. Niyato, and Z. Han, Dynamic Spectrum Access and Management in Cognitive Radio Networks, Cambridge University Press, 2009.

[3] Q. Zhao and B.M. Sadler, “A Survey of Dynamic Spectrum Access,” IEEE Signal Processing Magazine, vol. 24, no. 3, pp. 79-89, May 2007.

[4] I. F. Akyildiz , W. Y. Lee, M. C. Vuran, and S. Mohanty , “A Survey on Spectrum Management in Cognitive Radio Networks, ” IEEE Communications Magazine, vol. 46, no. 4, pp. 40-48, April 2008.

[5] M. J. Marcus, P.Kolodzy, and A. Lippman, “Reclaiming the vast wasteland: why unlicensed use of the white space in the TV bands will not cause interference to DTV viewers,” New America Foundation: Wireless Future Program Report, 2005.

[6] M.J. Marcus, “Unlicensed Cognitive Sharing of TV Spectrum: The Controversy at the Federal Communications Commission,” IEEE Communications Magazine, vol. 43, no. 5, May 2005.

[7] A. M. Wyglinski, M. Nekovee, and Y. T. Hou, Cognitive Radio Communications and Networks: Principles and Practice, Elsevier, Dec. 2009

[8] S. Haykin, “Cognitive Radio: Brain-empowered Wireless Communications”, IEEE Journal on Selected Areas in Communications, Special Issue on Cognitive Networks, vol. 23, pp. 201−220, Feb 2005.

[9] L. Xu, R. Tonjes, T. Paila, W. Hansmann, M. Frank, and M. Albrecht, “DRiVE−ing to the Internet: Dynamic Radio for IP services in Vehicular Environments,” In Proceeding of 25th Annual IEEE International Conference on Local Computer Networks, pp. 281-289 , 2000.

[10] G. Bansal, O. Duval, and F. Gagnon, “Joint Overlay and Underlay Power Allocation Scheme for OFDM-based Cognitive Radio Systems,” In Proceeding of IEEE VTC spring 2010, Taipei, Taiwan, 2010.

[11] Y. Zhang, J. Zheng and H. H. Chen, Cognitive Radio Networks: Architectures, Protocols, and Standards ,CRC Press, 2010.

[12] K.J.R. Liu, A.K. Sadek, W. Su, and A. Kwasinski, Cooperative Communications and Networking, Cambridge University Press, 2008.

[13] J. N. Laneman, D. N. C. Tse, and G. W. Wornell, “Cooperative Diversity in Wireless Networks: Efficient Protocols and Outage Behavior,” IEEE Trans. Inform. Theory, vol. 50, no. 12, pp. 3062-3080, Dec. 2004.

[14] G. J. Foschini and M. J. Gans, “On limits of wireless communications in a fading environment when using multiple antennas,” Wireless Personal Communications, vol. 6, pp. 311-335, 1998.

[15] E. Telatar, “Capacity of Multi-antenna Gaussian Channels,” European Trans. on Telecomm. vol. 10, pp 569-709, Nov. 1999.

[16] C. Anton-Haro, P. Svedman, M. Bengtsson,A. Alexiou,and A. Gameiro, “Cross-layer scheduling for multi-user MIMO systems,” IEEE Communications Magazine, vol.44, no.9, pp.39-45, Sep. 2006.

[17] P. Si, H. Ji, F.R. Yu and V.C.M. Leung, “Optimal Cooperative Cognitive Radio Systems with Spectrum Pooling,” IEEE Trans. Vehicular Technology, vol. 59, no. 5, pp. 1760-1768, May 2010.

[18] L. B. Le and E. Hossain, “Multihop cellular networks: Potential gains, research challenges, and a resource allocation framework,” IEEE Communications Magazine, vol. 45, no. 9, pp. 66-73, Sept. 2007.

[19] International Telecommunication Union (ITU), “Report on Climate Change”, Oct. 2008.

[20] IEA report, “CO2 Emissions from Fuel Combustion 2010 – Highlights,”, http://www.iea.org/co2highlights/co2highlights.pdf

[21] G. Koutitas and P. Demestichas, “ A Review of Energy Efficiency in Telecommunication Networks,” Journal of Telecommunication Forum (TELFOR), 2010.

[22] G. Koutitas, “Green Network Planning of Single Frequency Networks,” IEEE Transactions on Broadcasting, vol.56, no.4, pp.541-550, Dec. 2010.

[23] L. Herault, E. C. Strinati , O. Blume ,D. Zeller, Muhammad A. Imran, R. Tafazolli, Y. Jading ,J. Lundsjö and Michael Meyer, “Green Communications: a Global Environmental Challenge,” In Proceeding of 12th International Symposium on Wireless Personal Multimedia Communications, 2009.

[24] C. Han, T. Harrold, I. Krikidis, I. Ku, T. A. Le, S. Videv, J. Zhang, S. Armour, P. M. Grant, H. Haas, L. Hanzo, M. R. Nakhai, J. Thompson, and C.-X. Wang, “Green radio: radio techniques to enable energy efficient wireless networks,” available at http://eprints.ecs.soton.ac.uk/21431/

[25] K. Li, “Mobile Communications 2008: Green Thinking Beyond TCO Consideration,” In-Stat White paper, May 2008.

[26] T. Newman, R. Rajbanshi, A. Wyglinski, J. Evans, and G. Minden, “Population Adaptation for Genetic Algorithm-based Cognitive Radios,” ACM/Springer Mobile Ad Hoc Networks ,vol. 13, no. 5, pp. 442-451, 2008.

[27] R.T. Marler and J.S. Arora, “Survey of multi-objective optimization methods for engineering,” Structural and Multidisciplinary Optimization, vol. 26, no.6, pp. 369-395, April 2004.

[28] M. Elmusrati, H. El-Sallabi, and H. Koivo, " Applications of multi-objective techniques in radio resource scheduling of cellular communication systems," IEEE Transaction of Wireless Communication, vol. 7, no. 1,pp. 343-353 Jan. 2008.

[29] K. Deb, Multi-objective optimization using evolutionary algorithms, Wiley New York, 2001.

[30] P. Larrañaga and J. A Lozano, Estimation of Distribution Algorithms: A New Tool for Evolutionary Computation. Kluwer Academic Publishers, 2001.

[31] A.E. Eiben and J.E. Smith, Introduction to Evolutionary Computing, Springer Verlag, 2003.

[32] I. Maric and R. D. Yates, "Bandwidth and Power Allocation for Cooperative Strategies in Gaussian Relay Networks," IEEE Trans. Inform. Theory, vol. 56, no. 4, pp. 1880-1889, Apr. 2010.

[33] Y. Jing and H. Jafarkhani, "Single and multiple relay selection schemes and their achievable diversity orders," IEEE Transactions on Wireless Communications, vol. 8, no. 3, pp. 1414 - 1423, Mar. 2009.

[34] S. Kadloor and R. Adve, "Optimal Relay Assignment and Power Allocation in Selection Based Cooperative Cellular Networks," IEEE International Conference on Communications , 14-18 June, pp. 1-5, 2009.

[35] Y. Shi, S. Sharma, Y.T. Hou, and S. Kompella, "Optimal relay assignment for cooperative communications," In Proceedings of the 9th ACM international Symposium on Mobile Ad Hoc Networking and Computing , Hong Kong, China, pp. 3-12, 2008..

[36] A. K. Sadek, Z. Han, and K. J. R. Liu, "Distributed Relay-Assignment Protocols for Coverage Expansion in Cooperative Wireless Networks," IEEE Transactions on Mobile Computing, , vol.9, no.4, pp.505-515, April 2010.

[37] P. Zhang, Z. Xu, F. Wang, X. Xie, and L. Tu; , "A Relay Assignment Algorithm With Interference Mitigation For Cooperative Communication," In Proceedings of IEEE Wireless Communications and Networking Conference, April 2009.

[38] G. Farhadi and N. C. Beaulieu, “A Decentralized Power Allocation Scheme for Amplify-And-Forward Multi-Hop Relaying Systems,” In Proceedings of IEEE International Conference on Communications (ICC), May 2010.

[39] Y. T. Hou, Y. Shi, and H. D. Sherali, “Spectrum sharing for multi-hop networking with cognitive radios,” IEEE Journal on Selected Areas of Communications, vol. 26, no. 1, pp. 146-155, Jan. 2008.

[40] J. Zhu, Y. Zou, and B. Zheng, “Cooperative Detection for Primary User in Cognitive Radio Networks,” EURASIP Journal on Wireless Communications and Networking, 2009.

[41] R. Manna, R.H.Y. Louie, Yonghui Li, and B. Vucetic, “Cooperative Amplify-and-Forward relaying in cognitive radio networks,” In Proceedings of the Fifth International Conference Cognitive Radio Oriented Wireless Networks & Communications (CROWNCOM),June 2010.

[42] L.K.S. Jayasinghe and N. Rajatheva, "Optimal Power Allocation for Relay Assisted Cognitive Radio Networks," In Proceedings of 72nd IEEE Vehicular Technology Conference, Sep. 2010.

[43] H. Chun, F. Zhiyong,.Z. Qixun,Z. Zhongqi and X. Han, “A Joint Relay Selection, Spectrum Allocation and Rate Control Scheme in Relay-Assisted Cognitive Radio System,” In Proceedings of 72nd IEEE Vehicular Technology Conference, Sept 2010.

[44] Q. Xiaoyu, T. Zhenhui, X. Shaoyi and J. Li, “Combined Power Allocation in Cognitive Radio-Based Relay-Assisted Networks,” In Proceedings of IEEE International Conference Communications Workshops (ICC), 2010.

[45] J. Mietzner, L. Lampe and R. Schober, “ Distributed transmit power allocation for multihop cognitive-radio systems,” IEEE Transactions On Wireless Communications, vol. 8, no. 10, Oct 2009.

[46] H. Rasouli and A. Anpalagan, “SNR- and BER-based power allocation in wireless relay networks with MRC at destination,” In Proceedings of IEEE Biennial Symposium on Communications, May 2010.

[47] S.-W. Han, H. Kim, Y Han and V.C.M. Leung, “Cooperative Access for Cognitive Radios to Guarantee QoS for Cell Edge Primary Users,” In Proceedings of IEEE PIMRC, Tokyo, Japan, Sep. 2009.

[48] S. Abdulhadi, M. Jaseemuddin and A. Anpalagan, “Joint routing and power allocation in DAF multi-hop cooperative adhoc networks,” In Proceedings of IEEE International Conference on Wireless and Mobile Computing, Oct. 2010

[49] Y. Ma, D. I. Kim, and Z. Wu, “Optimization of OFDMA-based Cellular Cognitive Radio Networks,” IEEE Trans. Comm.., vol. 58, pp. 2265-2276, Aug. 2010.

[50] H. Keshavarz, E. Hossain, S. Noghanian, and D. I. Kim, “Perturbation Analysis of Spectrum Sharing in Cognitive Radio Networks,” IEEE Trans. Wireless Comm., vol. 9, pp. 1564-1570, May 2010

[51] Z. Hasan, G. Bansal, E. Hossain, and V. K. Bhargava, “Energy-efficient power allocation in OFDM-based cognitive radio systems: A risk-return model,” IEEE Transactions on Wireless Communications, vol. 8, no. 12, , pp. 6078-6088, Dec. 2009.

[52] G. Bansal, M. J. Hossain and V. K. Bhargava, “Optimal and suboptimal power allocation schemes for OFDM-based Cognitive Radio systems,” IEEE Trans. Wireless Comm.., vol. 7, no. 11, pp.4710-4718, Nov. 2008.

[53] X. Kang, R. Zhang, Y.-C. Liang, and H. K. Garg. “On Outage Capacity of Secondary Users in Fading Cognitive Radio Networks with Primary User's Outage Constraint,” In Proceedings of IEEE GLOBECOM 2009.

[54] X. Kang, H. K. Garg, Y.-C. Liang, and R. Zhang, “Power Allocation for OFDM-Based Cognitive Radio Systems with Hybrid Protection to Primary Users,” In Proceedings of IEEE GLOBECOM 2009.

[55] D. I. Kim, L. Le, and E. Hossain, “Joint Rate and Power Allocation for Cognitive Radios in Dynamic Spectrum Access Environment,” IEEE Trans. Wireless Comm., vol. 7, pp. 5517-5527, Dec. 2008.

[56] Z. Li, L. Gao, X. Wang, X. Gao, and E. Hossain, “Pricing for uplink power control in cognitive radio networks,” IEEE Transactions on Vehicular Technology, vol. 59, no. 4, May 2010.

[57] W. Ren, X. Xiao, and Q. Zhao, “Minimum-Energy Multicast Tree in Cognitive Radio Networks,” In Proceedings of IEEE Asilomar Conference on Signals, Systems, and Computers, Nov. 2009.

[58] D. Ngo, C. Tellambura, and H. Nguyen, “Efficient Resource Allocation for OFDMA Multicast Systems with Spectrum-sharing Control,” IEEE Transactions on Vehicular Technology, vol. 58, no. 9, pp. 4878-4889, Nov. 2009.

[59] D. Ngo, C. Tellambura, and H. Nguyen, “Resource Allocation for OFDMA-based Cognitive Radio Multicast Networks with Primary User Activity Consideration,” IEEE Transactions on Vehicular Technology, vol. 59, no. 4, pp. 1668-1679, May 2010.

[60] R. Wang, V.K.N. Lau, C. Ying, K. Huang, B. Chen and X. Yang, “Decentralized Fair Resource Allocation for Relay-Assisted Cognitive Cellular Downlink Systems,” In Proceedings of IEEE International Conference on Communications, 2009.

[61] J. Guo, S.Gu, X. Wang, H. Yu and M. Guizani, “Subchannel and Power Allocation in OFDMA-Based Cognitive Radio Networks,” In Proceedings of IEEE International Conference on Communications (ICC), 2010.

[62] M. Adnan, S. Haoqiu, W. Yafeng, Y. Dacheng and W. Xiang, “Multicast based Dual Amplify and Forward relay scheme for 2-hop networks,” In Proceedings of IEEE Latin-American Conference on Communications, pp.1-5, 10-11 Sep. 2009.

[63] L. B. Le and E. Hossain, “Resource allocation for spectrum underlay in cognitive wireless networks,” IEEE Transactions on Wireless Communications, vol. 7, no. 12, pp. 5306-5315, Dec. 2008.

[64] K. Hamdi, W. Zhang, and K. B. Letaief, “Opportunistic spectrum sharing in cognitive MIMO wireless networks,” IEEE Transactions on Wireless Communications, vol. 8, no. 8, pp. 4098-4109, Aug. 2009.

[65] R. Zhang, “On peak versus average interference power constraints for protecting primary users in cognitive radio networks,” IEEE Transactions on Wireless Communications vol 8 no 4 pp 2112-2120, 2009.

[66] A. T. Hoang, Y.-C. Liang, and M. Habibul Islam, “ Power Control and Channel Allocation in Cognitive Radio Networks with Primary Users' Cooperation,” IEEE Trans. Mobile Computing, vol 9 no3 pp 348-360, 2010.

[67] H. Rasouli and A. Anpalagan, “Cooperative subcarrier allocation for an OFDM relaying system with grouped users,” Wireless Personal Communications, 2010.

[68] S. Senthuran, A. Anpalagan and O. Das, “Cooperative subcarrier and power allocation for a two-hop decode-and-forward OFCDM based relay network,” IEEE Transactions on Wireless Communications, vol. 8, no 9, pp. 4797-4805, Sep. 2009.

[69] L. Zhang, Y. Xin, and Y.-C. Liang, “Weighted sum rate optimization for cognitive radio MIMO broadcast channels,” IEEE Transactions on Wireless Communications, vol. 8, no. 6, pp. 2950-2959, 2009.

[70] R.Wang and V.K.N.Lau, “Joint Cross-Layer Scheduling and Spectrum Sensing for OFDMA Cognitive Radio Systems,” IEEE Transactions on Wireless Communications, vol. 8, no. 5, May 2009.

[71] Y. Cui, V.K.N. Lau, and R. Wang, “Distributive Subcarrier, Power, and Rate Allocation for Relay-Assisted OFDMA Cellular Systems with Imperfect System State Knowledge,” IEEE Transactions on Wireless Communications, vol. 8, no. 10, Oct. 2009.

[72] S. Gao, L. Qian and D. Vaman, “Distributed energy efficient spectrum access in cognitive radio wireless ad hoc networks,” IEEE Transactions on Wireless Communications, vol.8, no.10, pp.5202-5213, Oct. 2009.

[73] S. Sadr, A. Anpalagan and K. Raahemifar, “Radio resource allocation algorithms for downlink of multiuser OFDM communication systems,” IEEE Communications Surveys & Tutorials, vol. 11, no 3, Third Quarter, pp. 1-15, 2009.

[74] Y. Zhang, C. Ji, Y. Liu, W. Q. Malik, D. C. O'Brien, and D. J. Edwards, “A low complexity user scheduling algorithm for uplink multiuser MIMO systems,” IEEE Transactions on Wireless Communications, vol. 7, no. 7, pp. 2486−2491, Jul. 2008.

[75] Z. Shen, R. Chen, J. G. Andrews, R. W. Heath, Jr., and B. L. Evans, “Sum-capacity of multiuser MIMO broadcast channel with block Diagonalization ,” IEEE Transactions on Wireless Communications, vol.6 no. 6, June 2007.

[76] R. C. Elliott and W. A. Krzymień, “On the convergence of genetic scheduling algorithms for downlink transmission in multi-user MIMO systems,” Wireless Personal Communications, Sep. 2010.

[77] X. Zhang and J. Lee, “Low complexity MIMO scheduling with channel decomposition using capacity upper bound,” IEEE Transactions on Communications, vol. 56, no. 6, pp. 871−876, June 2008.

[78] Z. Min and T. Ohtsuki, “An improved user selection algorithm in multiuser MIMO broadcast,” In Proceedings of IEEE Personal, Indoor and Mobile Radio (PIMRC) ,Sep. 2009

[79] X. Zhang, E.A. Jorswieck, B. Ottersten, and A. Paulraj, “User selection schemes in multiple antenna broadcast channels with guaranteed performance,” In Proceedings of 8th IEEE Workshop on Signal Processing Advances in Wireless Communications SPAWC, 2007.

[80] B.C. Lim, W.A. Krzymień, and C. Schlegel, “Efficient sum rate maximization and resource allocation in block diagonalized space-division multiplexing”, IEEE Transactions on Vehicular Technology, vol. 58, no. 1, pp. 478-483, Jan. 2009.

[81] R. Urgaonkar and M. J. Neely, "Opportunistic Scheduling with Reliability Guarantees in Cognitive Radio Networks," In Proceedings of IEEE INFOCOM, Phoenix, AZ, April 2008.

[82] W. Zong; S.Shao, Q. Meng and W. Zhu, “Joint user scheduling and beamforming for underlay cognitive radio systems,” In Proceedings of 15th Asia-Pacific Conference on Communication (APCC), pp.99-103, Oct. 2009.

[83] Q. Meng, W. Zong, S. Shao, W. Zhu and B. Zheng, “A Near Fair User Scheduling Scheme in Cognitive Radio Networks,” In Proceedings of 5th International Conference on Wireless Communications, Networking and Mobile Computing, 2009.

[84] A. Bayesteh and A. K. Khandani, “On the user selection for MIMO broadcast channels,” In Proceedings of IEEE ISIT 2005.

[85] A. Khisti, T. Alpcan, J. P. Singh and H. Boche, “A Hybrid Game Approach for Joint User Selection and Power Allocation over Unlicensed Spectrum Bands,” In Proceedings of 47th Annual Allerton Conference on Comm., Control, and Computing 2009.

[86] E. Jorswieck and R. Mochaourab , “Beamforming in Underlay Cognitive Radio: Null-Shaping Constraints and Greedy User Selection,” In Proceedings of International Conference on Cognitive Radio Oriented Wireless Networks and Communications (CrownCom), pp. 1 - 5, Cannes, France, Jun 2010.

[87] B. Zayen, M. Haddad, H. Menouni, A. Øien and E. Geir, “Binary power allocation for cognitive radio networks with centralized and distributed user selection strategies,” Physical Communications, vol.1, no. 3, pp. 183-193, Sep. 2008.

[88] J. Wang, D. J. Love, and M. D. Zoltowski, “User Selection for MIMO Broadcast Channel with Se-quential Water-Filling,” In Proceedings of 44th Annual Allerton Conference on Comm., Control, and Computing, Monticello, IL, Sept. 27-29, 2006.

[89] K. Hamdi, W. Zhang, and K. B. Letaief, “Uplink scheduling with QoS provisioning for cognitive radio systems,” In Proceedings of IEEE International Wireless Communications and Networking Conference (WCNC 2007), Hong Kong, Mar. 11-15, 2007.

[90] L. Chaoyuan L, Z. Shidong, L. Yunzhou and W. Tingchang, “Low complexity user selection for MIMO broadcast channels,” In Proceedings of 19th IEEE International Symposium on Personal, Indoor and Mobile Radio Communications, (PIMRC), 2008.

PART 1: RELAY ASSIGNMENT

CHAPTER 2: RELAY ASSIGNMENT AND POWER ALLOCATION FOR CRS

The performance of a cooperative communication system can be improved by using multiple relays, rather than a single relay, which convey the same information to the destination [1] [2]. A larger number of relays in general increase the diversity order and the channel capacity. However, in a cognitive radio system (CRS), a large number of relays can collectively cause a significant level of interference to the primary users. In a multi-user CRS in which the users' signals are separated by frequency division, one can reduce the inference level in each frequency band by cleverly grouping relays and assigning each group to different frequency bands. In this chapter, we focus on the problem of assigning multiple relays to the secondary users in a CRS so that the sum-capacity of CRS is maximized under the constraint that the interference to the primary users is below a specified threshold. For relay assignment, we consider a CRS that employs amplify and forward (AF) relays in shared band mode. In shared band AF scheme, all the relays assigned to any destination transmit in a same time slot and in the same frequency band [1] [2]. We consider a CRS comprising single source node, multiple destination nodes (multiple secondary users), and multiple relays.

In our work, we propose relay assignment schemes with continuous and discrete power allocation. Finding an optimal interference-aware multiple relay assignment can be computationally extensive because of the combinatorial nature of the problem. Exhaustive Search Algorithm (ESA) evaluates all possible relay assignments, which is computationally inefficient. For relay assignment and power allocation, we propose low-complexity algorithms for both continuous and discrete power allocation.

The main contribution of this work is the formulation of the optimization framework for multiple relay assignment in multiuser CRS with power allocation (both discrete and continuous power allocation). The proposed multiple relay assignment and power allocation is a non-convex mixed[1] integer non-linear programming (NC-MINLP) problem. In the context of the proposed framework, we propose efficient algorithms for multiple relay assignment and power allocation. For comparison, we provide an upper bound on the sum-rate capacity in the relay assignment problem. A detailed performance analysis is examined to show the effect of different system parameters (e.g., interference threshold level, number of primary users, number of secondary users, relay power levels etc.) on the performance of the proposed scheme.

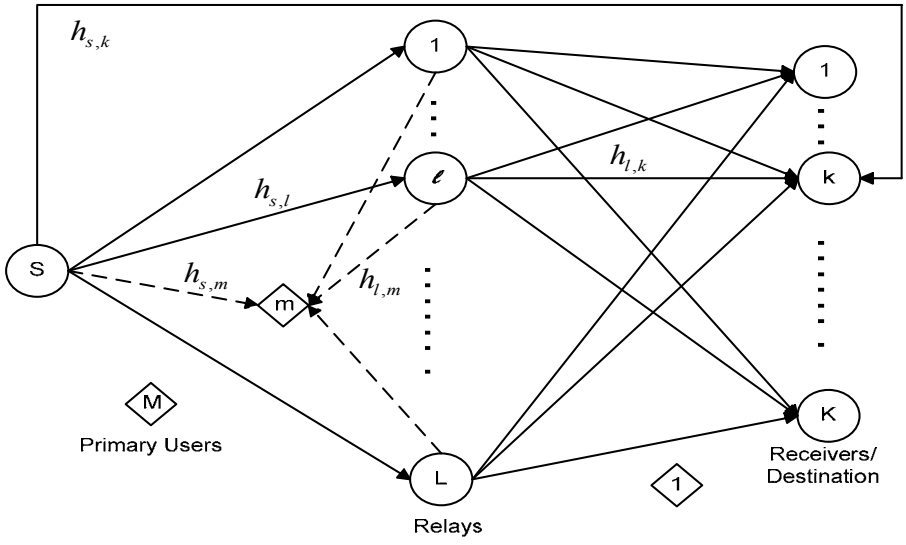

Fig. 2.1 Relay Assisted Cognitive Radio Network.

[1] For discrete power control, the relay assignment problem is a non-convex integer programming problem.

Table 2.1 Notations used in chapter 2.

Symbol	Definition
K	Number of secondary users
M	Number of primary users
L	Number of relays
$h_{s,l}$	Channel gain from source to the lth relay
$h_{s,k}$	Channel gain from source to the kth secondary user
$h_{l,k}$	Channel gain from lth relay to the kth secondary user
$g_{l,m}$	Channel gain from lth relay to the mth primary user
$g_{s,m}$	Channel gain from source to the mth primary user
P_s^k	Transmission power of source to kth secondary user
W	Bandwidth of non overlapping frequency bands to each secondary user
P_L	Set of relays' discrete power levels. $P_L = \left\{0, p^{max}/\lambda, 2p^{max}/\lambda, ..., p^{max}\right\}$
p_l^{max}	Maximum allowed transmission power of the lth relay
$I_{m,k}^{max}$	Maximum allowed interference at mth primary user on the kth secondary user's band
$\varepsilon_{l,k}$	Binary assignment indicator indicating whether relay l is assigned to the kth secondary user
Λ	A matrix where element $\Lambda(l,k)$ denotes individual SNR contribution of relay l at kth secondary user
Ψ	Set of relays that individually satisfy the interference constraints at all the primary users with non zero transmission power level
Γ^l	Summation of individual interference contribution of relay l at all the primary users i.e. $\Gamma^l = \sum_{m=1}^{M} I(l,m)$
$\tilde{k}$	User receiving maximum individual SNR
Θ	A vector where element $\Theta(l) = \arg\max_{k\in(1,2,..,K)} \Lambda(l,k) \quad \forall l \in \Psi$ represents the user where relay l generates its maximum individual SNR

2.1 Problem Formulation

We consider a two-hop cooperative CRS, which comprises one transmitting node (source), K receiving nodes (secondary users), and L relay nodes. Our system model also includes M primary users, for which the

transmission power of the cognitive radio nodes (secondary users) must be limited. *M* primary users can mean, as well as primary user devices, *M* geographic locations or regions in which the strengths of the cognitive radio signals must be constrained. Each relay, transmitter and receiver is equipped with a single antenna. We denote by $h_{s,l}$ the channel from the source to the *l*th relay, $h_{s,k}$ the channel from the source to the *k*th secondary user, $h_{l,k}$ the channel from the *l*th relay to the *k*th secondary user, $g_{s,m}$ the channel from the source to the *m*th primary user, and $g_{l,m}$ the channel from the *l*th relay to the *m*th primary user. In our system, a central controller (also referred to as the spectrum manager) jointly assigns relays to the secondary users and decides the relays' power levels. We assume that the central controller has perfect knowledge of the channel gains $h_{s,l}$, $h_{l,k}$ and $g_{l,m}$. We consider a two-step shared-band AF scheme for cooperative communication [1] [2]. In our system model, each secondary user will receive the data destined to it in its designated frequency band that does not overlap with other users' bands. We assume that all users are given the same bandwidth in the radio spectrum. Each relay will transmit and receive in the same frequency band. We denote by p_l, the transmission power of the *l*th relay. We denote by $\eta(p_l, l, m) = p_l \left| g_{l,m} \right|^2$, the interference power contributed to the *m*th primary user from the *l*th relay with power p_l.

We denote by P_s^k the transmission power of the source in the user band indexed by *k*. We assume that a relay assigned to the *k*th user filters in the received signal in the band indexed by *k* and then amplifies and transmits the signal in the same band. In our system mode, the source's transmission and the relays' transmission are separated in time. Each symbol is transmitted in two time slots−in the first time slot by the source and in the second time slot by the relays. Thus, in the first time slot, the signal received by the *l*th relay (after listening to the *k*th user's band) can be written as $\sqrt{P_s^k} h_{s,l} s + Z_l$, where complex-valued *s* represents the transmitted symbol and Z_l represents the complex-

valued white Gaussian noise at l_{th} relay. In our system model, symbol value *s* is normalized so that $E\left(|s|^2\right)=1$ and $N_0^{'}/2$ is the power spectral density of the noise Z_l. The noise power N, in watts, in each user band can be written as $N=\left(N_0^{'}/2\right)2W=N_0^{'}W$, where *W* is the bandwidth of each user band [10]. In the second time slot, the relays amplify the received signal and re-transmit the amplified signal. We are considering a system in which each relay can be assigned to only one user while a user can receive data from multiple relays. The channel capacity of the *k*th user with *L* relays using AF relaying is [1] [2]

$$C_k=\frac{1}{2}\log\left[1+\frac{P_s^k\left|h_{s,k}\right|}{N}+\frac{P_s^k}{N}\frac{\left(\sum_{l=1}^{L}\left|h_{s,l}h_{l,k}\right|\beta_l\sqrt{p_l}\right)^2}{1+\sum_{l=1}^{L}\left(\beta_l\left|h_{l,k}\right|\sqrt{p_l}\right)^2}\right] \tag{2.1}$$

where $\beta_l=\left(P_s^k\left|h_{s,l}\right|^2+N\right)^{-1/2}$. Our joint relay assignment and power allocation problem in a CRS is to determine the assignment of relays to the secondary users and the relays' powers, p_l, *l=1,2,...,L,* in order to maximize the sum-capacity $\sum_k C_k$ under the constraint that interference to the primary users within a specified value. The sum-capacity expression for shared AF in (2.1) is not a concave function of relay powers. We define $\varepsilon_{l,k}$ as a binary assignment indicator:

$$\varepsilon_{l,k}=\begin{cases}1 & \textit{if the } l\text{th } \textit{relay is assigned to the kth receiver}\\ 0 & \textit{otherwise}\end{cases}$$

The interference aware relay assignment problem can be defined as the following mixed integer non-linear programming problem:

$OP1:$

$$\max_{\substack{\{p_l \\ \varepsilon_{lk}, P_s^k\}}} \sum_{k=1}^{K} \frac{1}{2} \log_2 \left[1 + \frac{P_s^k \left| h_{s,k} \right|}{N} + \frac{P_s^k}{N} \frac{\left(\sum_{l=1}^{L} \frac{\varepsilon_{l,k} \left| h_{s,l} h_{l,k} \right| \beta_l \sqrt{p_l}}{\sqrt{P_s^k \left| h_{s,l} \right|^2 + N}} \right)^2}{1 + \sum_{l=1}^{L} \frac{\left| h_{l,k} \right|^2 p_l}{P_s^k \left| h_{s,l} \right|^2 + N}} \right]$$

subject to

$$\begin{aligned}
&C1: \ \sum_{k=1}^{K} \varepsilon_{l,k} \le 1, \qquad \forall l \\
&C2: \ \sum_{l=1}^{L} \varepsilon_{l,k} p_l \left| g_{l,m} \right|^2 \le I_{m,k}^{max}, \quad \forall (m,k) \\
&C3: \ P_s^k \left| g_{s,m} \right|^2 \le I_{m,k}^{max}, \quad \forall (m,k) \\
&C4: \ 0 \le P_s^k \le P_s^{max}, \quad \forall k \\
&C5: \ 0 \le p_l \le \sum_{k=1}^{K} \varepsilon_{l,k} p_l^{max}, \quad \forall l \\
&C6: \ \varepsilon_{l,k} \in \{0,1\}, \forall (l,k)
\end{aligned} \tag{2.2}$$

where p_l^{max} is the maximum allowable transmission power from the *l*th relay, and $I_{m,k}^{max}$ is the maximum tolerable interference at the *m*th primary user in the *k*th secondary user's band. The constraint *C*1 assures that a relay can only be assigned to one user. The constraints *C*2 and *C*3 are the interference constraints for source and relay transmissions respectively. The constraints *C*4 and *C*5 are the power constraints for source and relay respectively. The constraint *C*5 ensures that if the *l*th relay is not assigned to any user then the transmit power of the *l*th relay should be zero. The proposed multiple relay assignment and power allocation in *OP*1 is a non-linear mixed integer programming problem. An exhaustive search algorithm (ESA) for (2.2) would evaluate all the possible relay assignments and for each assignment determines the power of each relay. The number of different relays assignments increases exponentially with the number of relays and the number of the secondary users. Moreover, even for a given relay assignment, $\{\varepsilon_{l,k} | l = 1,2,..,L, k = 1,2,...,K\}$, the objective in (2.2) is not a

concave function of the source's and relays' power levels, so this continuous optimization is not a convex optimization problem. High-speed communications demand an assignment scheme with low computational complexity. This chapter proposes heuristic algorithms that have good performance and yet have relatively low computational complexity.

2.1.1 Decoupling of source power

Optimization problem (2.2) has three sets of decision variables: the relay assignment represented by $\{\varepsilon_{l,k}\}$, relay transmission power represented by $\{p_1, p_2, \ldots . p_L\}$, and the source's transmission power represented by $\{P_s^k \mid k = 1, 2, .., K\}$. We first note a special structure of the optimization problem (2.2). For any choice of relay assignment represented by $\{\varepsilon_{l,k}\}$ and relay transmission power represented by $\{p_1, p_2, \ldots . p_L\}$, the objective function is an increasing function of variable P_s^k, the source transmission power. In addition, the only constraints on variable P_s^k are $P_s^k \left|g_{s,m}\right|^2 \le I_{m,k}^{max}, \forall m$ and $0 \le P_s^k \le P_s^{max}$, which can be simplified to $0 \le P_s^k \le \min\left\{ P_s^{max}, \frac{I_{1,k}^{max}}{\left|g_{s,1}\right|^2}, \frac{I_{2,k}^{max}}{\left|g_{s,2}\right|^2}, \cdots, \frac{I_{M,k}^{max}}{\left|g_{s,M}\right|^2} \right\}$, and variable P_s^k do not appear in any other constraints in (2.2). That is, the interval constraint $0 \le P_s^k \le \min\left\{ P_s^{max}, \frac{I_{1,k}^{max}}{\left|g_{s,1}\right|^2}, \frac{I_{2,k}^{max}}{\left|g_{s,2}\right|^2}, \cdots, \frac{I_{M,k}^{max}}{\left|g_{s,M}\right|^2} \right\}$ of P_s^k, is decoupled from all other constraints in (2.2). Therefore, problem (2.2) can be written as:

$$\max_{\left\{p_l,\varepsilon_{lk}\ \middle|\substack{l=1,2,..,L\\k=1,2,..,K}\right\}}\left[\begin{array}{l}\max\limits_{P_s^k,k=1,2,...,K}\sum\limits_{k=1}^{K}\frac{1}{2}\log_2\left\{1+\frac{P_s^k\left|h_{s,k}\right|}{N}+\frac{P_s^k}{N}\frac{\left(\sum\limits_{l=1}^{L}\frac{\varepsilon_{l,k}\left|h_{s,l}h_{l,k}\right|\sqrt{p_l}}{\sqrt{P_s^k\left|h_{s,l}\right|^2+N}}\right)^2}{1+\sum\limits_{l=1}^{L}\frac{\left|h_{l,k}\right|^2p_l}{P_s^k\left|h_{s,l}\right|^2+N}}\right\}\\ \text{subject to}\quad C3:\ P_s^k\left|g_{s,m}\right|^2\le I_{m,k}^{max},\quad\forall(m,k)\\ \qquad\qquad C4:\ 0\le P_s^k\le P_s^{max},\quad\forall k\end{array}\right]$$

subject to

$$C1:\ \sum_{k=1}^{K}\varepsilon_{l,k}\le 1,\qquad\forall l$$

$$C2:\ \sum_{l=1}^{L}\varepsilon_{l,k}p_l\left|g_{l,m}\right|^2\le I_{m,k}^{max},\quad\forall(m,k)$$

$$C5:\ 0\le p_l\le\sum_{k=1}^{K}\varepsilon_{l,k}p_l^{max},\quad\forall l$$

$$C6:\ \varepsilon_{l,k}\in\{0,1\},\forall(l,k)$$

or equivalently,

$$\max_{\left\{p_l,\varepsilon_{lk}\ \middle|\substack{l=1,2,..,L\\k=1,2,..,K}\right\}}\left[\begin{array}{l}\max\limits_{P_s^k,k=1,2,...,K}\quad\sum\limits_{k=1}^{K}\frac{1}{2}\log_2\left\{1+\frac{P_s^k\left|h_{s,k}\right|}{N}+\frac{P_s^k}{N}\frac{\left(\sum\limits_{l=1}^{L}\frac{\varepsilon_{l,k}\left|h_{s,l}h_{l,k}\right|\sqrt{p_l}}{\sqrt{P_s^k\left|h_{s,l}\right|^2+N}}\right)^2}{1+\sum\limits_{l=1}^{L}\frac{\left|h_{l,k}\right|^2p_l}{P_s^k\left|h_{s,l}\right|^2+N}}\right\}\\ \text{subject to}\quad 0\le P_s^k\le\min\left\{P_s^{max},\frac{I_{1,k}^{max}}{\left|g_{s,1}\right|^2},\frac{I_{2,k}^{max}}{\left|g_{s,2}\right|^2},\cdots,\frac{I_{M,k}^{max}}{\left|g_{s,M}\right|^2}\right\},\forall k\end{array}\right]$$

$$\text{subject to} \quad C1: \ \sum_{k=1}^{K} \varepsilon_{l,k} \le 1, \qquad \forall l$$

$$C2: \ \sum_{l=1}^{L} \varepsilon_{l,k} p_l \left| g_{l,m} \right|^2 \le I_{m,k}^{max}, \quad \forall (m,k)$$

$$C5: \ 0 \le p_l \le \sum_{k=1}^{K} \varepsilon_{l,k} p_l^{max}, \quad \forall l$$

$$C6: \ \varepsilon_{l,k} \in \{0,1\}, \forall (l,k)$$

For any choice of relay assignment $\{\varepsilon_{l,k}\}$ and relay transmission power $\{p_1, p_2, \ldots . p_L\}$, the inner maximization,

$$\max_{\{P_s^k, k=1,2,\ldots,K\}} \ \sum_{k=1}^{K} \frac{1}{2} \log_2 \left\{ 1 + \frac{P_s^k \left| h_{s,k} \right|}{N} + \frac{P_s^k}{N} \frac{\left(\sum_{l=1}^{L} \frac{\varepsilon_{l,k} \left| h_{s,l} h_{l,k} \right| \sqrt{p_l}}{\sqrt{P_s^k \left| h_{s,l} \right|^2 + N}} \right)^2}{1 + \sum_{l=1}^{L} \frac{\left| h_{l,k} \right|^2 p_l}{P_s^k \left| h_{s,l} \right|^2 + N}} \right\}$$

$$\text{subject to} \quad 0 \le P_s^k \le \min \left\{ P_s^{max}, \frac{I_{1,k}^{max}}{\left| g_{s,1} \right|^2}, \frac{I_{2,k}^{max}}{\left| g_{s,2} \right|^2}, \cdots, \frac{I_{M,k}^{max}}{\left| g_{s,M} \right|^2} \right\}, \forall k$$

has a nice structure. Namely, the constraint on $\left(P_s^1, P_s^2, \ldots, P_s^k, \ldots, P_s^K\right)$ is a rectangular constraint and the objective function is separable. Therefore, the maximization can be achieved by performing the maximization over single variable P_s^k,

$$\max_{P_s^k} \quad \frac{1}{2}\log_2\left\{1+\frac{P_s^k\left|h_{s,k}\right|}{N}+\frac{P_s^k}{N}\frac{\left(\sum_{l=1}^{L}\frac{\varepsilon_{l,k}\left|h_{s,l}h_{l,k}\right|\sqrt{p_l}}{\sqrt{P_s^k\left|h_{s,l}\right|^2+N}}\right)^2}{1+\sum_{l=1}^{L}\frac{\left|h_{l,k}\right|^2 p_l}{P_s^k\left|h_{s,l}\right|^2+N}}\right\}$$

$$\text{subject to} \quad 0\le P_s^k \le \min\left\{P_s^{max},\frac{I_{1,k}^{max}}{\left|g_{s,1}\right|^2},\frac{I_{2,k}^{max}}{\left|g_{s,2}\right|^2},\cdots,\frac{I_{M,k}^{max}}{\left|g_{s,M}\right|^2}\right\}$$

individually for k=1,2,..,*K*. The objective function is monotonically increasing function of P_s^k and the constraints set is an interval (Appendix A). Therefore, for any choice of relay assignment $\{\varepsilon_{l,k}\}$ and relay transmission power $\{p_1, p_2, \ldots. p_L\}$, the maximizing source power P_s^k is $\min\left\{P_s^{max},\frac{I_{1,k}^{max}}{\left|g_{s,1}\right|^2},\frac{I_{2,k}^{max}}{\left|g_{s,2}\right|^2},\cdots,\frac{I_{M,k}^{max}}{\left|g_{s,M}\right|^2}\right\}$ for each *k*. We denote the optimal source power as

$$\bar{P}_s^k = \min\left\{P_s^{max},\frac{I_{1,k}^{max}}{\left|g_{s,1}\right|^2},\frac{I_{2,k}^{max}}{\left|g_{s,2}\right|^2},\cdots,\frac{I_{M,k}^{max}}{\left|g_{s,M}\right|^2}\right\}. \tag{2.3}$$

With $P_s^k = \bar{P}_s^k$,the optimization problem (2.2) is reduced to

$$OP2:$$

$$\max_{\substack{\{p_l\}_{l=1,2,..,L}\\ \{\varepsilon_{lk}\}_{k=1,2,..,K}}} \sum_{k=1}^{K}\frac{1}{2}\log_2\left[1+\frac{\bar{P}_s^k\left|h_{s,k}\right|}{N}+\frac{\bar{P}_s^k}{N}\frac{\left(\sum_{l=1}^{L}\frac{\varepsilon_{l,k}\left|h_{s,l}h_{l,k}\right|\sqrt{p_l}}{\sqrt{\bar{P}_s^k\left|h_{s,l}\right|^2+N}}\right)^2}{1+\sum_{l=1}^{L}\frac{\left|h_{l,k}\right|^2 p_l}{\bar{P}_s^k\left|h_{s,l}\right|^2+N}}\right] \tag{2.4}$$

subject to

$$C1, C2, C5, C6 \ \ of \ \ OP1$$

In the next section, we will present a low complexity sub-optimal algorithm for solving problem *OP*2.

2.2 Algorithm for Relay Assignment with Continuous Power

In this section, we present an iterative joint relay assignment and power allocation (IJRAPA) scheme for the multiuser CRS. The proposed IJRAPA is a two-phase algorithm. In the first phase, the algorithm, based on the channel conditions, assigns the relays to the secondary users. In the second phase, the algorithm iteratively allocates power to the relays. The Tables 2.2 and 2.3 show the pseudo code of the proposed algorithm.

2.2.1 Phase 1: Relay assignment

In this algorithm, the channel gains between the relays and the secondary users play a key role in relay assignment. For each relay *l*, the algorithm compares the channel gains from it to all secondary users, $|h_{l,1}|,|h_{l,2}|,\cdots,|h_{l,k}|,\cdots,|h_{l,K}|$. Then, the algorithm assigns relay *l* to the secondary user to which relay *l* has the best channel. That is, relay *l* is assigned to secondary user $\arg\max_{k\in\{1,2,..,K\}}|h_{l,k}|$. The Table 2.2 shows the pseudo code for relay assignment. First, we will describe the notation used in the pseudo code, and then we will describe the relay assignment algorithm.

We denote by *H* the $L\times K$ channel matrix and by L_k the set of relays assigned to *k*th user. At the start, the algorithm generates a vector $\Theta(l)=\arg\max_{k\in(1,2,..,K)} H(l,k),\ \forall l\in\Psi$ that contains the index of the secondary users that has highest channel gain with the relays. After getting the relay and secondary user pairs, the algorithm iteratively determines the subset of relays that are assigned to each secondary user −e.g., at the *k*th iteration, based on Θ, the algorithm gets the L_k subset of relays that are assigned to the *k*th user −i.e.,

$\varepsilon_{l,k}=1, \forall l \in L_k$. After getting the subset L_k, the algorithm iteratively allocates power to each relay in the subset L_k.

2.2.2 Optimization of Relay Transmission Power for a Given Relay Assignment

A relay assignment $\left\{\varepsilon_{l,k} \middle| l=1,2,..,L, k=1,2,...,K\right\}$ is also specified by subsets L_k, $k=1,2,...,K$. For a given relays assignment, power levels of the assigned relays can be optimized. The formulation of such an optimization problem is simply obtained by fixing $\left\{\varepsilon_{l,k} \middle| l=1,2,..,L, k=1,2,...,K\right\}$ in Problem *OP*2. That is,

$$OP2a:$$

$$\max_{\{p_l | l=1,2,..,L\}} \sum_{k=1}^{K} \frac{1}{2}\log_2\left[1+\frac{\bar{P}_s^k \left|h_{s,k}\right|}{N}+\frac{\bar{P}_s^k}{N}\frac{\left(\sum_{l\in L_k}\left|h_{s,l}h_{l,k}\right|\beta_l\sqrt{p_l}\right)^2}{1+\sum_{l\in L_k}\frac{\left|h_{l,k}\right|^2 p_l}{\bar{P}_s^k\left|h_{s,l}\right|^2+N}}\right]$$

$$subject\ to$$

$$\sum_{l\in L_k} p_l \left|g_{l,m}\right|^2 \le I_{m,k}^{max}, \quad \forall(m,k)$$

$$0 \le p_l \le p_l^{max}, \quad \forall l \in L_k, k=1,2,..,K$$

Problem *OP2a* has a nice separable structure, which is mainly attributed to the separation of frequency bands among different users k=1,2,...,K. Namely, in order to solve Problem *OP2a,* one can solve the following problem for k=1,2,...,K:

$$OP2a-k:$$

$$\max_{\{p_l|l\in L_k\}} \frac{1}{2}\log_2\left[1+\frac{\overline{P}_s^k\left|h_{s,k}\right|}{N}+\frac{\overline{P}_s^k}{N}\frac{\left(\sum_{l\in L_k}\left|h_{s,l}h_{l,k}\right|\beta_l\sqrt{p_l}\right)^2}{1+\sum_{l\in L_k}\frac{\left|h_{l,k}\right|^2 p_l}{\overline{P}_s^k\left|h_{s,l}\right|^2+N}}\right]$$

subject to

$$C1:\ \sum_{l\in L_k} p_l\left|g_{l,m}\right|^2 \le I_{m,k}^{max},\quad \forall(m)$$

$$C2:\ 0\le p_l\le p_l^{max},\quad \forall l\in L_k$$

Solving Problems *OP2a-k* for *k*=1,2,...,*K* is a divide-and-conquer approach to solving *OP2a* and is more efficient in terms of computational complexity. However, Problem *OP2a-k* is not a convex optimization problem. In the next subsection, we present an efficient suboptimal algorithm for solving Problem *OP2a-k.*

2.2.3 Phase 2: Power Allocation

In Problem *OP2a-k,* the objective is to maximize the capacity for secondary user *k*, and the high power gain of the channel $\left|h_{l,k}\right|^2$ from a relay *l* in L_k to user *k*'s receiver is favourable to the channel capacity for user *k*. On the other hand, the high power gain of the channel from relay *l* to primary users is not favourable because that adds interference to the primary users. For developing a heuristic optimization algorithm, we can view the channel gain from the *l*th relay to the *k*th secondary user $\left|h_{l,k}\right|^2$ as profit taken from investing unit transmission power to relay *l*. We also view channel gain from the *l*th relay to its primary users as loss. In particular, our algorithm views $\max\left(\left|g_{l,1}\right|^2,\left|g_{l,2}\right|^2,\cdots,\left|g_{l,M}\right|^2\right)$ as loss incurred from investing unit transmission power to relay *l*. At the start of the power allocation phase, the algorithm sorts the relays in the subset L_k according to the profit to loss ratio. After sorting, the algorithm greedily allocates power to

the relays in the subset L_k in the sorted order from the relay with the highest profit to loss ratio to the lowest.

Now, we will describe the algorithm in detail. Table 2.3 provides the pseudo code for power allocation routine for Problem *OP*2a-k. Initially, in this routine, the relays' powers are set to zero. We denote by Λ_p the set of relays whose power is already allocated. Initially Λ_p is empty. The algorithm allocates maximum power to that relay that has the maximum ratio of channel gains $h_{l,k}$ to the channel gain with the worst primary user. We define a function '*sortindex'* which sorts the relays according to the ratio $\frac{\left|h_{l,k}\right|^2}{\max\left(\left|g_{l,1}\right|^2,\left|g_{l,2}\right|^2,\cdots,\left|g_{l,M}\right|^2\right)}$ in descending order. The function '*sortindex'* returns a vector that consists of the relay indices according to the sorted values. The algorithm iterates over the relay indices in the sorted order. In each iteration, it stores one relay from the sorted relays to Λ_p.

The objective of Problem *OP*2a-*k* is in the form of

$$\frac{1}{2}\log_2\left[1+\frac{\overline{P}_s^k\left|h_{s,k}\right|}{N}+\gamma_k\right],$$

where $\gamma_k=\left(\frac{\left(\sum_l\left|h_{s,l}\right|\left|h_{l,k}\right|\beta_l\sqrt{p_l}\right)^2}{1+\sum_l\left(\beta_l\left|h_{l,k}\right|\sqrt{p_l}\right)^2}\right)$ and $\beta_l=\left(P_s^k\left|h_{s,l}\right|^2+N\right)^{-1/2}$, and the objective monotonically increasing with γ_k. Thus, we can solve *OP*2a-*k* by maximizing

$$\gamma_k=\left(\frac{\left(\sum_l\left|h_{s,l}\right|\left|h_{l,k}\right|\beta_l\sqrt{p_l}\right)^2}{1+\sum_l\left(\beta_l\left|h_{l,k}\right|\sqrt{p_l}\right)^2}\right).$$

We observe that γ_k is not increasing with respect to $p_l, \forall l \in L_k$. By taking $\frac{\partial \gamma_k}{\partial p_j}$, we observe that γ_k is non-decreasing with respect to p_j when $p_j \leq \left[\frac{|h_{s,j}| \left(1 + \sum_{l \neq j} \left(\beta_l |h_{l,k}| \right)^2 p_l \right)}{\beta_j |h_{j,k}| \left(\sum_{l \neq j} |h_{s,l}| |h_{l,k}| \beta_l \sqrt{p_l} \right)} \right]^2$ (see Appendix C). With the help of above observation, the power of the selected relay is determined using the equation

$$p_a = \min \left(\frac{I_{m,k}^{\max} - I_m^{Sum}}{g_{a,m}} \forall m, p_a^{max}, \left[\frac{|h_{s,a}| \left(1 + \sum_{l \neq a, l \in \Lambda_p} \left(\beta_l |h_{l,k}| \right)^2 p_l \right)}{\beta_a |h_{a,k}| \left(\sum_{l \neq a, l \in \Lambda_p} |h_{s,l}| |h_{l,k}| \beta_l \sqrt{p_l} \right)} \right]^2 \right)$$

The minimum of all three entries not only satisfies the interference and maximum power constraint but also ensures that the allocated power lies within the range of values for which the cost function is non-decreasing with respect to p_a. Then the algorithm determines the total interference generated by this allocated power. The algorithm continues until the set L_k becomes empty. The algorithm will terminate when all the users get their assigned relays.

Table 2.2 Iterative Joint Relay Assignment and Power Allocation (IJRAPA)

Main Algorithm	**Flops**
***Initialization*:** $H(l,k)=\left\|h_{l,k}\right\|^2 \ \forall (l,k)$	

$1:\Theta(l):=\underset{k\in(1,2,..,K)}{\arg\max} H(l,k) \ \ l=1,2,..,L$;
While $k \le K$
2: $L_k := \{l \mid \Theta(l)=k\}$
3: ***If*** $L_k \neq \varnothing$ ***Then***
Power Allocation Routine
Endif
EndWhile
***Output*:** Θ , $p_l, \forall l$
	1: LK
	
	2: K
	3: $K\left\|L_k\right\|^2(1+M)$
	$+2K\left\|L_k\right\|(1+M)$
	$+2KM$

Table 2.3 Power Allocation Routine

***Input*:** i=1,k, L_k, $g_{l,m}$, $h_{s,l}, h_{l,k}, I_m^{\max}, \beta_l \ \ \forall l \in L_k$	**Flops**
1: $p_l = 0, \forall l \in L_k, \ I_m^{Sum} = 0, \forall m, \Lambda_p = \varnothing, p^{Sum} = 0$	
2: $A = sortindex\left(\dfrac{\left\|h_{l,k}\right\|^2}{\max\left(\left\|g_{l,1}\right\|^2, \left\|g_{l,2}\right\|^2, \cdots, \left\|g_{l,M}\right\|^2\right)}, \forall l \in L_k\right)$	2: $\left\|L_k\right\|\log\left(\left\|L_k\right\|\right)$
While $i \le \left\|L_k\right\|$	
3: $a = A(i)$	3: 1
4: $\Lambda_p = \Lambda_p \cup \{a\}$;	4: 1
5: $p_a = \min\left(\left(\dfrac{I_m^{\max} - I_m^{Sum}}{g_{a,m}} \forall m\right), p_a^{max}, \left[\dfrac{\left\|h_{s,a}\right\|\left(1+\sum_{l\neq a, l\in\Lambda_p}\left(\beta_l\left\|h_{l,k}\right\|\right)^2 p_l\right)}{\beta_a\left\|h_{a,k}\right\|\left(\sum_{l\neq a, l\in\Lambda_p}\left\|h_{s,l}\right\|\left\|h_{l,k}\right\|\beta_l\sqrt{p_l}\right)}\right]^2\right)$	5: $2M+4\left\|L_k\right\|$ 6: $2M$ 7: 1
6: $I_m^{Sum} := I_m^{Sum} + p_a\left\|g_{l,m}\right\|^2 \ \ \forall m$;	
7: $i := i+1$	
EndWhile	
OutPut: $p_l \ \ \forall l \in L_k$	

2.2.4 Complexity Analysis

Tables 2.2 and 2.3 describe the complexity of proposed IJRAPA scheme. Complexity is measured in terms of flops Υ. A flop is defined as a real floating-point operation [8]. A real addition, multiplication or division is counted as one flop. A complex addition is counted as two flops and a complex multiplication has four flops. The multiplication of a *p*×*q* matrix with a *q*×*m* matrix takes approximately *2pqm* flops. Addition and removal of an element from a set takes one flop. The logical operator (e.g. comparison etc.) and assignment operator take one flop [8]. From Tables 2.2 and 2.3, we can observe that the IJRAPA takes approximately $K\left(M\left|L_k\right|^2+\left|L_k\right|\log\left(\left|L_k\right|\right)+2\left|L_k\right|+2M\left|L_k\right|+2\left|L_k\right|M\right)+2K+LK$ flops. To get the flop count Υ_{IJRAPA}, we set $\left|L_k\right|=L$. The flop count Υ_{IJRAPA} is

$$\begin{aligned}\Upsilon_{IJRAPA} &\approx K\left(ML^2+L\log\left(L\right)+2L+2ML+2LM\right)+2K+LK\\ &\approx O\left(KML^2\right)\end{aligned}$$

2.2.5 Performance Results with Continuous Power

As mentioned in section 2.1, for given realization of integer variables, the optimization problem in (2.2) is not a concave function of the relay powers due to the term $\gamma_k=\dfrac{\left(\sum_{l=1}^{L}\left|h_{s,l}h_{l,k}\right|\beta_l\sqrt{p_l}\right)^2}{1+\sum_{l=1}^{L}\left(\beta_l\left|h_{l,k}\right|\sqrt{p_l}\right)^2}$. Thus, even for a given realization of integer variables, convex optimization techniques cannot be applied to the resulting optimization problem. For comparison, we provide an upper bound on the sum-rate capacity of the relay assignment problem. The proposed upper bound is concave for a given realization of integer variables. The upper bound can be derived by using the Cauchy Schwarz inequality [5]

$$\frac{\left(\sum_{l=1}^{L}\left|h_{s,l}\right|\left|h_{l,k}\right|\beta_l\sqrt{p_l}\right)^2}{1+\sum_{l=1}^{L}\left(\left|h_{l,k}\right|\beta_l\sqrt{p_l}\right)^2} \le \frac{\left(\sum_{l=1}^{L}\left(\left|h_{s,l}\right|\right)^2\right)\sum_{l=1}^{L}\left(\left|h_{l,k}\right|\beta_l\right)^2 p_l}{1+\sum_{l=1}^{L}\left(\left|h_{l,k}\right|\beta_l\right)^2 p_l} \tag{2.5}$$

Appendix B shows that the upper bound is a concave function of relay powers. Fig. 2.2 shows the comparison of the upper bound (UB) with the exact values of the objective function. We consider the scenarios with relays power $p_l = \{P_s/10, P_s/50, P_s/100\}$. Fig.2.2 shows that the proposed bound is tight when the numbers of relays are less.

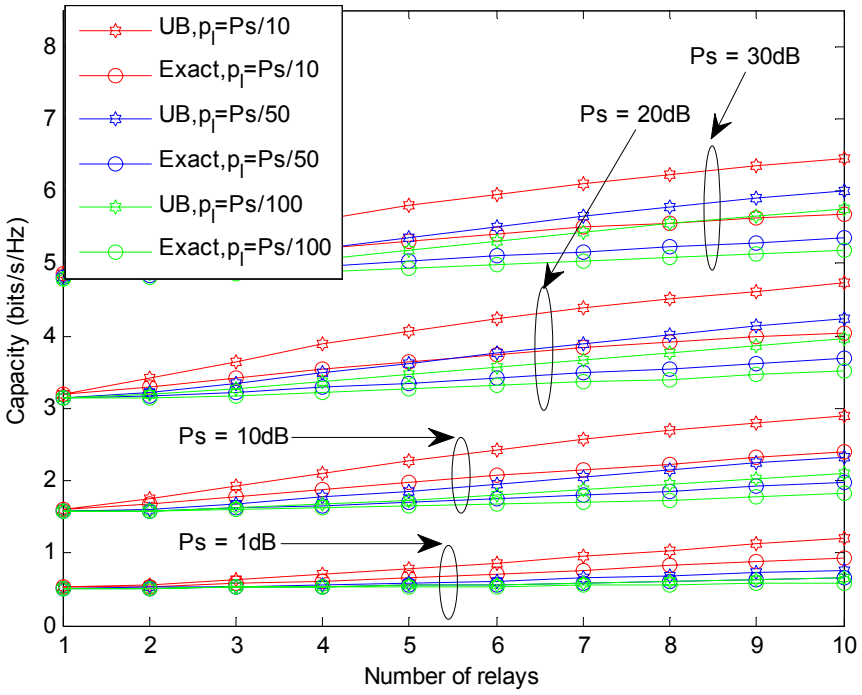

Fig. 2.2 Upper Bound on the AF channel capacity

We compare the proposed IJRAPA with exhaustive search algorithm that uses upper bound (ESA-UB) for power allocation. In ESA-UB, for each set of assigned relays, we run a convex optimization to allocate the relays power. We also include an iterative joint relay assignment algorithm that uses upper bound,

as mentioned in (2.5), for relays power allocation. We call this algorithm as iterative joint relay assignment with upper bound IJRA-UB. In IJRA-UB, relays are assigned using the algorithm mentioned in Table 2.2. For each set of assigned relays, the relays powers are allocated using conventional convex optimization techniques that uses upper bound as mentioned in (2.3). In the simulation results, the channel gains between source, relays and destinations have an independent complex Gaussian distribution.

In Fig. 2.3, we present the plot of sum-capacity versus the interference threshold with the parameters (*L, M, K*) = (6, 1, 3) for different $p_l^{\max}$. There are two scenarios with $p_l^{\max}$ = {1, 10} watts. We assume that each user's occupies a band of bandwidth 1 MHz. The results show that the performance of IJRAPA is close to that of ESA-UB and IJRA-UB. The Fig. 2.3 also show that the sum-capacity increases with the interference threshold because the feasible set of the optimization problem with lower interference threshold is a subset of the feasible set of the optimization problem with higher interference threshold. In Fig. 2.4, we present the plot of sum-capacity versus the interference threshold for different numbers of relays and primary users. We use the scenario (*L*,*M*,*K*) = (6,1,3) and (3,3,3). The results show that the performance of IJRAPA is close to that of ESA-UB and IJRA-UB. We observe that the sum-capacity increases with the number of relays as more relays mean more degrees of freedom in relay assignment. We also observe that the sum-capacity decreases with the increase in the number of primary users because the optimization problem has more number of constraints to satisfy. In Fig. 2.5, we present the plot of sum-capacity versus number of primary users. The parameters are (*L*, *K*) = (5, 3). Fig. 2.5 shows the variation in sum-capacity with the increase in the number of primary users. In this result, we observe that sum-capacity decreases as the number of primary users increase. This is because the relay assignment needs to satisfy more interference constraints as the number of primary users increases.

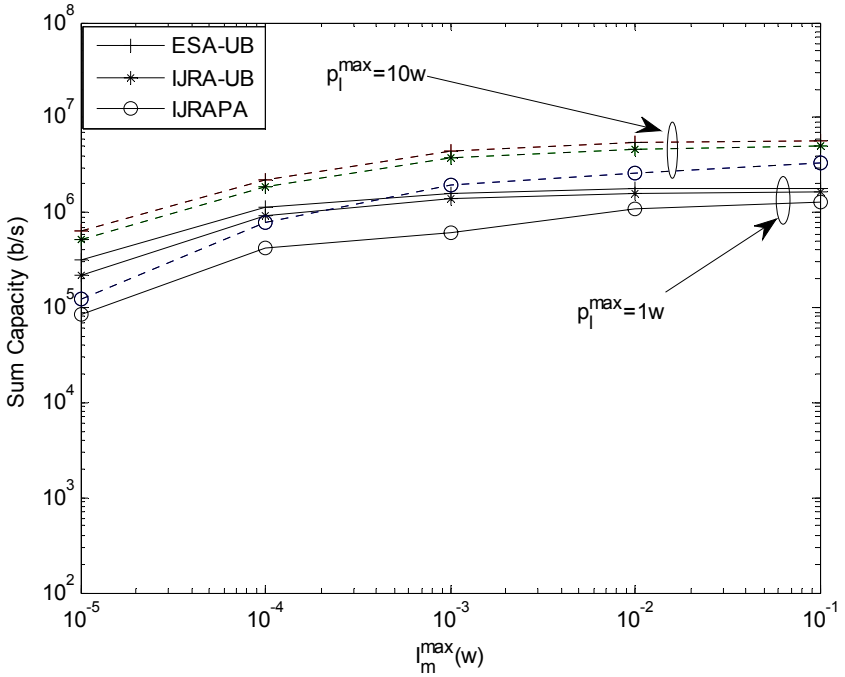

Fig. 2.3 Sum-rate capacity vs. Interference comparison. The parameters are L = 7, K = 3,M = 1, $p_s = 10\text{w}, p_l = \{10\text{w}, 1\text{w}\}$

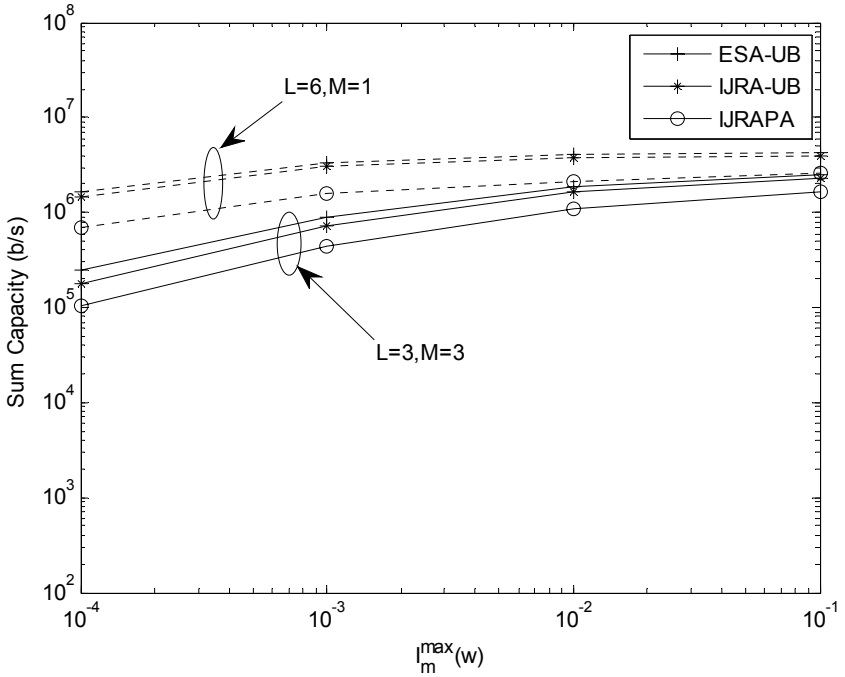

Fig. 2.4 Sum-rate capacity vs. Interference comparison. The parameters are K = 3, $p_s = 10\text{w}$, L = {6,3}, M = {1,3}

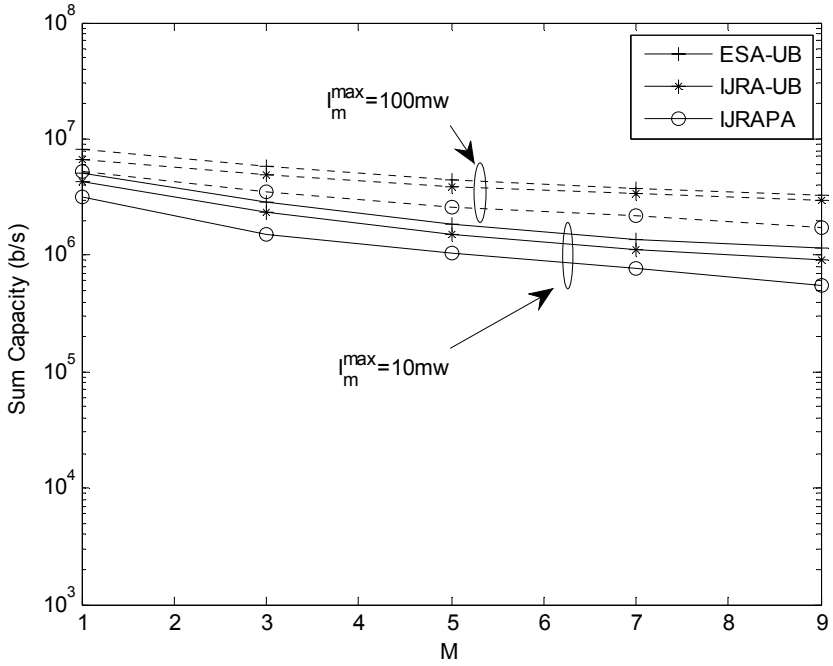

Fig. 2.5 Sum-rate capacity vs. number of primary user's comparison. The parameters are *L = 5, K* = 3, $I_{m,k}^{\max} = \{10mw, 1mw\}$

2.3 Algorithm for Relay Assignment with Discrete Power Allocation

The use of continuous relay power can lead to inefficient utilization of the available bandwidth as more number of control bits may be required to express the assigned relay power. Discrete power allocation (DPA) helps in simplifying the end-to-end control channel traffic. The assumption of DPA is also relevant to the networks, which deploy low cost relays that do not have sophisticated circuitry to support transmissions on arbitrary power levels.

In this work, we consider inexpensive relays that can operate only at a finite number of transmission power levels. Let P_L be the set of relay power levels comprising $\lambda+1$ uniformly spaced discrete power levels −i.e., $P_L = \left\{0, \frac{p_l^{max}}{\lambda}, \frac{2p_l^{max}}{\lambda}, ..., p_l^{max}\right\}$. We denote by $|P_L|$ the cardinality of set P_L. For discrete power allocation, the problem OP2 is changed to

$OP3:$

$$\max_{\substack{\{p_l \mid l=1,2,..,L \\ \varepsilon_{lk} \mid k=1,2,..,K}} \sum_{k=1}^{K} \frac{1}{2} \log_2 \left[1 + \frac{\overline{P}_s^k \left| h_{s,k} \right|}{N} + \frac{\overline{P}_s^k}{N} \left(\frac{\left(\sum_{l=1}^{L} \varepsilon_{l,k} \left| h_{s,l} h_{l,k} \right| \beta_l \sqrt{p_l} \right)^2}{1 + \sum_{l=1}^{L} \left(\beta_l \left| h_{l,k} \right| \sqrt{p_l} \right)^2} \right) \right] \tag{2.6}$$

subject to

$$C1, C2, C5, C6 \ \ of \ \ OP1$$

$$C7: \ \ p_l \in P_L, \forall l$$

The proposed multiple relay assignment and discrete power allocation in *OP*3 is a non-convex non-linear integer programming problem. An exhaustive search algorithm for *OP*3 evaluates all the possible relay assignments power levels. The computational complexity of the optimal relay assignment algorithm (e.g. exhaustive search algorithm) increases exponentially with the number of relays and power levels. For efficient relay assignment and discrete power allocation in the multiuser CRS, we propose a low-complexity interference aware greedy assignment (IAGA) algorithm. The proposed algorithm, in each iteration, assigns a relay or a set of relays to the secondary user that gives maximum SNR and satisfies the interference constraints at the primary users.

2.3.1 IAGA for Discrete Power Allocation

One of the basic ideas in designing this algorithm is that we assign a relay to the secondary user *k* only if the channel between that relay and the secondary user *k* is best among all the secondary users and the relay satisfies the interference constraint at all M primary users. In order to make the description of this algorithm clear, we will use an example system and often interject an illustration from this example system in our algorithm description. Tables 2.4 and 2.5 present the pseudo code and examples of IAGA respectively (For better understanding of the algorithm, a flow diagram of IAGA is also shown in appendix D). In the example of Table 2.5, we consider a system comprising three secondary users K_1, K_2 and K_3, two primary users M_1, M_2, and seven relays

L_1, L_2, … ,L_7. The interference thresholds of primary users M_1 and M_2 is 10mw and 20mw in each secondary user's band respectively.

The IAGA is performed in two stages. At stage 1, the algorithm determines the transmission power, p_l, of each relay *l* and computes some other quantities for stage 2. Let us denote by $\eta(p,l,m) \equiv p\left|g_{l,m}\right|^2$ the interference caused by relay *l* on primary user *m* with power p_l. In stage 1, the algorithm sets the transmission power, p_l, of each relay *l* to

$$p_l^* := \max\left\{p \in P_L \mid \eta(p,l,m) \equiv p\left|g_{l,m}\right|^2 \le I_{m,k}^{max} \forall (m,k)\right\}$$

Note that $p_l\left|g_{l,m}\right|^2$ can be interpreted as the interference the *l*th relay would cause on primary user *m* if no other relay were transmitting at that time. In words, the algorithm at stage 1 sets the transmission power of each relay as high as possible with the constraint that the interference it individually causes on each primary user is within its interference constraint (interference tolerance level). Note that such a transmission power level for some relay can be '0' if every positive power value in set P_L individually causes interference on some primary user above its tolerance level. The relays with power level set to '0' are removed from consideration; it means at the end of stage one, the algorithm selects the relays that individually satisfy the interference constraints at all the primary users. We denote the set of selected relays as Ψ. For each of these selected relays and power levels, the algorithm evaluates the individual SNR contribution by each relay at each secondary user −that is, the individual SNR that each secondary user would have if it does not receive a signal from the source or other relays. These SNR contributions from the relays are stored in matrix Λ. Table 2.5(a) illustrates the values stored in matrix Λ. The algorithm then calculates the aggregated or sum−interference, $\Gamma^l \equiv \sum_{m=1}^{M} \eta(p_l^*,l,m)$, from each relay to the primary users. Table 2.5(a) illustrates the transmission power levels of all the relays determined as p_l^*, the individual SNRs in Λ, and the individual

interferences $\eta\left(p_l^*, l, m\right)$ computed in stage 1. Note that relay L_7 is removed from further consideration for assignment in subsequent steps as its individual interference contribution violates the interference constraints.

In stage 2, at each iteration, the algorithm determines the set of relays assigned to a secondary user in a greedy manner. For clarity of exposition, we now use our example system to illustrate the steps of stage 2. From Table 2.5(a), for each relay, we select the user where it generates its maximum individual SNR− e.g., relay L_1 generates maximum SNR at user K_1 as we have $\Lambda(1,1) = 8 > 3 = \Lambda(1,2)$ and $\Lambda(1,1) = 8 > 5 = \Lambda(1,3)$. As mentioned earlier, we assign a relay to the secondary user *k* only if that relay has the best channel to the user *k* among all the secondary users. Thus, in Table 2.5(b) for each relay, we retain the SNR value of that relay/user pair where the relay has the best channel gain. The selection of relay/user pair from Table 2.5(a) in this manner results in Table 2.5(b), where e.g. for relay L_1 the bins for $\Lambda(1,2)$ and $\Lambda(1,3)$ are blanked. Among these selected relay/user pairs, the pair that has the highest SNR value is chosen and the corresponding user is denoted as $\tilde{k}$. For illustration, in Table 2.5(b), $\Lambda(2,3)$ has the highest individual SNR among all entries of Λ and $\tilde{k} = K_3$. The relays whose individual SNR contributions are maximum at user $\tilde{k}$ can be potentially assigned to that user. From Table 2.5(b), these relays are L_1, L_5 and L_6 and they constitute the set *R*. Then, the algorithm checks whether the cumulative interference level generated by these three relays at the primary users is below the required tolerance level. We observe from Table 2.5(b) that the cumulative interference from these three relays violates the interference threshold of M_1 −i.e., $\Delta_1 = \eta(p_1^*,1,1) + \eta(p_5^*,5,1) + \eta(p_6^*,6,1) = (8+1+6) > I_1^{max}(10)$. In this algorithm, if the relays in set *R* violate the interference constraints at any of the primary users, then the relay with the highest sum interference $\Gamma^l = \sum_{m=1}^{M} \eta\left(p_l^*, l, m\right)$ is removed from further consideration for relay assignment. From Table 2.5(b), it is observed that relay L_6 has the highest sum interference

among the relays in set *R* as sum interferences from L_2, L_5, and L_6 are 8+5 = 13, 3+1 = 4 and 6+10 = 16 respectively. Therefore, relay L_6 is removed from set *R* and Ψ. Since the remaining relays, L_2 and L_5, together satisfy the interference constraints, they are both assigned to the user K_3 as done in Table 2.5(c). The relays and users that have been already assigned are no longer considered for the rest of the algorithm, as illustrated by the blanks in Table 2.5(c). These steps are repeated until all the remaining relays are assigned or removed from consideration. The subsequent steps are illustrated in tables 2.3(c) − 2.3(f).

We now present a step-by-step description of the pseudo code of stage 2 given in Table 2.4. In line 2 of stage 2 in Table 2.4, for each relay a user, that receives the maximum SNR from it, is chosen and stored in the variable Θ as

$$\Theta(l) := \arg\max_{k \in (1,2,..,K)} \Lambda(l,k) \quad \forall l \in \Psi$$

Line 3 determines the relay-secondary user pair that has the maximum SNR which is mathematically expressed as

$$\overline{\Lambda} := \max\left\{\Lambda(1,\Theta(1)), \Lambda(2,\Theta(2)), ..., \Lambda(L,\Theta(L))\right\}$$

In line 4, the user $\tilde{k}$ which has the highest SNR is determined as $\tilde{k} = \Theta(l) \;\; s.t. \;\; \Lambda(l,\Theta(l)) = \overline{\Lambda}$. The relays that generate maximum SNR at user $\tilde{k}$ are determined from the set Θ and stored in the set *R* in line 5.

In lines 6-15 of stage 2, the algorithm iterates over the relays in the set *R*. In each iteration, for every primary user *m* the sum of the interference levels generated by the relays in the set *R* (on primary user *m*) is evaluated as $\Delta_{m,\tilde{k}} := \sum_{r \in R} \eta\left(p_r^*, r, m\right), \; \forall m$. If the interference constraints, $\Delta_{m,\tilde{k}} \le I_{m,\tilde{k}}^{max}, \forall m$ are satisfied then the capacity of the user $\tilde{k}$ is calculated for the relays in set *R*, the assigned relays are removed from the sets R and Ψ. If the interference constraint is violated at any primary user then we choose the relay *r* (from the set *R*) that

causes maximum sum interference (as given by Γ^r). The selection of relay *r* is mathematically written as $r := \arg\max_{l \in R} \Gamma^l$. The selected relay *r* is removed from the set *R* and Ψ. Note that the retention of relay *r* in the set Ψ may increase the capacity of the system but it also increases the complexity of our algorithm. By the end of first iteration over the set Ψ, the user $\tilde{k}$ has its assigned relays. Lines 2-16 are repeated till $\Psi = \varnothing$.

Table 2.4 IAGA

IAGA	Flops
INITIALIZATION: $\Lambda(l,k) = 0 \ \forall (l,k), \Gamma^l = 0 \ \forall (l), C_k = 0, \forall k, \Psi = \varnothing$	
STAGE 1: 1***:For*** *l*=1 *to L* 2: $p_l^* := \max\left\{p_l \in P_L \mid \eta(p_l,l,m) \equiv p_l \left\|g_{l,m}\right\|^2 \le I_{m,k}^{max} \forall (m,k)\right\}$ 3: ***If*** $p_l^* \neq 0$ 4: $\Lambda(l,k) = \frac{p_l^*}{N}\left\|h_{l,k}\right\|^2$; 5: $\Gamma^l = \sum_{m=1}^{M} \eta(p_l^*,l,m)$; 6: $\Psi := \Psi \bigcup \{l\}$; 7: ***else*** 8: $\eta(p_l^*,l,m) = 0$; 9: ***EndIf*** 10:***EndFor***	2: $2M\left\|P_L\right\|$ 3: *1* 4:*2K* 5:*M* 6:1 8:1
STAGE 2: 1: ***While*** $\Psi \neq \varnothing$ 2: $\Theta(l) = \arg\max_{k \in (1,2,..,K)} \Lambda(l,k) \quad \forall l \in \Psi$; 3: $\bar{\Lambda} = \max\left\{\Lambda(1,\Theta(1)), \Lambda(2,\Theta(2)), ..., \Lambda(L,\Theta(L))\right\}$; 4: $\tilde{k} = \Theta(l) \ s.t. \ \Lambda(l,\Theta(l)) = \bar{\Lambda}$ 5: $R = \{l \mid \Theta(l) = \tilde{k}\}$ 6: **While** $R \neq \varnothing$ 7: $\Delta_m = \sum_{r \in R} \eta(p_l^*,l,m), \ \forall m$ 8: ***if*** $\Delta_{m,\tilde{k}} \le I_{m,\tilde{k}}^{\max}, \forall m$ 9: $C_{\tilde{k}}$ = *Apply Eq. (2.1) for R*; 10: $\Lambda(l,\tilde{k}) = 0, \forall l$, , $\Psi = \Psi \setminus R$ and *Goto* 1*:* 11: ***else*** 12: $r = \arg\max_{l \in R} \Gamma^l$; 13: $\eta(p_r^*,r,m) = 0$; $\Gamma(r) = 0$; *R* := *R* \ *r*, $\Psi := \Psi \setminus r$; 14: ***EndIf*** 15: ***EndWhile*** 16: $\Lambda(l,\tilde{k}) = 0, \forall l$ 17:***EndWhile***	2:*KL* 3:*K* 4:*L* 5:1 6: *LM* 7: *M* 8: $11L^2$ 9: *M* 12: *L*
OUTPUT: $\sum_{k=1}^{K} C_k$	*K*

Table 2.5 Example of IAGA

Symbol '−' represents a relay that can be assigned and '×' represents a relay that has been removed from consideration from further relay assignment

First Iteration							Second Iteration					
	p_l^*	Λ			$\eta(p_l^*,l,m)$			Λ			$\eta(p_l^*,l,m)$	
		K_1	K_2	K_3	M_1	M_2		K_1	K_2	K_3	M_1	M_2
L_1, −	p^{max}	8	3	5	6	13	L_1, −	8			6	13
L_2, −	p^{max}	15	18	50	8	5	L_2, −			50	8	5
L_3, −	$\frac{3p^{\max}}{\lvert P_L \rvert}$	49	23	44	2	7	L_3, −	49			2	7
L_4, −	p^{max}	8	39	2	10	15	L_4, −		39		10	15
L_5, −	p^{max}	20	22	26	1	1	L_5, −			26	1	1
L_6, −	$\frac{p^{max}}{\lvert P_L \rvert}$	9	1	40	6	10	L_6, −			40	6	10
L_7, ×	0						L_7, ×					
(a) Illustration of Stage1 of IAGA, Columns K_1, K_2 and K_3, denote individual SNR contribution of each relay at secondary user K_1-K_3 respectively. Column 1 (p_l^*) and 5 (M_1,M_2) denote the interference contributed by each relay individually at each primary user and the selected power level of each relay respectively.							(b) Selection of user $\tilde{k}=K_3$ and relays to be assigned to user $\tilde{k}$ i.e. set $R = \{L_2, L_5, L_6\}$.					

Third Iteration						Fourth Iteration					
	Λ			$\eta(p_l^*,l,m)$			Λ			$\eta(p_l^*,l,m)$	
	K_1	K_2	K_3	M_1	M_2		K_1	K_2	K_3	M_1	M_2
L_1, −	8			6	13	L_1, −	8			6	13
L_2, K_3						**L_2, K_3**					
L_3, −	49			2	7	L_3, −	**49**			2	7
L_4, −		39		10	15	L_4, −		39		10	15
L_5, K_3						**L_5, K_3**					
L_6, ×						L_6, ×					
L_7, ×						L_7, ×					
(c)Relays L_2 and L_5 are assigned to user $\tilde{k} = K_3$. Relay L_6 is removed from set R due to violation of interference constraints at M_1						(d) Selection of user $\tilde{k}=K_1$ and relays to be assigned to user $\tilde{k}$ i.e. set $R = \{L_1, L_3\}$.					

Fifth Iteration						Sixth Iteration					
	Λ			$\eta(p_l^*,l,m)$			Λ			$\eta(p_l^*,l,m)$	
	K_1	K_2	K_3	M_1	M_2		K_1	K_2	K_3	M_1	M_2
L_1, K_1						L_1, K_1					
L_2, K_3						L_2, K_3					
L_3, K_1						L_3, K_1					
$L_4, -$		39		10	15	L_4, K_2					
L_5, K_3						L_5, K_3					
$L_6, \times$						$L_6, \times$					
$L_7, \times$						$L_7, \times$					
(e) Relays L_1 and L_3 are assigned to user K_1. In the next iteration user $\tilde{k}=K_2$ is selected and the relay in set R is L_4						(f) Relay L_4 is assigned to user $\tilde{k}=K_2$.					

2.3.2 Fairness aware IAGA

In this subsection, we modify the IAGA to consider the fairness in the relay assignment. We use access proportional fairness (APF) and rate proportional fairness (RPF) schemes for relay assignment [6]. In APF, all the secondary users will get approximately same number of assigned relays, i.e., each user will get $\lfloor L/K \rfloor$ relays. To incorporate APF in our formulations, we need to add one more constraint to the optimization problems *OP*1, *OP*2 and *OP*3. Mathematically:

$$\sum_{l=1}^{L} \varepsilon_{l,k} \geq \left\lfloor \frac{L}{K} \right\rfloor, \qquad \forall k = 1,2,\cdots,K$$

For APF, a little change is required to the stage 2 of IAGA. In stage 2, if any user is assigned $\lfloor L/K \rfloor$ number of relays then that user cannot be assigned any more relays. The rest of the algorithm is same as IAGA.

In RPF, every secondary user *k* gets a rate proportional to its weight factor α_k. In RPF, we compute the capacity ratio $A(k) = \frac{C_k}{\sum_{k=1}^{K} C_k \alpha_k}$. We find the

user that has minimum capacity ratio $\tilde{k} = \arg\min_{k=1,2,\ldots,K} A(k)$. We select a relay that gives maximum SNR to the user $\tilde{k}$ and individually satisfies the interference constraint at all the primary users. The selected relay is then assigned to user $\tilde{k}$. For fairness comparison, we are using Jain's fairness index as performance metric [7]. The Jain's fairness index is defined as

$$Jain's\ Fairness\ Index = \frac{\left[\sum_{k=1}^{K} C_k\right]^2}{K\sum_{k=1}^{K}\left[C_k\right]^2}$$

2.3.3 Complexity Analysis

The main advantage of the proposed algorithm is its low implementation complexity. In this section, we will compare the complexity of the proposed algorithm (IAGA) with the exhaustive search algorithm (ESA), which achieves an exactly optimal solution.

Table 2.4 describes the complexity of IAGA operations. First, we will describe the complexity of the objective function and the constraints. The term inside the log in equation (2.1) requires approximately 11*L* flops. The interference constraint for each primary user requires $2L|P_L|$ flops. The sum interference $\sum_{m=1}^{M}\eta(p_l^*, l, m)$ for each relay requires *M* flops. IAGA takes approximately $L(3M|P_L| + 2K + M + 2)$ flops for first stage and $11L^3 + L^2(K + 2M + 2) + L(K + 1)$ for second stage. Therefore the total number of flops Υ_{IAGA} require by IAGA is

$$\begin{aligned}\Upsilon_{IAGA} &\approx 11L^3 + L^2(K + 2M + 2) + L(3M|P_L| + 3K + M + 3) \\ &\approx O\left(L^3 + L^2K + L^2M\right)\end{aligned} \tag{2.7}$$

From the above complexity analysis, we conclude that IAGA has a polynomial-time complexity with respect to number of relays and number of secondary users. The computational complexity of ESA is $O\left(K^L\right)$.

2.3.4 Relay Assignment Results with Discrete Power Levels

We present the simulation results of the proposed IAGA. The performance of proposed IAGA algorithm is compared with 1) exhaustive search with upper bound (ESA-UB), 2) exhaustive search with discrete power allocation (ESA-Discrete) and 3) one-to-one exhaustive search assignment. For ESA-UB, a conventional convex optimization technique is used to determine the power of all the relay assignment subsets. The disadvantage of this approach is that for ESA we have to compute power allocation over all the possible relay assignments. One-to-one ESA obtains an optimal solution for one-to-one relay assignment. One-to-one relay assignment is formulated by adding an additional constraint in *OP3* where a user can only get data from one relay i.e. $\sum_{l=1}^{L} \varepsilon_{l,k} = 1 \forall k$ and a relay can send data to only one user i.e. $\sum_{k=1}^{K} \varepsilon_{l,k} = 1 \forall l$. Comparison between IAGA and one-to-one ESA helps us to show the effect of multiple relay assignments in the cognitive radio system. In the simulation results, the channel gains between source, relays and destinations have an independent complex Gaussian distribution.

In Figs. 2.6 and 2.7, we present the plot of sum-capacity versus interference threshold, $I_{m,k}^{\max}$. We used the scenarios (L, K, M, $\lambda, P_s^{max}, p_l^{max}$) = (6, 4, 4, 1, 10w, 1w) and (5, 3, 4, 2, 10w, 1w) . Bandwidth assign to each user is 1 MHz. We observe that sum-capacity increases with the interference threshold because a feasible set of the optimization problem with lower interference threshold is a subset of a feasible set of the optimization problem with higher interference threshold. In Figs. 2.8 and 2.9, we present the sum-capacity versus the number of relays. We used two different scenarios (K, M, $\lambda, P_s^{max}, p_l^{max}$, $I_{m,k}^{\max}$) = (4, 1, 1, 10w, 1w, 10mw) and (2, 4, 2, 10w, 5w, 1mw). From these results, we

observe that the sum-capacity increases with the number of relays. This is because more relays in the system give more degrees of freedom in assigning the relays to the secondary users. In Fig. 2.10, we present the sum-capacity versus number of primary users. The parameters are (*L*, *K*, $\lambda, P_s^{max}, p_l^{max}, I_{m,k}^{\max}$) = (5, 2, 1, 10w, 1w, 1mw). Fig. 2.10 illustrates the variation in sum-capacity with the increase in the number of primary users. In this result, we observe that sum-capacity decreases as the number of primary users increases. This is because the relay assignment needs to satisfy more interference constraints as the number of primary users increases. From the numerical results, Figs 2.13 and 2.14 and Tables 2.6 and 2.7, we can see that IAGA converges to with in 86 percent of that obtained by ESA-Discrete algorithm at low interference threshold and 96 percent at high interference threshold.

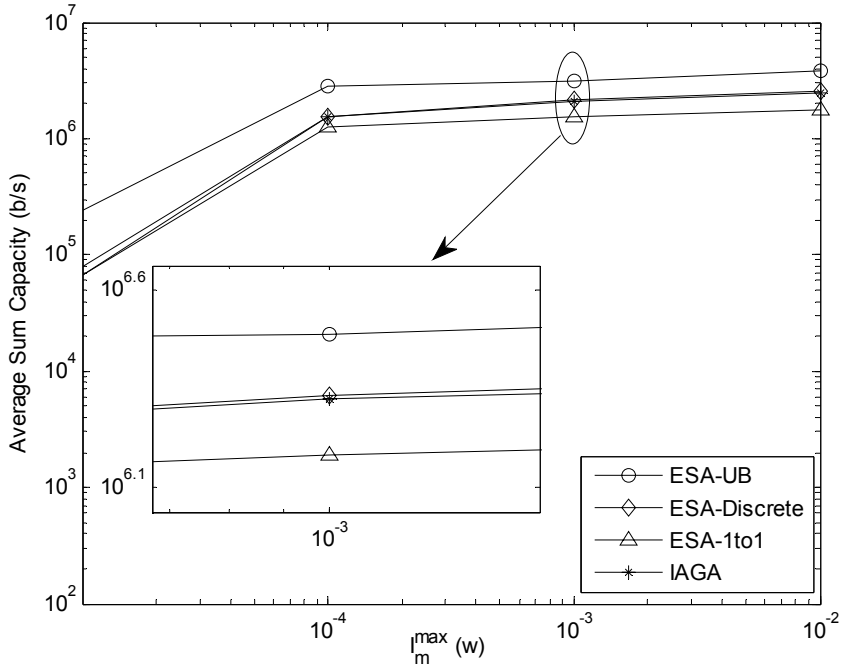

Fig. 2.6 Sum-capacity vs. maximum interference threshold to primary users with *L*=6, *K*= 4, *M*= *4,* $\lambda = 1$, P_s^{max} =*10w* and $p_l^{max} = P_s^{max}/10$, $p_l \in \left\{0, p_l^{max}\right\}\ \forall l$

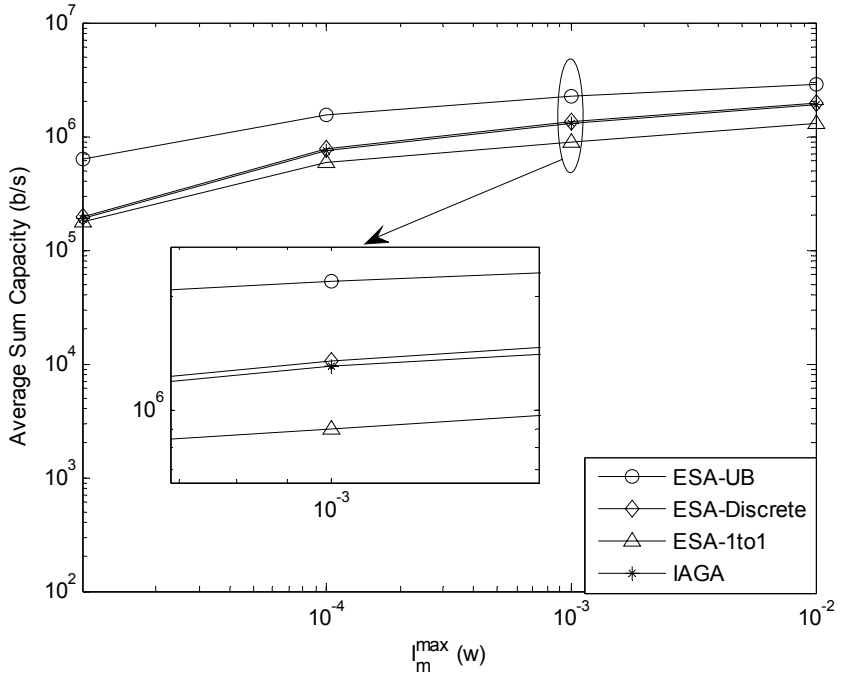

Fig. 2.7 Sum-capacity vs. maximum interference threshold to primary users with *L*=5, *K*=3, *M*= *4*, $\lambda = 2$, P_s^{max} =*10w*, $p_l^{max} = P_s^{max}/10$, $p_l \in \left\{0, p_l^{max}/2, p_l^{max}\right\}$

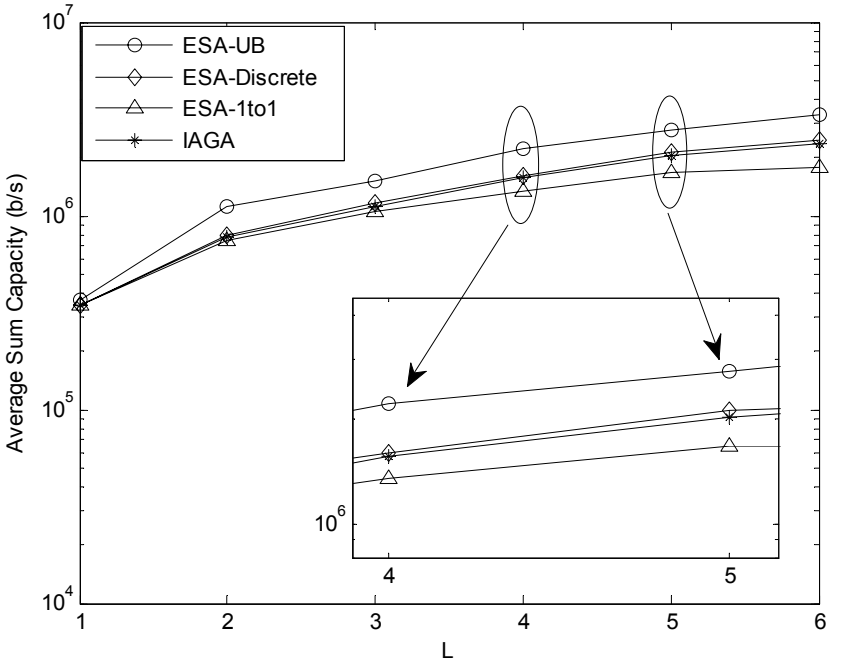

Fig. 2.8 Sum-capacity vs. number of relays with K = 4, M= 1, $\lambda = 1$, P_s^{max} =10w, $p_l^{max} = P_s^{max}/10$, $p_l \in P_L = \left\{0, p_l^{max}\right\}$ $\forall l$ and $I_{m,k}^{max}$ = 10mw $\forall m$

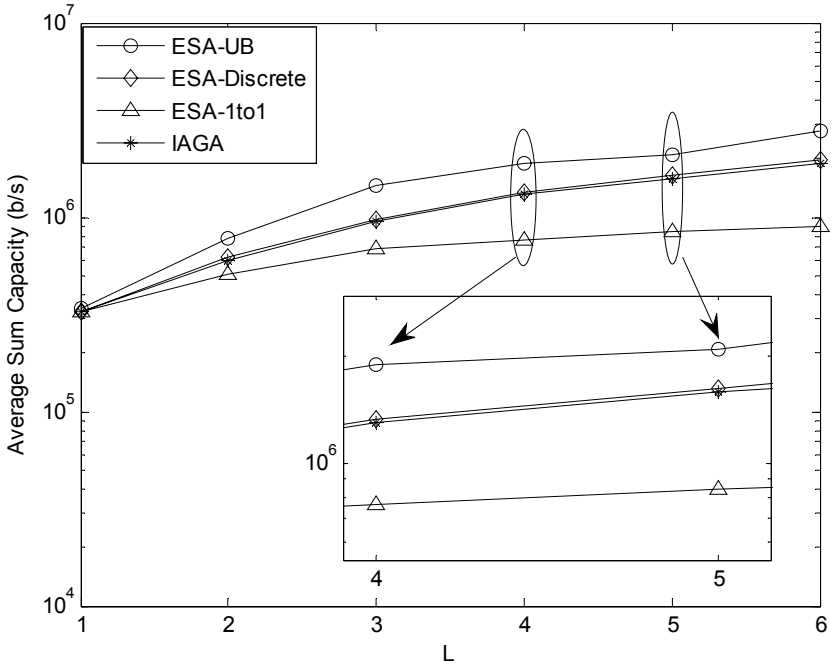

Fig. 2.9 Sum-capacity vs. number of relays with K = 2, M= 2, $\lambda = 2$, P_s^{max} =10watt, $p_l^{max} = P_s^{max}/10$, $p_l \in \left\{0, p_l^{max}/2, p_l^{max}\right\} \forall l$ and $I_{m,k}^{max}$ = 1mw $\forall m$

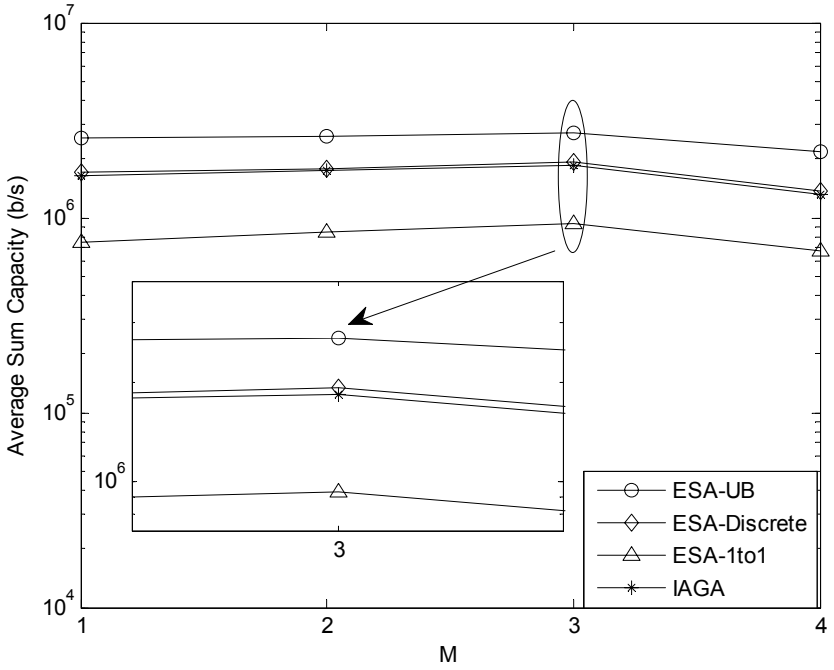

Fig. 2.10 Sum-capacity vs. number of primary users with K = 2, L= 5, $\lambda = 1$, P_s^{max} =10watt, $p_l^{max} = P_s^{max}/10$, $p_l \in \left\{0, p_l^{max}\right\} \forall l$, and $I_{m,k}^{max}$ = 1mw $\forall m$

In Figs. 2.11 and 2.12, we present the results of the proposed IAGA with access proportional fairness (APF) and rate proportional fairness (RPF). In these Figs., y-axis shows the capacity of each secondary user and the x-axis presents the index of each secondary users. We compare the IAGA with IAGA-RPF and IAGA-APF. We use two scenarios (*M*, *K*, $\lambda, P_s^{max}, p_l^{max}$, $I_{m,k}^{\max}$, α_k) = (10, 10, 1, 5w, 0.5w, 1mw,*1/K*) and (10, 10, 1, 10w, 1w, 10mw,*1/K*). For Fig. 2.11 (a) and (b), the fairness index for (IAGA, IAGA-APF, IAGA-RPF) are (0.4174, 0.6698, 0.6417) and (0.7438, 0.9159, 0.8929) respectively. Similarly, for Fig. 2.12 (a) and (b), the fairness index for (IAGA, IAGA-APF, IAGA-RPF) are (0.3733, 0.6727, 0.7465) and (0.746, 0.9684, 0.9440) respectively. The fairness index shows that IAGA- APF and IAGA-RPF fairness is higher than simple IAGA without fairness.

To check the feasibility of the proposed algorithms for practical implementation, in Table 2.8, we present the number of flops required by ESA, IAGA, and IJRAPA for different parameter settings (i.e., different search space size). The comparison shows that the number of flops required by IAGA and IJRAPA algorithms is much less than that of ESA.

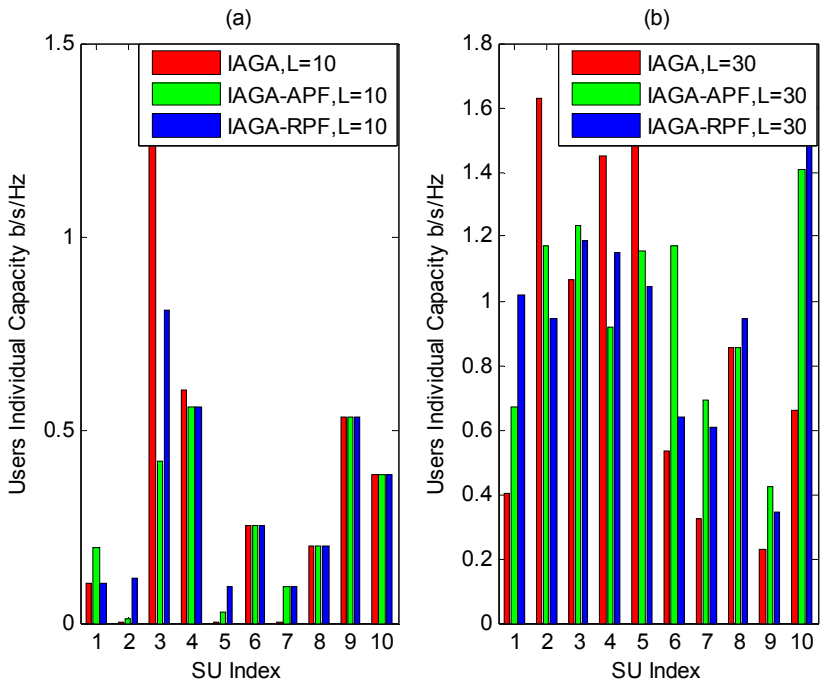

Fig. 2.11 User's individual capacities vs. user index with K = 10, M= 10, $\lambda = 2$, P_s^{max} =10w, $p_l^{max} = P_s^{max}/10$, and $I_{m,k}^{max}$ = 10mw for $\forall m$

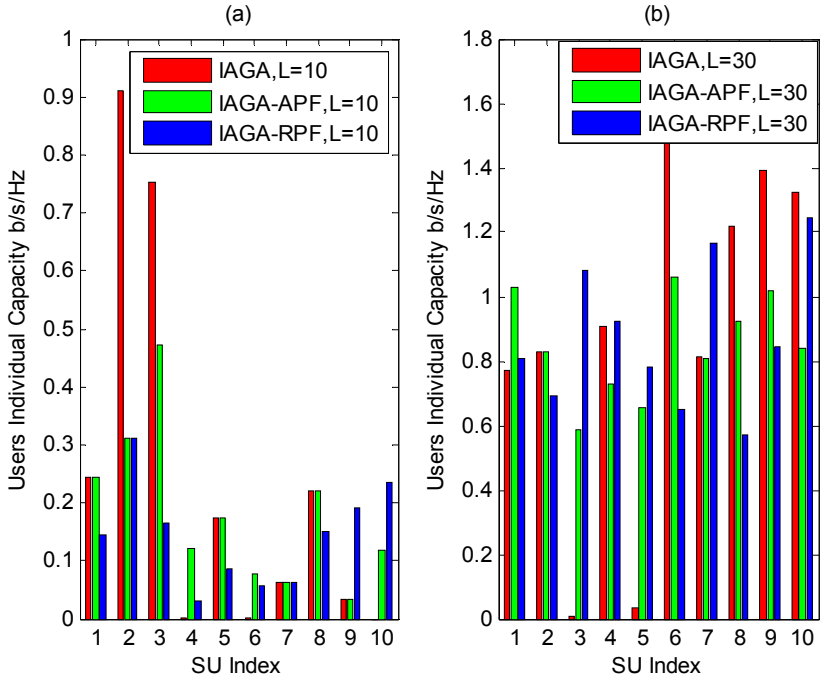

Fig. 2.12 User's individual capacities vs. user index with K = 10, M= 10, $\lambda = 4$ P_s^{max} =5w, $p_l^{max} = P_s^{max}/10$, and $I_{m,k}^{max}$ = 1mw for $\forall m$

Table 2.6 Percentage IAGA performance to ESA-Discrete for different $I_{m,k}^{\max}$

Parameters [K,L,M,λ]	$I_{m,k}^{\max}=10^{-5}$	$I_{m,k}^{\max}=10^{-4}$	$I_{m,k}^{\max}=10^{-3}$	$I_{m,k}^{\max}=10^{-2}$
[4,6,4,1] (Fig. 2.6)	86.57%	98.97%	98.72%	98.70%
[3,5,4,2] (Fig. 2.7)	96.64%	97.09%	96.25%	96.26%

Table 2.7 Percentage IAGA performance to ESA-Discrete for different *L*

Parameters [K,M,λ, $I_{m,k}^{\max}$]	**L = 2**	**L = 3**	**L = 4**	**L = 5**	**L = 6**
[4,4,1,10mw] (Fig.2.8)	97.81%	97.74%	96.83%	96.13%	95.80%
[3,4,2,1mw] (Fig. 2.9)	97.44%	98.54%	97.82%	97.78%	95.67%

Table 2.8 Number of flops required by ESA, IAGA and IJRAPA

Parameters [K,L,M,λ]	**ESA**	**IAGA**	**IJRAPA**
[5,5,1,5]	3125	395	1710
[8,5,10,16]	32768	3296	4710
[10,5,1,1]	100000	790	1910
[10,10,1,1]	1.0000e+010	2540	12770
[10,10,4,8]	1.0000e+010	6200	14330
[20,10,1,1]	1.0240e+013	5080	14070
[30,10,1,1]	5.9049e+014	7620	15370
[30,20,1,1]	3.4868e+029	27120	103540
[30,30,1,1]	2.0589e+044	58620	330510
[30,30,10,16]	2.0589e+044	318360	361290

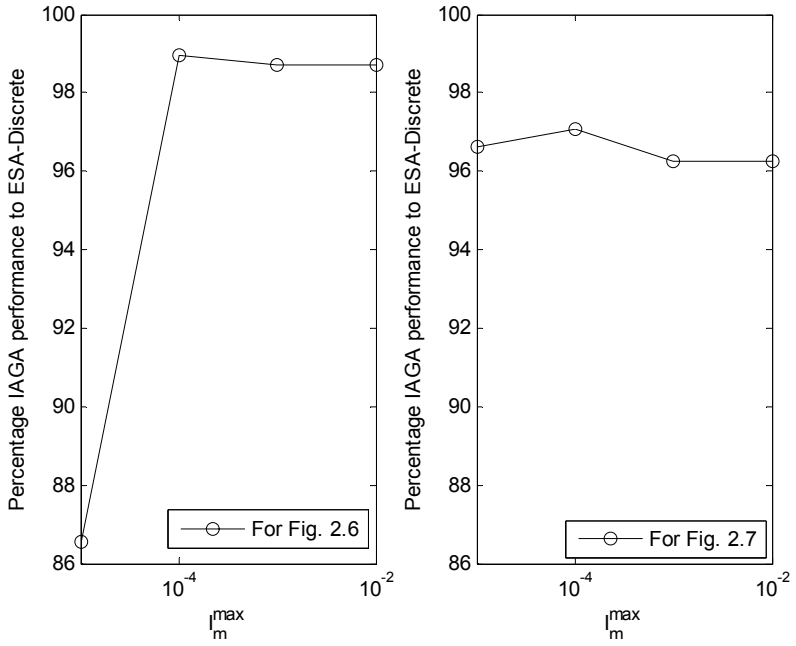

Fig. 2.13 Percentage IAGA performance to ESA-Discrete for different $I_{m,k}^{\max}$

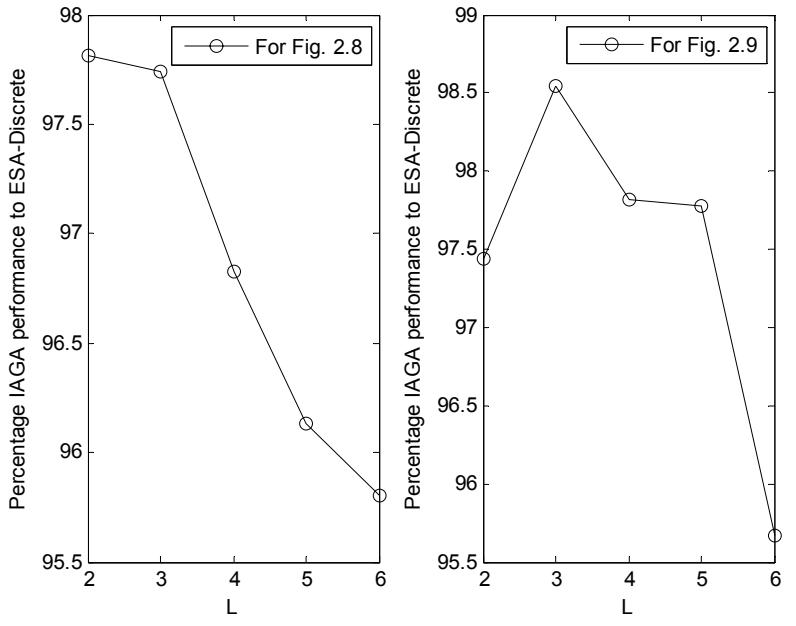

Fig. 2.14 Percentage IAGA performance to ESA-Discrete for different $I_{m,k}^{\max}$

2.4 Summary

In this chapter, we formulated an optimization problem for determining joint source/relays' transmission power levels and relay assignment in a CRS. We have shown that the assignment of source transmission power and the relays' transmission power levels are separable − i.e., the optimization (2.2) is reduced to the optimization (2.4). Then, we presented algorithms for discrete and continuous power allocation and relay assignment. The proposed algorithms have low computational complexity and the performance results are comparable to the exhaustive search algorithm and better than one to one ESA. The simple model and low implementation complexity makes the proposed algorithms suitable candidates for solving complex communication problems like interference aware multiple relay assignment in real-time.

2.5 Chapter References

[1] Y. Jing and H. Jafarkhani, "Single and multiple relay selection schemes and their achievable diversity orders," IEEE Transactions on Wireless Communications, vol. 8, no. 3, pp. 1414 - 1423, Mar. 2009.

[2] I. Maric and R. D. Yates, "Bandwidth and Power Allocation for Cooperative Strategies in Gaussian Relay Networks," IEEE Trans. Inform. Theory, vol. 56, no. 4, pp. 1880-1889, Apr. 2010.

[3] E. Hossain, D. Niyato, and Z. Han, Dynamic Spectrum Access and Management in Cognitive radio system, Cambridge University Press, 2009.

[4] Q. Zhao and B.M. Sadler, "A Survey of Dynamic Spectrum Access," IEEE Signal Processing Magazine, vol. 24, no. 3, pp. 79-89, May, 2007

[5] M. Abramowitz and I. A. Stegun, Handbook of Mathematical Functions with Formulas, Graphs, and Mathematical Tables, 9th Ed., New York: Dover Publications, 1970

[6] Y. Ma and D. I. Kim, "Rate-Maximization Scheduling Schemes for Uplink OFDMA," IEEE Trans. Wireless Comm., vol. 8, pp. 3193-3205, June 2009.

[7] R. Jain, D. Chiu, and W. Hawe, “A quantitative measure of fairness and discrimination for resource allocation in shared computer systems," Digital Equip. Corp., Littleton, MA, DEC-TR-301, Sep. 1984.

[8] G. H. Golub and C. F. Van Loan, Matrix Computations, the Johns Hopkins Univ. Press, 1983.

[9] H. Kwon, H. Seo, S. Kim, and B. G. Lee, “Generalized CSMA/CA for OFDMA Systems: Protocol Design, Throughput Analysis, and Implementation Issues,” IEEE Transactions on Wireless Communications, vol. 8 no. 8 pp 4176-4187, 2009.

[10] T. Cover and J. Thomas, Elements of Information Theory , Wiley & Sons, NY, 2nd Ed. 2006.

CHAPTER 3: GREEN RESOURCE ALLOCATION

According to the International Telecommunication Union (ITU) report [1] [2], primary sources of global warming (CO_2 emissions) are electricity generation, transport vehicles, buildings, and agricultural by-products. World Energy Outlook (WEO) has forecasted that by the year 2030, the demand of electricity will be twice as high as compared to the current demand, driven by the rapid growth in population and by the continuous increase in the residential and commercial electrical devices [3].

The information and communication technologies (ICTs) (especially the wireless sector) contribute significantly to CO_2 emissions [1] [2] [3]. The ICTs sector is responsible for approximately five percent of the global electricity demand and CO_2 emission [6] [7]. The CO_2 emission from the ICTs sector is equivalent to the airline industry [2] [7]. The Global e-Sustainability Initiative (GeSI) reported that during the year 2002, the ICTs and their related infrastructure caused 150 mega tons of CO_2 emissions, and by the year 2020 they will cause 350 mega tons of CO_2 emissions [4] [5]. Fig. 3.1 shows major sectors in ICTs and their estimated contribution in CO_2 emissions in year 2002 and 2020.

The main aim of green ICTs is to minimize the CO_2 emissions. Research in green ICTs will enable the communication system designer to develop and design the communication systems that will use power more efficiently and thus contribute to reducing the CO_2 emissions. There are a number of approaches to green ICTs. One approach is to use renewable energy (i.e., energy generation from natural resources such as sunlight, wind, rain, tides, and geothermal heat). Another approach is to design low power electronics components and design energy saving algorithms for ICTs operations [4].

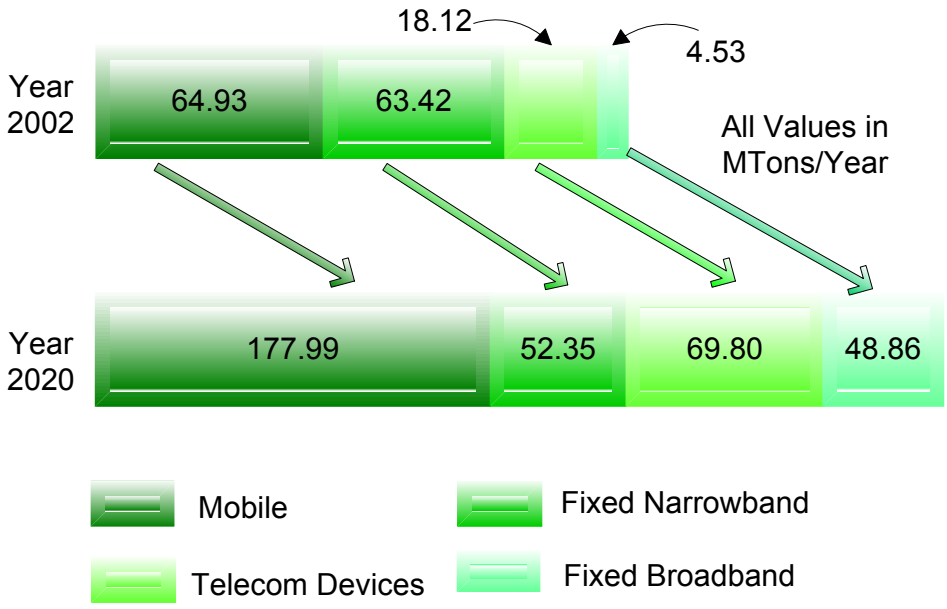

Fig. 3.1 CO_2 emission estimate by GeSI in Mega Tones/Year

In the last few years, there has been increasing efforts towards green ICTs. A comprehensive survey on green networking is presented in [4]. A green planning for wireless network is presented in [5]. In [6], authors presented the concept of energy efficiency in telecommunication networks. A detailed discussion about ICTs footprint and its impact on the environment is presented in [8] [9] and [10]. In [11], authors described a variable power/bandwidth efficient modulation strategy to save the battery life of the communication device. Information and technology companies like Google and Microsoft have already started working towards green ICTs [21] [22].

In the context of green communication, cooperative communication can contribute to reducing the CO_2 emissions. In this chapter, we present a multi-objective optimization framework that jointly solves the problem of spectrum sharing and reducing CO_2 emissions. In particular, we propose a green multi-objective optimization framework for joint relay assignment and power allocation in cooperative CRS.

3.1 Multi-objective Optimization

Multi-objective optimization (MOO) is used in many complex engineering optimization problems [12] − [15]. In typical MOO problems, different objectives can conflict with each other. Optimization with respect to any particular objective can give unacceptable results with respect to other objectives [14]. For resource allocation in green cooperative cognitive radio network (GCCRN), we have two conflicting objectives, maximize the sum-capacity and minimize the CO_2 emissions. Determining the optimal set of decision variables for a single objective− e.g. CO_2 emissions minimization can result in a non-optimal set with respect to other objectives, e.g. sum-capacity maximization. Two widely used methods to solve multi-objective optimization are weighted sum method and constraint objective method [12] – [15]. In the weighted sum method (WSM), a weighted sum of the multiple objective function is considered as the metric to minimize (maximize). In WSM, the weight of each objective is proportional to its importance placed for decision-making. A general WSM multi-objective optimization problem is expressed as follows:

$$\begin{aligned}
&\min \quad f(x) = \sum_{i}^{Q} w_i f_i(x) \\
&subject\ to \\
&\quad g_j(x) \le 0, j = 1, 2, ..., D \\
&\quad h_i(x) = 0, i = 1, 2, ..., E \\
&\quad \sum_{i=1}^{Q} w_i = 1
\end{aligned}$$

where *Q* is the number of objective functions, *D* is the number of inequality constraints; *E* is the number of equality constraints. In the constraint objective method [14], each objective is transformed into a constraint. In our formulation, we will use weighted sum method.

An important task in designing the weighted sum MOO is to normalize objective functions so that each objective function has same range of values. A weighted-sum method [14] for MOO, without normalization, would result in a

biased fitness function–e.g., if the value of one objective function is in the range [0, 1] and the value of second objective is in the range [0, x] (where $1 \le x < \infty$) then the second objective produces bias in the weighted fitness function. In this work, we normalized all the objective values within the range [0, 1]. For normalization, we divide each objective function with its upper bound. We formulate the GCCRN MOO in a way that the range of combined objective function is always within 0 and 1.

3.2 Green Relay Assignment for GCCRN

We consider a two-hop wireless network with one transmitter (source), *K* receivers (secondary users), *L* relays, and *M* primary users. Each relay, transmitter, and receiver is equipped with a single antenna. We denote by $h_{s,l}$, the channel from the source to the *l*th relay, $h_{l,k}$ the channel from the *l*th relay to the *k*th secondary user, and $g_{l,m}$ the channel from the *l*th relay to the *m*th primary user. We denote by p_l, the *l*th relay's transmission power. We consider a two-step amplify-and-forward (AF) scheme [16]. In our system model, each user will receive the data on a separate frequency band. Each relay will transmit and receive in the same frequency band. We define $\varepsilon_{l,k}$ as a binary assignment indicator

$$\varepsilon_{l,k} = \begin{cases} 1 & if\ the\ lth\ relay\ is\ assigned\ to\ the\ kth\ receiver \\ 0 & otherwise \end{cases}$$

The channel capacity of the *k*th user for amplify and forward relaying is [16] [17]

$$C_k = \frac{1}{2}\log\left[1 + \frac{P_s^k}{N}\left(\frac{\left(\sum_{l=1}^{L}\varepsilon_{l,k}\left|h_{s,l}h_{l,k}\right|\beta_l\sqrt{p_l}\right)^2}{1+\sum_{l=1}^{L}\left(\beta_l\left|h_{l,k}\right|\sqrt{p_l}\right)^2}\right)\right] \tag{3.1}$$

where $\beta_l = \left(\sqrt{P_s^k \left| h_{s,l} \right|^2 + N/2} \right)^{-1}$. Our first objective is to maximize the sum-rate capacity $\sum_{k=1}^{K} C_k$. As mentioned in section 3.1, to normalize the first objective between 0 and 1, we will divide the sum-rate capacity with $\sum_{k=1}^{K} C_k^{\max}$, where $C_k^{\max}$ is an upper bound on the capacity of the *k*th secondary user. We use the following upper bound, which is obtained from Schwartz inequality:

$$\log\left[1+\frac{P_s^k}{N}\left(\frac{\left(\sum_{l=1}^{L}\left|h_{s,l}\right|\left|h_{l,k}\right|\beta_l\sqrt{p_l}\right)^2}{1+\sum_{l=1}^{L}\left(\left|h_{l,k}\right|\beta_l\sqrt{p_l}\right)^2}\right)\right] \le \log\left[1+\frac{P_s^k}{N}\left(\frac{\left(\sum_{l=1}^{L}\left(\left|h_{s,l}\right|\right)^2\right)\sum_{l=1}^{L}\left(\left|h_{l,k}\right|\beta_l\right)^2 p_l}{1+\sum_{l=1}^{L}\left(\left|h_{l,k}\right|\beta_l\right)^2 p_l}\right)\right]$$

Mathematically, we can write the objective of the sum-rate capacity as

$$\overline{f}_c = \frac{\sum_{k=1}^{K} C_k}{\sum_{k=1}^{K} C_k^{\max}} \tag{3.2}$$

The second objective is to reduce the CO_2 emissions. The CO_2 emissions are measured in grams. If *P* is the power used in the transmission and *X* is a constant in grams/watt then the product of *P* and *X* (i.e., *PX*) represents the CO_2 emissions in grams. The value of *X* is different for different types of material (fuel) used for electricity generation. There are three major sources of fuel for electricity generation. These fuels are oil, gas, and coal. The value of *X* for lignite/brown coal, natural gas, crude oil and diesel oil is 940, 370, 640, and 670 grams/watt, respectively [6] − [8]. We define by $E_l^{CO_2} = \sum_{l=1}^{L} X p_l$, the CO_2 emissions due to the *l*th relay. We can write the objective of CO_2 emissions as

$$f_{CO2} = \left(\frac{\sum_{l=1}^{L} \varepsilon_{l,k} E_{l}^{CO_2}}{\sum_{l=1}^{L} \varepsilon_{l,k} E_{l^{\max}}^{CO_2}} \right) \tag{3.3}$$

where $E_{l^{\max}}^{CO_2} = \sum_{k=1}^{K} Xp_l^{max}$. To define a single objective, we can transform the maximization objective $\overline{f}_c$ into minimization using the relation $f_c = 1 - \overline{f}_c$. Mathematically, we can write the MOO for GCCRN as

$$\begin{aligned}
&OP1: \\
&\min_{\varepsilon, p_l} \quad \{ \mathrm{w}_1 f_c + \mathrm{w}_2 f_{CO2} \} \\
&subject\ to \\
&\qquad C1: \ \sum_{k=1}^{K} \varepsilon_{l,k} \le 1, \forall l \\
&\qquad C2: \ \sum_{l=1}^{L} p_l g \left| h_{l,m} \right|^2 \le I_{m,k}^{max}, \quad \forall (m,k) \\
&\qquad C3: \ 0 \le p_l \le \sum_{k=1}^{K} \varepsilon_{l,k} p_l^{max}, \quad \forall l \\
&\qquad C4: \ \varepsilon_{l,k} \in \{0,1\}
\end{aligned} \tag{3.4}$$

The formulation in (3.4) is a multi-objective non-convex mixed integer non-linear programming problem. The objective function in (3.4) is bounded by zero and one. In (3.4), the constraint *C*1 assures that a relay can only be assigned to one secondary user, *C*2 is the interference constraint, the constraints *C*3 and *C*4 jointly ensure that if the *l*th relay is not assigned to any secondary user then the transmission power of the *l*th relay should be zero. In the next section, we will present a low-complexity hybrid estimation-of-distribution algorithm (EDA) for GCCRN MOO problem.

3.3 Hybrid EDA for GCCRN MOO Problem

In this section, we will present a hybrid scheme for GCCRN multi-objective problem. The proposed scheme is a combination of an evolutionary estimation-of-distribution algorithm for power allocation and an iterative greedy algorithm for relay assignment. Evolutionary algorithms (EAs) in general have been often used

to solve multi-objective optimization problems. Evolutionary Algorithms are inspired by the theory of biological evolution. Candidate solutions to a multi-objective optimization problem are represented as individuals in the population. In EAs, the objective function value of a candidate solution indicates the fitness of the individual, which is associates with the concept of natural selection [18]. Unlike other evolutionary algorithms such as the genetic algorithm, in EDA, the individuals are generated without the crossover and mutation operators. Instead, in EDA, a new population is generated based on a probability distribution, which is estimated from the best-selected individuals of the previous iterations [19]. In general, EDA is used for discrete optimization problems; however, we introduce EDA for continuous domain to allocate power to the relays. Table 3.1 illustrates the parameters and notations used in continuous EDA (CEDA).

Table 3.1 Parameters and notations of CEDA

F	Fitness function
W_{High}	Upper limit of the EDA search window
W_{Low}	Lower limit of the EDA search window
Δ_l	The population (the set of individuals) at the *l*th iteration and $\lvert\Delta_l\rvert$ denotes its cardinality
η_l	The set of best candidate solutions selected from set Δ_l at the *l*th iteration.
p_s	The selection probability. The EDA selects $p_s\lvert\Delta_l\rvert$ individuals from the set Δ_l to make up the set η_l.
I_{Ter}	The maximum number of iterations

In CEDAs, each individual can be designated by an *L*-dimensional real-valued vector. For GCCRN MOO problem. In our implementation of CEDA, each individual represents the transmission power of the relays. We denote by a row vector $\boldsymbol{P} = (p_1, p_2, \cdots, p_L)$ as an individual where p_i is the transmission power of the *i*th relay. The transmission power of the *i*th relay is bounded by W_{Low} and W_{High} where W_{Low} and W_{High} are the lower and upper limit of EDA search window. In

each iteration, the CEDA maintains a population of individuals. The population is denoted by set Δ_l . We denote by $|\Delta_l|$, the number of individuals in the population. Population Δ_l can be specified by the following matrix

$$\Lambda_{CEDA} = \begin{pmatrix} \boldsymbol{P}^1 \\ \boldsymbol{P}^2 \\ \vdots \\ \boldsymbol{P}^{|\Delta_l|} \end{pmatrix} = \begin{pmatrix} p_1^1 & p_2^1 & \vdots & p_L^1 \\ p_1^2 & p_2^2 & \vdots & p_L^2 \\ \cdots & \cdots & \cdots & \cdots \\ p_1^{|\Delta_l|} & p_2^{|\Delta_l|} & \vdots & p_L^{|\Delta_l|} \end{pmatrix} \tag{3.5}$$

where superscript *j* in the row vector $P^j = \left(p_1^j, p_2^j, p_3^j, ..., p_L^j\right)$ indexes an individual in the population. A flow diagram of EDA algorithm is shown in Fig. 3.2. The CEDA applied to the GCCRN MOO problem can be described in the following steps:

Step 0*: Generate an initial population* Δ_0*. Each element of matrix* Λ_{CEDA} *is obtained from the following formula:*

$$p_i^j = W_{Low} + \left(W_{High} - W_{Low}\right) \times rand, \forall i = 1,2,..,n, j = 1,2,...,\left|\Delta_0\right| \tag{3.6}$$

where W_{Low} *= 0,* W_{High} *=* p_l^{max} *and 'rand' is a random number generated from a uniform distribution between 0 and 1. For iterations l = 1,2, ...,*I_{Ter} *, follow Step 1 through Step 7:*

Step 1*: Evaluate the individuals in the current population* Δ_{l-1} *according to the fitness function F. Sort the candidate solutions (individuals in the current population) according to their fitness orders.*

Step 2*: In this step, the algorithm determines the assignment variable* $\varepsilon = \left[\varepsilon_{1,1}, \varepsilon_{1,2}, .., \varepsilon_{1,K}, .., \varepsilon_{l,k}, .., \varepsilon_{L,K}\right]$ *for each individual heuristically. We propose an iterative relay assignment algorithm that generates a feasible* $\varepsilon = \left[\varepsilon_{1,1}, \varepsilon_{1,2}, .., \varepsilon_{1,K}, .., \varepsilon_{l,k}, .., \varepsilon_{L,K}\right]$ *and repairs each individual such that constraints C2 and C3 are satisfied. The algorithm is described in section 3.3.2. At the end of this step, the algorithm has a population, which comprises individuals with*

feasible relays' power levels and the associated assignment variables $\varepsilon = \left[\varepsilon_{1,1}, \varepsilon_{1,2}, .., \varepsilon_{1,K}, .., \varepsilon_{l,k}, .., \varepsilon_{L,K} \right]$.

Step 3*: In this step, the cost function is evaluated to determine the fitness values for each individual in the population, and the individuals are sorted according to their fitness values. If the convergence criteria (e.g. number of iterations) is satisfied, then terminate; else, go to step 4.*

Step 4*: Select the best* $\rho_s \left| \Delta_{l-1} \right| = \left| \eta_{l-1} \right|$ *candidate solutions (individuals) from the current population* Δ_{l-1}*. This selected population is used to compute the mean and standard deviation.*

Step 5*: Determine the mean 'm' and standard deviation 'σ'. Based on these estimates of 'm' and 'σ,' update the search window bounds* W_{Low} *and* W_{High} *as* $W_{Low} = m - \sigma$ *and* $W_{High} = m + \sigma$.

Step 6*: Generate new* $\left| \Delta_l \right| - \left| \eta_{l-1} \right|$ *individuals on the basis of this new estimated* W_{Low} *and* W_{High} *using equation* (3.6)*. Combine these newly generated* $\left| \Delta_l \right| - \left| \eta_{l-1} \right|$ *individuals with members of* η_{l-1} *to form a new population* Δ_l .

Step 7*: Go to step one and repeat the steps.*

Even with this simple application of CEDA, the simulation results show that it has very good performance. In addition, we were able to modify this basic EDA algorithm and even further improve the algorithm's performance. The modification includes the introduction of thresholds in CEDA to avoid premature convergence. We name this algorithm as Modified EDA (MEDA). In the next section, we will explain the MEDA.

3.3.1 Modified EDA

During the execution of CEDA, the difference between the search window bounds W_{Low} and W_{High} *may* diminishes as the iterations proceeds. This may cause the CEDA to get stuck in a search space and result in premature

convergence. The premature convergence may occur if the difference between W_{Low} and W_{High} diminishes to an extremely small value. In that case, at every future iteration, the algorithm will generate nearly same power levels. We suggest restoring the W_{Low} and W_{High} to their initial values ($W_{Low} = 0$ and $W_{High} = p_l^{max}, l = 1, 2, .., L$) when the difference between W_{Low} and W_{High} is less than a pre-specified threshold γ −i.e.

$$
\begin{aligned}
&if\ W_{High} - W_{Low} \le \gamma \\
&\quad W_{Low} = 0,\ \ W_{High} = p_l^{\max} \\
&endif
\end{aligned}
$$

The above steps are illustrated in Fig. 3.3. In section 3.4, we present some experimental results, which show the effect of threshold on the performance of EDA. Now, we will describe the iterative greedy algorithm for relay assignment.

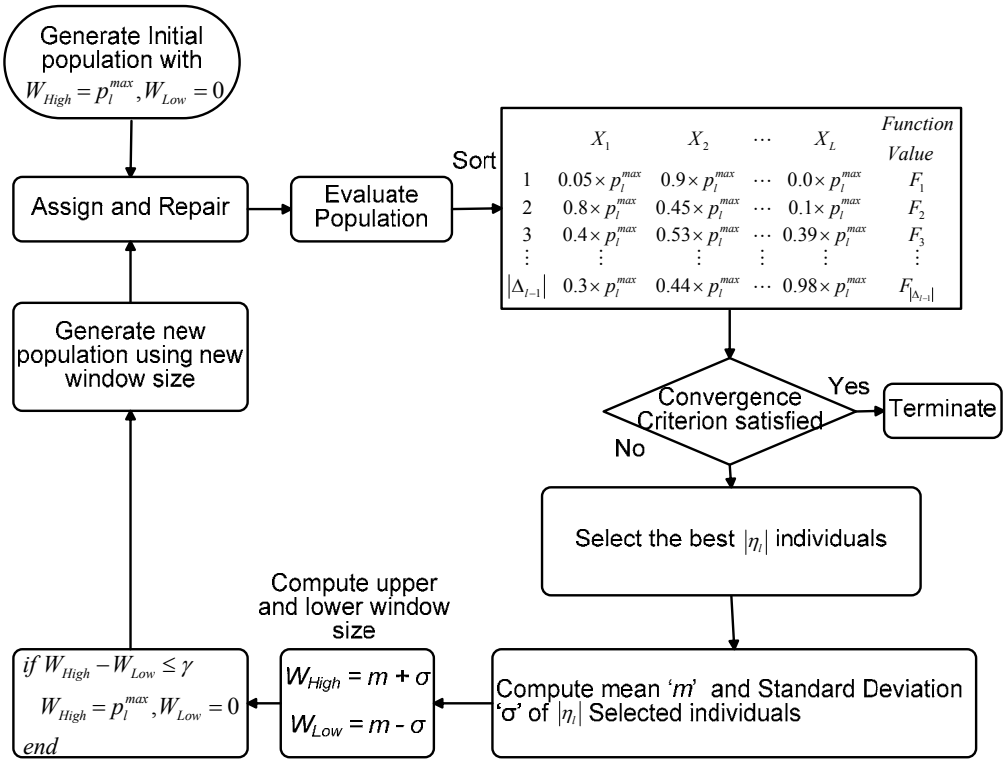

Fig. 3.2 Flow diagram for continuous EDA

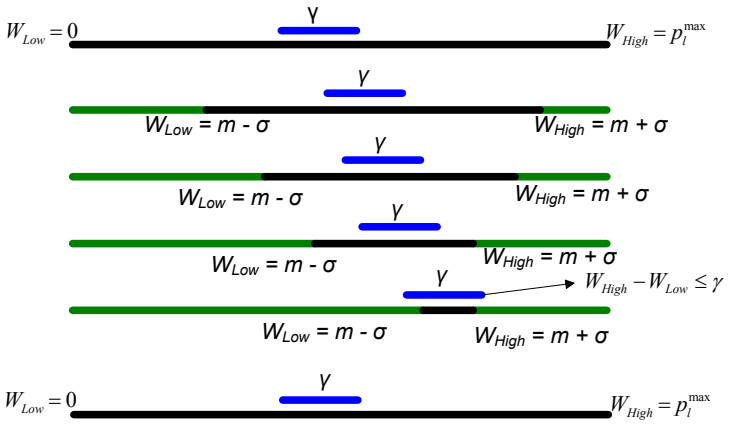

Fig. 3.3 Continuous EDA with threshold

Table 3.2 Iterative greedy relay assignment for each EDA individual

NOTE: This routine will be executed on each EDA individual in the population. This table illustrates the relay assignment for the EDA individual indexed by j.

***INITIALIZATION*:**

$S(l)=0, \forall l$,*k = 1*; *C*(*k*)= 0, $\forall k$,*l* = 1;

Step 1:

While $l \le L$

1: $S(l)=\underset{k\in\{1,2,\ldots,K\}}{\arg\max}\ \dfrac{\left|h_{sl}\right|^2\left|h_{l,k}\right|^2}{max\left(\left|g_{l1}\right|^2,\left|g_{l2}\right|^2,\cdots\left|g_{lM}\right|^2\right)}$;

2: *l:=l+1*

End While

Step 2:

$p_l^j := \min\left(\dfrac{I_m^{\max}}{\left|g_{lm}\right|^2}\forall m, p_l^j\right), \forall l$; /*power of the *l*th element of the jth individual*/

While $k \le K$

1: $\Psi_k = \{l \mid S(l)=k\}$

2: ***If*** $\Psi_k \neq \varnothing$

3*: l = 0;*

4: ***While l = 0***

5: ***If*** (*is interference constraint satisfied with* Ψ_k) = *FALSE*

6: l=Get the relay with largest interference;

7: $\Psi_k := \Psi_k \setminus \{l\}$;

8: ***Else***

9: *l = 1;*

10: *C(k) = Get the capacity from eq.* (3.1) *using* Ψ_k

11: ***End If***

12: ***End While***

13: ***End If***

14: k := k+1;

End While

3.3.2 Iterative Greedy Algorithm

In this section, we present an iterative greedy relay assignment algorithm, which determines the assignment variable $\varepsilon = \left[\varepsilon_{1,1}, \varepsilon_{1,2}, .., \varepsilon_{1,K}, .., \varepsilon_{l,k}, .., \varepsilon_{L,K} \right]$ for each individual heuristically. The proposed algorithm also converts any infeasible individual to feasible individual. Table 3.2 shows the pseudo code of the iterative greedy algorithm[2].

The proposed algorithm has two steps. In the first step, based on the channel conditions, relays are assigned to the secondary users without satisfying the interference constraint. In the second step, the algorithm performs final assignment under the constraint that interference to the primary users is satisfied..

3.3.2.1 Step 1: Relay Assignment without Interference Constraint

For developing this algorithm, we can view the product of channel gain from the *l*th relay to the *k*th secondary user and channel gain from source to the *l*th relay as $\left|h_{l,k}\right|^2 \left|h_{sl}\right|^2$ as profit (throughput) . We also view channel gain from the *l*th relay to its primary users as loss (interference). In particular, our algorithm views $max\left(\left|g_{l1}\right|^2, \left|g_{l2}\right|^2, \cdots \left|g_{lM}\right|^2\right)$ as loss. The algorithm in Step 1 temporarily assigns each relay to the secondary user that gives the maximum profit to loss ratio. Mathematically, for each relay *l*, the algorithm temporarily assigns secondary user:

$$S(l) = \underset{k \in \{1,2,...,K\}}{\arg\max} \frac{\left|h_{sl}\right|^2 \left|h_{l,k}\right|^2}{max\left(\left|g_{l1}\right|^2, \left|g_{l2}\right|^2, \cdots \left|g_{lM}\right|^2\right)},$$

where *S* is an *L*-dimensional vector that stores this temporary assignment. At the end of Step 1, relays are assigned to the secondary users with the power

[2] This algorithm (routine) will be executed on each EDA individual (sample). Table 3.2 illustrates the relay assignment for the CEDA's relay power vector sample indexed by *j*. .

assignment $p_l^j, l = 1,2,..,L$ may violate the interference constraint. In Step 2 of the algorithm, based on temporary relay assignment in Step 1, the algorithm performs joint relay assignment and power allocation such that the interference constraint is satisfied at each primary user.

3.3.2.2 Step 2: Final Relay Assignment with Interference Constraint

In the second step, the algorithm performs final assignment under the constraint that interference to the primary users is satisfied.

Note that the relays' power levels randomly generated by the EDA algorithm can violate the constraint of limited interference to the primary users. At the start of the second step, the algorithm starts repairing the relays' power levels if they violate an interference constraint. First, the algorithm examines for each relay *l* whether its transmission power would still violate any interference constraint even if all other relays' power level were set to zero. We denote by p_l^j, the relay *l*'s power level in the *j*th sample drawn by the EDA, in accordance with expression (3.5). If p_l^j violates any of the interference constraint, $I_m^{\max}$, even under the assumption that other relays' transmission power levels are all set o 0, then the algorithm first makes the following adjustment:

$$p_l^j := \min\left(\frac{I_1^{\max}}{|g_{l1}|^2}, \frac{I_2^{\max}}{|g_{l2}|^2}, \cdots, \frac{I_M^{\max}}{|g_{lM}|^2}, p_l^j\right), \forall l \tag{3.7}$$

After the power adjustment, the algorithm iterates over the secondary users and completes the final assignment of relays.

At the *k*th iteration, the algorithm determines the set of relays Ψ_k that are temporarily assigned to the *k*th secondary user in Step 1. Then, the algorithm checks whether the relays in the set Ψ_k satisfies the interference constraint at all the primary users. If the relays in the set Ψ_k violate the interference constraint at any primary user, then the algorithm iteratively removes the relay from the set

Ψ_k that causes maximum interference to the primary users. This relay removal process continues until the relays in the set Ψ_k satisfy the interference constraint. The algorithm will terminate when all the secondary users get their assigned relays.

Table 3.3 Explanation of abbreviations used in simulation results

DP-EDA	Decrease in power using EDA
DP-GA	Decrease in power using GA
DSC-EDA	Decrease in sum-capacity using EDA
DSC-GA	Decrease in sum-capacity using GA
(M)-EDA-f	Performance of (Modified)-EDA on combined fitness function
(M)-EDA-fc	Performance of (Modified)-EDA on f_c
(M)-EDA-fCO_2	Performance of (Modified)-EDA on f_{CO2}

3.3.3 Numerical Results

In all simulations, the channel gains between source, relays and destinations have independent complex Gaussian distribution. All the simulations are performed using Monte Carlo runs. Each result is an average of two thousand independent simulation runs. We compare the results of Hybrid EDA and MEDA with standard continuous genetic algorithm [20]. Table 3.3 describe the notations used in the simulation results.

In Figs. 3.4, 3.5 and 3.6, we present the trade-off plots of sum-capacity and power. The trade-off is calculated between the green communication and without green communication. Trade-off is presented as percentage decrease in sum-capacity (DSC) and percentage decrease in power consumption (DP). To get the result without green communication, we set w_1 = 1 and w_2 = 0. Figs. 3.4 and 3.5 show the effect of green communication by changing the values of weights w_1 and w_2. The results show that when w_2 is more than w_1 there is more reduction in CO_2 emissions (percentage decrease in power). The reduction in CO_2 emissions comes at the cost of throughput reduction. From the results, we can observe that CO_2 emissions will decrease by 50 to 70 percent at the cost of 10 to 30 percent loss of throughput when $w2 \geq w1$. The different weights settings are suitable for different geographical conditions and regulatory policies. The results also show that performance of EDA is better than GA. Fig. 3.6 illustrate

the trade-off plots of sum-capacity and power for different *L, K* and $I_m^{\max}$. Results show that there is less decrease in power at $I_m^{\max}$ = 10m*w* as compared with $I_m^{\max}$ = 1*w*. This due to the fact that lower interference threshold itself makes the CRS as a green communication device and there is less freedom for further improvement.

Figs 3.7 and 3.8 present the iterations vs. fitness plot for different number of relays and users. The parameters are (*M,* p_l^{max}, I_m^{max},*w*1,*w*2) = (1,10w,10mw,0.5,0.5) and (1,10w,1w,0.5,0.5). From Figs. 3.7 and 3.8, we can see that performance of MEDA is better than EDA and GA. A simple EDA and GA can get stuck in local optimum after few iterations. We can also note that the fitness values with large relays and less number of users (e.g., *L* = 20, *K*=10) is better than fitness values with less relays and large number of users (e.g., *L* = 10, *K* = 20). This is because with the large number of relays and less number of secondary users there is more freedom in assigning the relays to the secondary users.

Figs. 3.9 and 3.10 present the performance of EDA, MEDA and GA on each objective function. The parameters for Figs. 3.8 and 3.9 are (*M*, p_l^{max}, I_m^{max},*K,w*1,*w*2) = (1,10w,10mw,10,0.5,0.5) and (*M*, p_l^{max}, I_m^{max},*L,w*1,*w*2) = (1,10w,1w,L,0.5,0.5) . The results shows per iteration performance of both EDA and MEDA is better than GA on the fitness function and the individual objective functions.

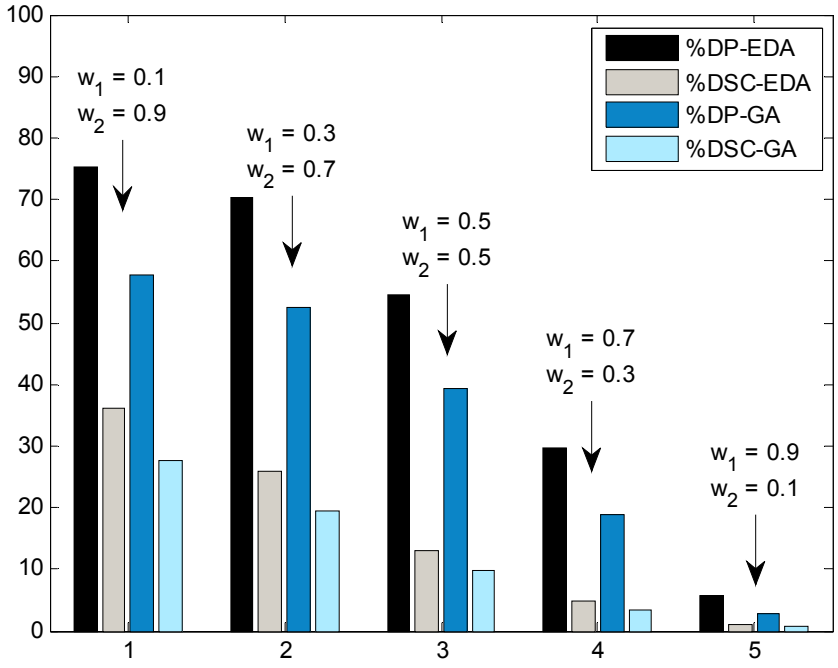

Fig. 3.4 Power and sum-capacity trade-off plot with K = 10, L = 10, $I_m^{\max} = 10mw$

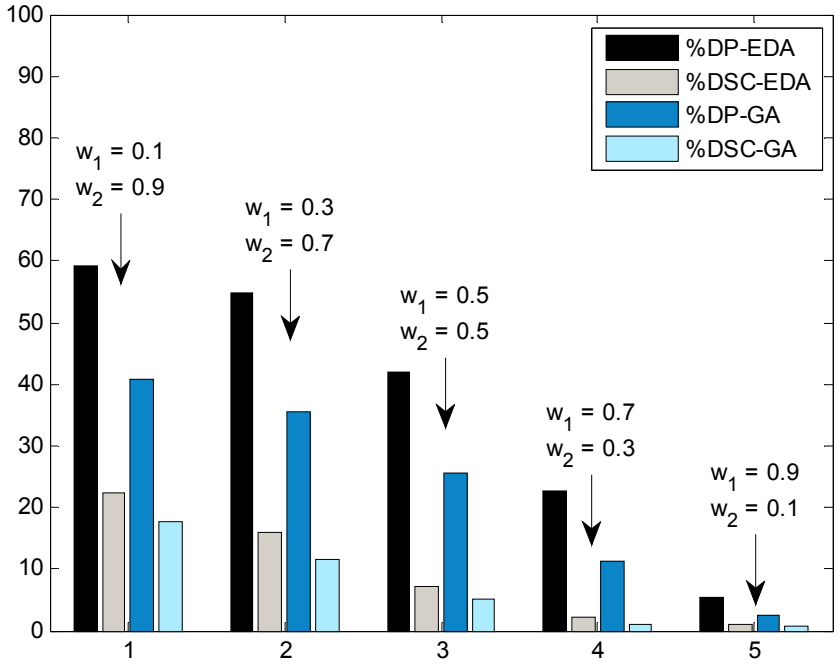

Fig. 3.5 Power and sum-capacity trade-off plot with K = 20, L = 10, $I_m^{\max} = 10mw$

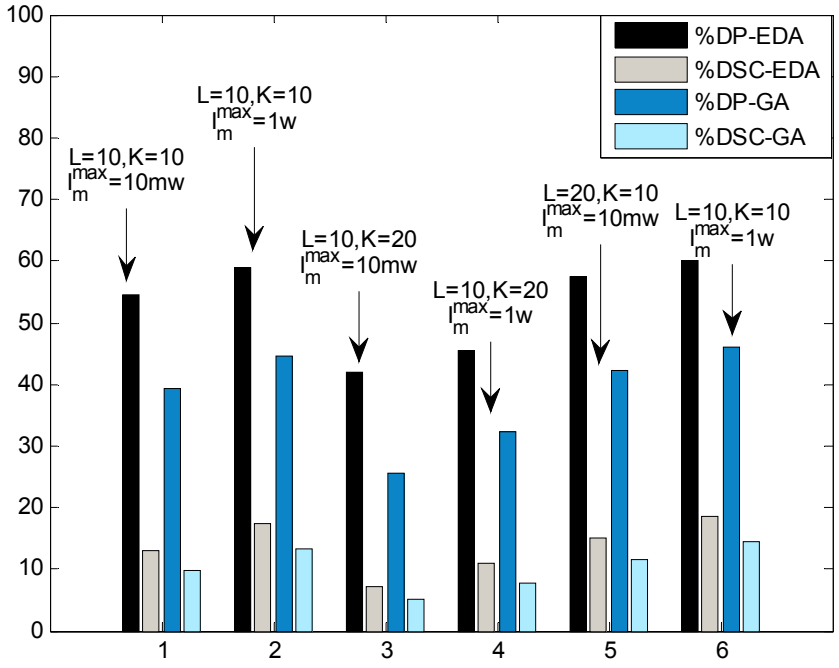

Fig. 3.6 Power and sum-capacity trade-off plot with (K,L, $I_m^{\max}$) = (10/20,10/20,10mw/1mw)

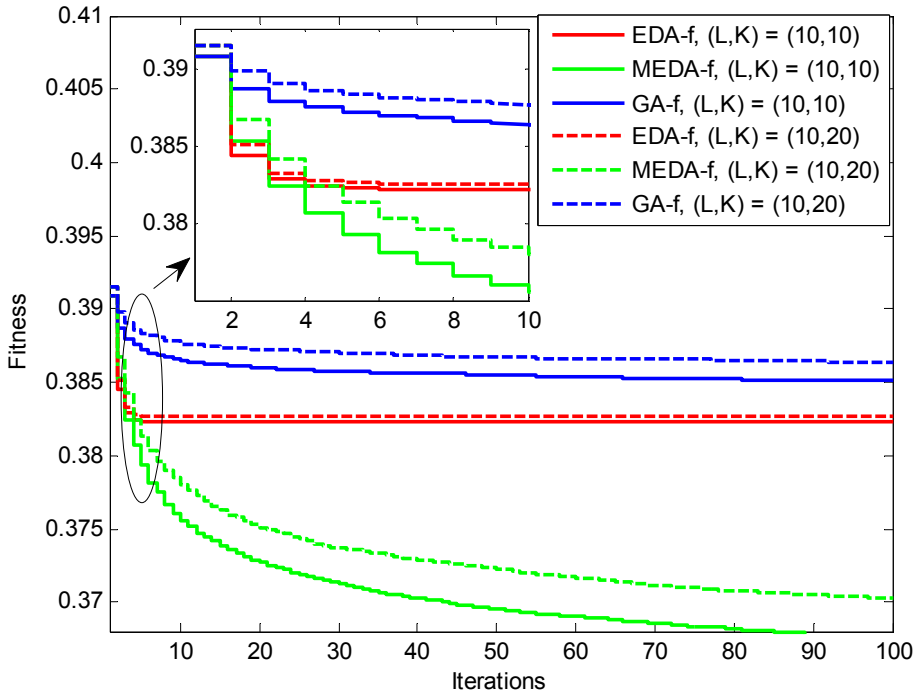

Fig. 3.7 Iterations vs. Fitness plot for different (L,K) configuration. The parameters are (M, p_l^{max}, I_m^{max},w1,w2)=(1,10w,10mw,0.5,0.5)

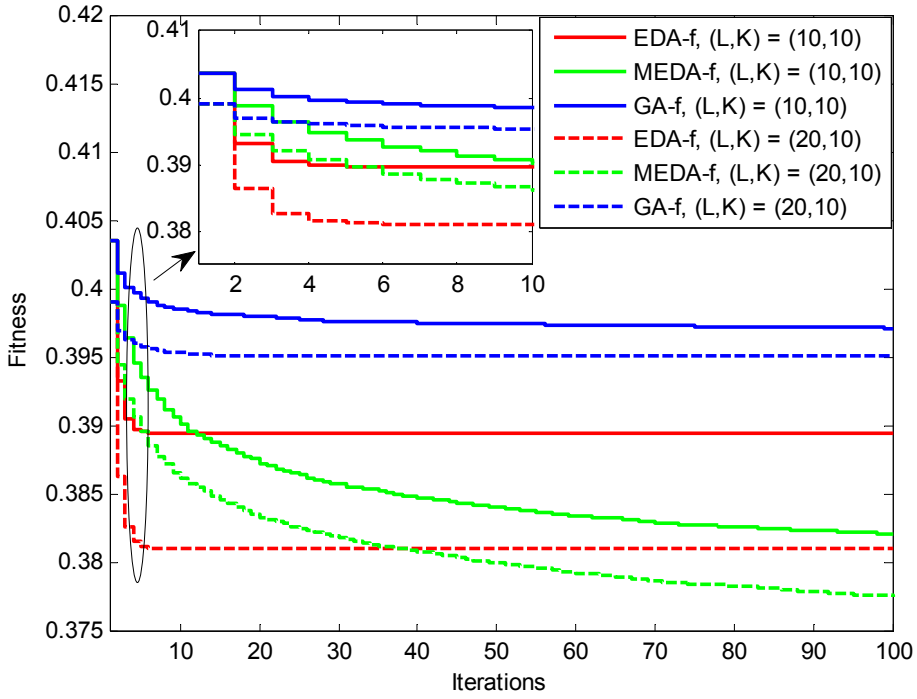

Fig. 3.8 Iterations vs. Fitness plot for different (L,K) configuration. The parameters are (M, p_l^{max}, I_m^{max},w1,w2)=(1,10w,1w,0.5,0.5)

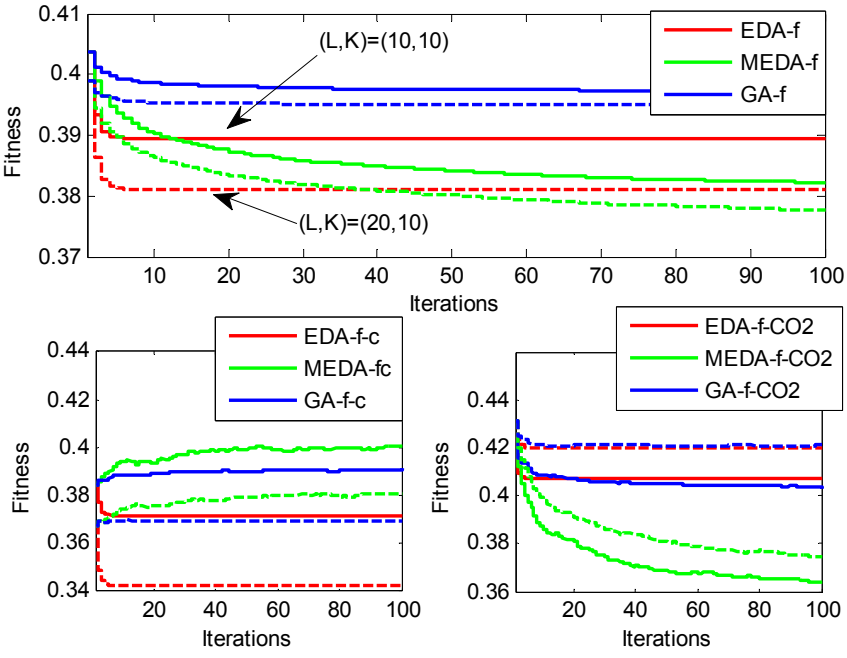

Fig. 3.9 Iterations vs. Fitness plot for different number of relays. The parameters are (M, p_l^{max}, I_m^{max},K ,w1,w2)=(1,10w,1w,20, 0.5 0.5

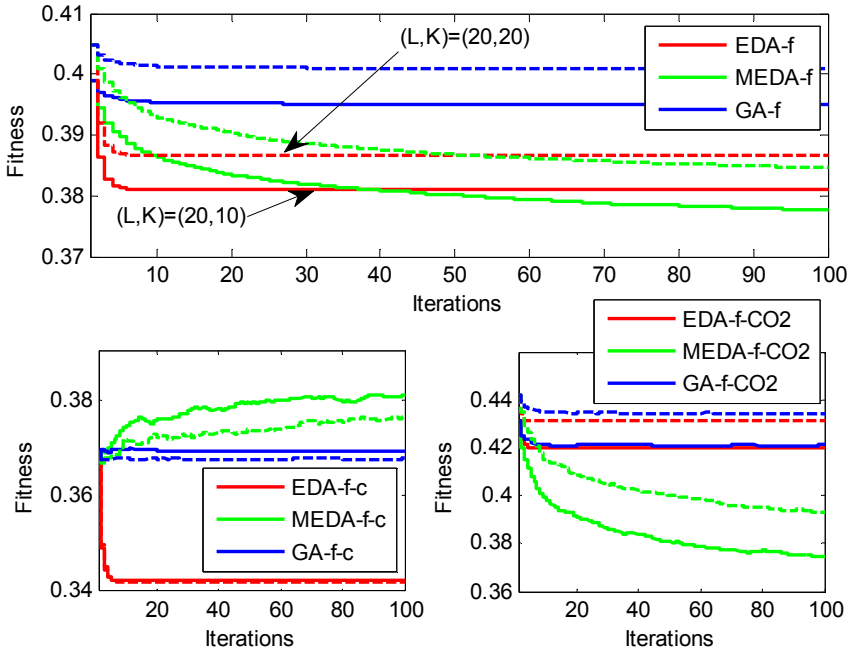

Fig. 3.10 Iterations vs. Fitness plot for different number of relays. The parameters are (M, p_l^{max}, I_m^{max} ,L ,w1,w2)=(1,10w,1w,20, 0.5 0.5)

3.4 Summary

In this chapter, we presented a multi-objective framework for green resource allocation in multiuser cognitive radio network. Estimation-of-distribution algorithm with an iterative relay assignment scheme is used to solve the multi-objective optimization problem. Simple underlying concept and ease of implementation of the proposed algorithm make EDA a suitable candidate for green resource allocation.

3.5 Chapter References

[1] C. Han, T. Harrold, I. Krikidis, I. Ku, T. A. Le, S. Videv, J. Zhang, S. Armour, P. M. Grant, H. Haas, L. Hanzo, M. R. Nakhai, J. Thompson, and C.-X. Wang, "Green radio: radio techniques to enable energy efficient wireless networks," (available at *http://eprints.ecs.soton.ac.uk /21431/*)

[2] International Telecommunication Union (ITU), "Report on Climate Change," Oct. 2008.

[3] IEA report, “CO2 Emissions from Fuel Combustion 2010 – Highlights,” *http://www.iea.org/co2highlights/co2highlights.pdf*

[4] R. Bolla, R. Bruschi, F. Davoli, and F. Cucchietti, , "Energy Efficiency in the Future Internet: A Survey of Existing Approaches and Trends in Energy-Aware Fixed Network Infrastructures," IEEE Communications Surveys & Tutorials, (Accepted), (http://ieeexplore.ieee.org/stamp/stamp.jsp?tp=&arnumber=5522467&isnumber=5451756)

[5] Global e-Sustainibility Initiative (GeSI) Report, ”SMART 2020:Enabling the Low Carbon Economy in the Information Age,” Available at *http://www.smart2020.org/_assets/files/02_Smart2020Report.pdf*

[6] G. Koutitas, “Green Network Planning of Single Frequency Networks,” IEEE Transactions on Broadcasting, vol.56, no.4, pp.541-550, Dec. 2010.

[7] G. Koutitas, P. Demestichas, “A Review of Energy Efficiency in Telecommunication Networks,” Journal of Telecommunication Forum (TELFOR), 2010.

[8] K. Li, “Mobile Communications 2008: Green Thinking Beyond TCO Consideration,” In-Stat White paper, May 2008.

[9] L. Herault,E. C. Strinati ,O. Blume ,D. Zeller, Muhammad A. Imran, R. Tafazolli, Y. Jading ,J. Lundsjö and Michael Meyer, “Green Communications: a Global Environmental Challenge,” In *Proceeding of 12th International Symposium on Wireless Personal Multimedia Communications*, 2009.

[10] W. Vereecken, W. V. Heddeghem, D. Colle, M. Pickavet, and P. Demeester, “Overall ICT footprint and green communication technologies,” In Proceedings of 4th IEEE International Symposium on Communications, Control and Signal Processing (ISCCSP), 2010.

[11] D. Grace, J. Chen, T. Jiang, and P.D. Mitchell, “Using cognitive radio to deliver Green communications,” In Proceedings of 4th IEEE International Conference on Cognitive Radio Oriented Wireless Networks and Communications (CROWNCOM), 2009.

[12] R.T. Marler and J.S. Arora, “Survey of multi-objective optimization methods for engineering,” Structural and Multidisciplinary Optimization, vol. 26, no.6, pp. 369-395, April 2004.

[13] M. Elmusrati, H. El-Sallabi, and H. Koivo, “ Applications of multi-objective techniques in radio resource scheduling of cellular communication systems,” IEEE Transaction of Wireless Communication, vol. 7, no. 1,pp. 343-353 Jan. 2008.

[14] K. Deb, *Multi-objective optimization using evolutionary algorithms*, Wiley New York, 2001.

[15] T. Newman, R. Rajbanshi, A. Wyglinski, J. Evans, and G. Minden, “Population Adaptation for Genetic Algorithm-based Cognitive Radios,” ACM/Springer Mobile Ad Hoc Networks -- Special Issue on Cognitive Radio Oriented Wireless Networks and Communications ,vol. 13, no. 5, pp. 442-451, 2008.

[16] J. N. Laneman, D. N. C. Tse, and G. W. Wornell, “Cooperative Diversity in Wireless Networks: Efficient Protocols and Outage Behavior,” IEEE Trans. Inform. Theory, vol. 50, no. 12, pp. 3062-3080, Dec. 2004.

[17] I. Maric and R. D. Yates, “Bandwidth and Power Allocation for Cooperative Strategies in Gaussian Relay Networks,” In Proceedings of 38th Asilomar Conference on Signals, Systems and Computers, Pacific Grove, CA, Nov. 2004.

[18] A.E. Eiben and J.E. Smith, Introduction to Evolutionary Computing, Springer Verlag, 2003.

[19] P. Larrañaga and J. A Lozano, Estimation of Distribution Algorithms: A New Tool for Evolutionary Computation. Kluwer Academic Publishers, 2001.

[20] R.L. Haupt and S.E. Haupt, Practical Genetic Algorithms, Wiley-Interscience, 2004.

[21] R. H. Katz, “Tech Titans Building Boom,” IEEE Spectrum, vol. 46,pp. 40–54, Feb. 2009.

[22] R. Barga, “Cloud Computing – A Microsoft Research Perspective.” Keynote Speech at IEEE P2P 2009 Sept. 2009.

PART 2: SUBCARRIER ASSIGNMENT

CHAPTER 4: RESOURCE ALLOCATION IN COOPERATIVE MULTICAST CRS

In this chapter, we present resource allocation schemes for the cooperative multiuser multicast cognitive radio system (MMCRS). For resource allocation, we propose schemes that jointly assign subcarriers and relays to the multicast groups and allocate power to the relays in the cooperative MMCRS. We consider two separate optimization problems. In one optimization problem, we maximize the total throughput of the cooperative MMCRS under the constraint of acceptable interference to the primary users. In the other optimization problem, we maximize the throughput of the worst multicast group in the cooperative MMCRS under the constraint of acceptable interference to the primary users. For each optimization problem, we propose an iterative algorithm with polynomial time complexity.

4.1 Subcarrier Assignment for Sum-rate maximization

4.1.1 System Model

We consider an OFDMA based two-hop cooperative MMCRS with one transmitting node (source), *L* relay nodes, *N* subcarriers, and *G* traffic flows (*G* multicast groups). Each traffic flow is meant for a separate multicast group, and we assume that each secondary user belongs to only one multicast group at a time. We denote by $K_g, g = 1,2,\cdots,G$, the set of secondary users in the *g*th multicast group. The total number of secondary users in MMCRS will be $|K| = \sum_{g=1}^{G} |K_g|$, where $|K|$ is the cardinality of the set $K = \bigcup_{g=1}^{G} K_g$. Our system model also includes *M* primary users, for which the transmission power of the secondary users must be limited. Fig. 4.1 shows the cooperative MMCRS.

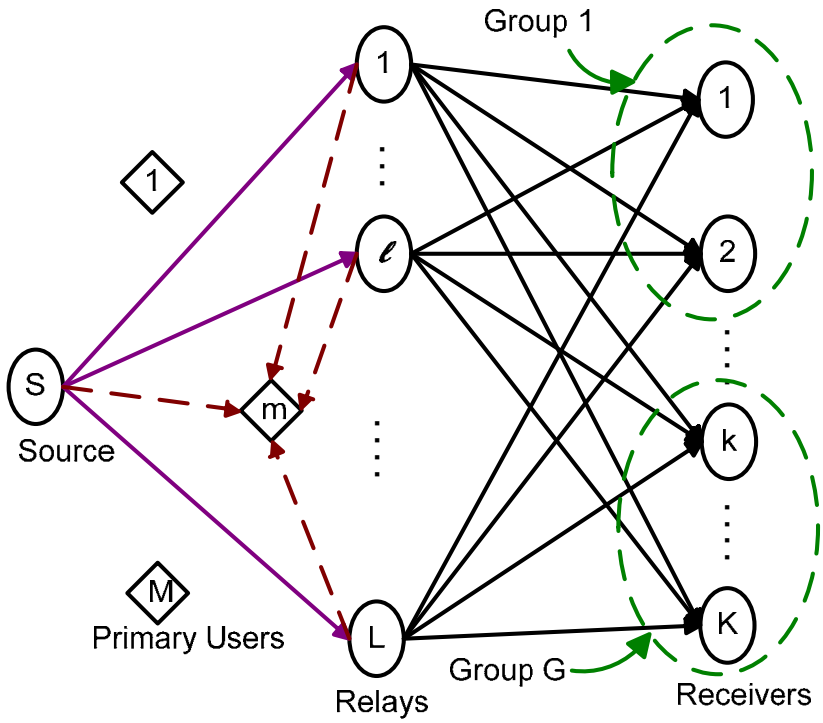

Fig. 4.1 Cooperative MMCRS.

We denote by h_{sl}^{n}, the channel from the source to the *l*th relay on the *n*th subcarrier, $h_{g,lk}^{n}$ the channel from the *l*th relay to the *k*th secondary user of group *g* on the *n*th subcarrier, and h_{lm}^{n} the channel from the *l*th relay to the *m*th primary user on the *n*th subcarrier. We denote by p_{l}^{max} the maximum allowable transmission power of the *l*th relay, p_{l}^{n} the transmission power of the *l*th relay on the *n*th subcarrier and by P_{s} the transmission power of the source. We assume that the central controller has the knowledge of channel gains h_{sl}^{n}, $h_{g,lk}^{n}$ and h_{lm}^{n} and there is a cooperation between primary and secondary user network to get the channel state information. The bandwidth of each subcarrier is *B*.

The central controller decides the joint subcarrier, power allocation and relay assignment. We define $\varepsilon_{g,l}^{n}$ as a binary assignment indicator

$$\varepsilon_{g,l}^{n} = \begin{cases} 1 & if\ the\ lth\ relay\ transmits\ to\ the\ gth\ group\ on\ the\ nth\ subcarrier \\ 0 & otherwise \end{cases}$$

Setting variable $\varepsilon_{g,l}^{n} = 1$ means that the system controller is giving subcarrier *n* to group *g* for data reception and having relay *l* forward the signal carried in subcarrier *n* (to group *g*).

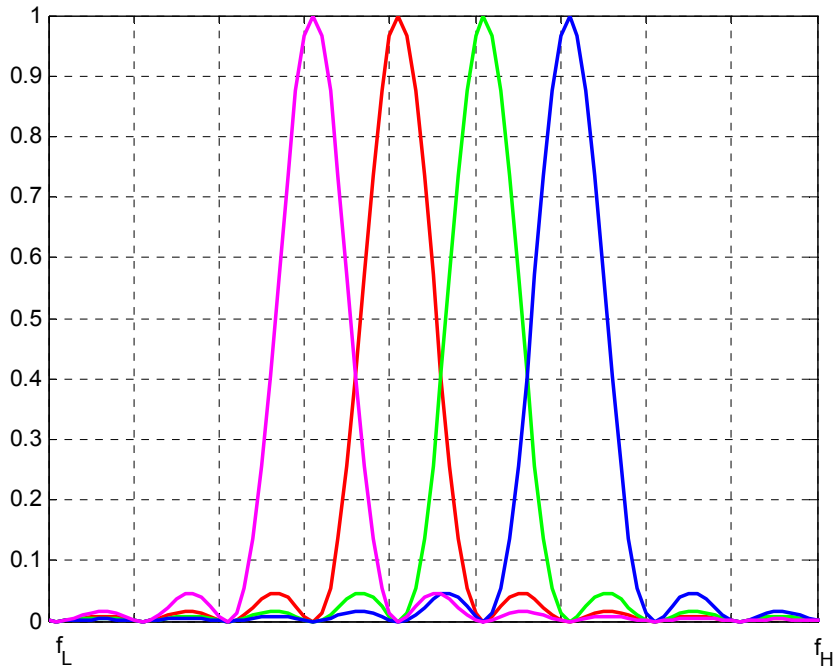

Fig. 4.2 Lower and upper limits of the primary band

The cumulative interference caused by transmission of all the *L* relays on primary users in *l*th relay's band can be written as,

$$\sum_{l=1}^{L}\sum_{n=1}^{N} p_l^n \left|h_{lm}^n\right|^2 \int_{f_L}^{f_U} \phi_l^n(f)df \le I_m^{max} \quad \forall m \tag{4.1}$$

where $p_l^n \phi_l^n(f)$ is the power spectral density of the *l*th relay on *n*th subcarrier and I_m^{max} is the interference limit defined by the regulatory body at each primary user. $\phi_l^n(f)$ can be written as [1]

$$\phi_l^n(f) = T_s \left(\frac{\sin \pi \left(f - f_c^n \right) T_s}{\pi \left(f - f_c^n \right) T_s} \right)^2 \tag{4.2}$$

where $f_c^n = (2n-1)B/2$ is the frequency of the *n*th subcarrier, T_s is the symbol duration, f_L and f_U represent lower and upper limit of the frequency band being used by the primary users (which is also shared by the secondary users) as shown in Fig 4.2.

We consider a two-step amplify-and-forward (AF) scheme, as given in [2] [3]. In such a system, conveyance of each symbol from the source to destination takes place in two time slots. In the first time slot, the source transmits its data symbol for each multicast group on the subcarriers assigned to the multicast group and its associated relays. In the second time slot, relays will transmit amplified signal to the users of a multicast group using the subcarriers assigned to them. In our system modes, we assume that different subcarriers are used to carry different data streams, and a multicast group can receive multiple streams of data through multiple subcarriers. We also assume that no two relays are allowed transmit on the same subcarrier in our subcarrier assignment. Sharing of a subcarrier among multiple relays is possible but it requires coherent combining of the signals transmitted from the different relays, which may be quite challenging in practical systems [8].

The capacity at the *g*th group using the *n*th subcarrier and the *l*th relay [2] [3] is

$$C_{g,l}^n = \log\left(1 + \min\left\{ S_{g,l}^{n,1}, S_{g,l}^{n,2}, \cdots, S_{g,l}^{n,|Kg|} \right\}\right)$$

where $S_{g,l}^{n,k} = \dfrac{\left|h_{sl}^n\right|^2 \left|h_{g,lk}^n\right|^2 P_s^n p_l^n}{\left|h_{sl}^n\right|^2 P_s^n + \left|h_{g,lk}^n\right|^2 p_l^n + 1}$ is the SNR received by the *k*th secondary user of the *g*th multicast group, if the *g*th multicast group is assigned with the *n*th subcarrier and the *l*th relay. For this capacity formula, we assumed that the

strength of the signal received directly from the source is negligible. It can be observed that the capacity of *g*th multicast group is equal to the capacity of the user (in the *g*th multicast group) with the worst channel conditions −i.e. $C_{g,l}^{n} = \log\left(1+S_{g,l}^{n,\tilde{k}}\right) \quad ,\tilde{k} = \arg\min_{k\in Kg}\left|h_{g,lk}^{n}\right|^{2}$. For notational convenience we define, $\left|\tilde{h}_{g,l}^{n}\right|^{2} = \min_{k\in Kg}\left|h_{g,lk}^{n}\right|^{2}$. We can rewrite $C_{g,l}^{n}$ as

$$C_{g,l}^{n} = \log\left(1+\frac{\left|h_{sl}^{n}\right|^{2}\left|\tilde{h}_{g,l}^{n}\right|^{2}P_{s}^{n}p_{l}^{n}}{\left|h_{sl}^{n}\right|^{2}P_{s}^{n}+\left|\tilde{h}_{g,l}^{n}\right|^{2}p_{l}^{n}+1}\right)$$

The main objective of the joint power, subcarrier allocation and relay assignment (JPSARA) is to maximize the total rate of the cooperative MMCRS under the constraint of acceptable interference to the primary users. Mathematically:

$$\begin{aligned}
&\max_{\boldsymbol{\varepsilon},\boldsymbol{p}} \sum_{g=1}^{G}\sum_{n=1}^{N}\sum_{l=1}^{L}\varepsilon_{g,l}^{n}C_{g,l}^{n} \\
&C1:\ \ p_{l}^{n} \geq 0 \ \ \forall(l,n), \\
&C2:\ \sum_{n=1}^{N}p_{l}^{n} \leq p_{l}^{max} \ \ \forall l \\
&C3:\ \sum_{l=1}^{L}\sum_{n=1}^{N}p_{l}^{n}\left|h_{lm}^{n}\right|^{2}\int_{f_L}^{f_U}\phi_{l}^{n}(f)df \ \leq I_{m}^{max} \quad \forall m \\
&C4:\ \sum_{g=1}^{G}\sum_{l=1}^{L}\varepsilon_{g,l}^{n} \leq 1, \ \forall n, \\
&C5:\ \varepsilon_{g,l}^{n} \in \{0,1\} \ \forall(l,g,n)
\end{aligned} \tag{4.3}$$

where *C*2 is the constraint on total transmission power of the relay, *C*3 is the interference constraint and constraint *C*4 ensures that no two relay transmit on a subcarrier. The proposed optimization problem in (4.3) is a mixed integer non-linear optimization problem. The complexity of exhaustive search for joint subcarrier and relay assignment increases exponentially with the number of

subcarriers, relays and groups. We now present a dual decomposition approach to solve the optimization problem in (4.3).

4.1.2 Dual Decomposition Algorithm

For dual decomposition, we can write the Lagrangian function as follows:

$$\begin{aligned}
&= \sum_{g=1}^{G}\sum_{n=1}^{N}\sum_{l=1}^{L}\varepsilon_{g,l}^{n}C_{g,l}^{n} + \sum_{l=1}^{L}\mu_l\left(p_l^{max} - \sum_{n=1}^{N}p_l^{n}\right) \\
&\quad + \sum_{m=1}^{M}\lambda_m\left(I_m^{max} - \sum_{l=1}^{L}\sum_{n=1}^{N}p_l^{n}I_{lm}^{n}\right) \\
&= \sum_{n=1}^{N}\left(\sum_{g=1}^{G}\sum_{l=1}^{L}\varepsilon_{g,l}^{n}C_{l,g}^{n} - \sum_{l=1}^{L}\mu_l p_l^{n} - \sum_{m=1}^{M}\lambda_m\sum_{l=1}^{L}p_l^{n}I_{lm}^{n}\right) \\
&\quad + \sum_{l=1}^{L}\mu_l p_l^{max} + \sum_{m=1}^{M}\lambda_m I_m^{max}
\end{aligned} \tag{4.4}$$

where $\mu_l, l = 1,2,...,L$ and $\lambda_m, m = 1,2,...,M$ are the dual variables for power and interference constraints respectively. The dual problem is

$$\begin{aligned}
&\min_{\boldsymbol{\lambda},\boldsymbol{\mu}} \quad \max_{\boldsymbol{\varepsilon},\boldsymbol{p}} \quad L\left(\boldsymbol{\varepsilon},\boldsymbol{p},\boldsymbol{\lambda},\boldsymbol{\mu}\right) \\
&subject\ to \\
&\qquad \sum_{g=1}^{G}\sum_{l=1}^{L}\varepsilon_{g,l}^{n} \le 1, \qquad \forall n \\
&\qquad p_l^{n} \ge 0, \varepsilon_{g,l}^{n} \in \{0,1\}, \forall\left(l,g,n\right)
\end{aligned}$$

Note that duality gap will not be zero due to the integer constraints. We can decompose (4.4) into *N* sub-problems, which can be independently solved for given $\boldsymbol{\lambda}$ and $\boldsymbol{\mu}$. The sub-problem at any subcarrier *n* is

$$\max_{\bar{\varepsilon},\bar{p}} \left(\sum_{g=1}^{G}\sum_{l=1}^{L} \varepsilon_{g,l}^{n} C_{g,l}^{n} - \sum_{l=1}^{L} \mu_l p_l^n - \sum_{m=1}^{M} \lambda_m \sum_{l=1}^{L} p_l^n I_{lm}^n \right)$$

$$\begin{aligned} &subject\ to \\ &\sum_{g=1}^{G}\sum_{l=1}^{L} \varepsilon_{l,g}^{n} \le 1, \qquad \forall n \\ &p_l^n \ge 0, \varepsilon_{g,l}^{n} \in \{0,1\} \forall g,l,n \end{aligned} \tag{4.5}$$

From (4.5), we can observe that for any fixed $\tilde{l}$ and $\tilde{g}$, we can find the power $\bar{p}$ by solving the following optimization

$$\begin{aligned} &\max \quad C_{\tilde{g},\tilde{l}}^{n} - \mu_{\tilde{l}} p_{\tilde{l}}^{n} - p_{\tilde{l}}^{n} \sum_{m=1}^{M} \lambda_m I_{lm}^{n} \\ &s.t.\ p_{\tilde{l}}^{n} \ge 0 \end{aligned} \tag{4.6}$$

From (4.6), we can get the p_l^n value of power from the following equation:

$$\frac{d}{dp_l^n}\left[\log\left(1 + \frac{\left|h_{sl}^n\right|^2 \left|\tilde{h}_{g,l}^n\right|^2 P_s^n p_l^n}{\left|h_{sl}^n\right|^2 P_s^n + \left|\tilde{h}_{g,l}^n\right|^2 p_l^n + 1} \right) - \mu_l p_l^n - p_l^n \sum_{m=1}^{M} \lambda_m I_{lm}^n \right] = 0,$$

which is equivalent to

$$\frac{\left|h_{sl}^n\right|^2 \left|\tilde{h}_{g,l}^n\right|^2 P_s^n \left(\left|h_{sl}^n\right|^2 P_s^n + 1\right)}{\left(\left|h_{sl}^n\right|^2 P_s^n + 1 + \left|\tilde{h}_{g,l}^n\right|^2 p_l^n + \left|h_{sl}^n\right|^2 \left|\tilde{h}_{g,l}^n\right|^2 P_s^n p_l^n\right)\left(\left|h_{sl}^n\right|^2 P_s^n + 1 + \left|\tilde{h}_{g,l}^n\right|^2 p_l^n\right)} - \mu_l - \sum_{m=1}^{M} \lambda_m I_{lm}^n = 0$$

With some mathematical manipulation, we can obtain

$$p_{\tilde{l}}^{n} = \max\left(0, \frac{\gamma_{\tilde{g},\tilde{l}}^{n} - 2 - \left|h_{s\tilde{l}}^n\right|^2 P_s^n}{2\left|\tilde{h}_{\tilde{g},\tilde{l}}^n\right|^2} \right)$$

where $\gamma_{\tilde{g},\tilde{l}}^{n}=\sqrt{\left|h_{s\tilde{l}}^{n}\right|^{4}\left(P_{s}^{n}\right)^{2}+4\frac{\left|h_{s\tilde{l}}^{n}\right|^{2}\left|\tilde{h}_{\tilde{g},\tilde{l}}^{n}\right|^{2}P_{s}^{n}}{\mu_{\tilde{l}}+\sum_{m=1}^{M}\lambda_{m}I_{lm}^{n}}}$. We denote by Ψ, a matrix whose each element is $\Psi\left(\tilde{g},\tilde{l}\right)$ the cost function using $p_{\tilde{l}}^{n}=\max\left(0,\frac{\gamma_{\tilde{g},\tilde{l}}^{n}-2-\left|h_{s\tilde{l}}^{n}\right|^{2}P_{s}^{n}}{2\left|\tilde{h}_{\tilde{g},\tilde{l}}^{n}\right|^{2}}\right)$. The optimal $\varepsilon_{g,l}^{n}$ for any subcarrier *n* will be

$$\varepsilon_{g,l}^{n}=\begin{cases}1 & (g,l)=(g^{*},l^{*})=\arg\max_{g,l}\Psi(g,l)\\ 0 & otherwise\end{cases} \tag{4.7}$$

The dual variable can be updated as

$$\begin{aligned}\lambda_{m}(t+1)&=\left[\lambda_{m}(t)+\alpha(t)\left(I_{m}^{max}-\sum_{l=1}^{L}\sum_{n=1}^{N}p_{l}^{n}I_{lm}^{n}\right)\right]^{+}\\ \mu_{l}(t+1)&=\left[\mu_{l}(t)+\beta(t)\left(p_{l}^{max}-\sum_{n=1}^{N}p_{l}^{n}\right)\right]^{+}\end{aligned} \tag{4.8}$$

where $\alpha(t)$ and $\beta(t)$ are the step size. A pseudo code for the dual decomposition is mentioned in Table 4.1.

Table 4.1 Dual Decomposition Algorithm.

Step1: *Initialize the dual variables* λ_m *and* μ_l *.*

Step2: *Calculate* $p_{\tilde{l}}^{n}=\max\left(0,\frac{\gamma_{\tilde{g},\tilde{l}}^{n}-2-\left|h_{s\tilde{l}}^{n}\right|^{2}P_{s}^{n}}{2\left|\tilde{h}_{\tilde{g},\tilde{l}}^{n}\right|^{2}}\right)$

Step3: *Get* $\Psi\left(\tilde{g},\tilde{l}\right)$ *and* $\varepsilon_{g,l}^{n}$ *using (4.7)*

Step4: *update dual variables using (4.8)*

Step5: *Go to Step 2 if convergence criterion is not satisfied*

4.1.3 Computational complexity of dual decomposition algorithm

We measure the computational complexity in terms of flops Υ [5]. In each subcarrier, approximately *GLM* flops are required to calculate Ψ and *GL* flops required to get the maximum of Ψ. It means a total of $GLMN + GLN$ flops for all *N* subcarriers. The update of dual variables required $GLMN + GLN + 3M + 3L$ flops. The overall complexity of algorithm will be $I_{sub}\left(2GLMN + 2GLN + 3M + 3L\right)$, where I_{sub} is the number of iterations for sub-gradient method. The complexity of proposed dual decomposition based algorithm will be more for large network size; also, more number of iterations will be required to converge to an acceptable solution. In the next section, we present a low-complexity iterative algorithm for joint subcarrier, relay assignment and power allocation (JPSARA).

4.1.4 Iterative Algorithm for JPSARA

For efficient subcarrier, power allocation and relay assignment in MMCRS, we present a low-complexity iterative greedy algorithm for joint power, subcarrier allocation and relay assignment (IJPSARA). The pseudo code of the proposed algorithm is shown in Table 4.2.

This iterative algorithm is based on the plausible reasoning that the signal-to-noise ratio of a secondary user on any subcarrier mostly depends on the transmission power of the relay assigned to the multicast group (to which this secondary user belongs) and the channel gain from this relay to the multicast group[3]. The objective of optimization (4.3) is to maximize the total sum-rate capacity in MMCRS. Further, in optimization (4.3), the interference constraints may not always allow assigning the best multicast group[4], the relays and subcarriers with which it has good channel condition. In this algorithm, we introduce a strategy that considers channel gains from both relay to the secondary user and relay to primary users while assigning relays to the multicast

[3] Means worst user of the group

[4] Best group is defined as the group with best worst channel condition among all the groups.

groups. The algorithm considers the channel gain between the relays and the secondary users as a profit (throughput) and the channel gain between the relays and the primary users as a loss (interference). We want to choose the relay for transmission that will give maximum profit to loss ratio. In other words, the algorithm assigns a relay to that multicast group with which it has the maximum ratio of channel gains with the secondary users to the channel gain with the worst primary user[5] −i.e. the algorithm first determines assigned relay, group and subcarrier using the expression

$$\left[\tilde{g},\tilde{l},\tilde{n}\right]=\underset{g\in\{1,2,\ldots,G\},l\in\{1,2,\ldots,L\},n\in\Gamma_N}{\arg\max}\frac{\left|h_{sl}^{n}\right|^2\left(\left|\tilde{h}_{g,l}^{n}\right|^2\right)}{max\left(\left|h_{l1}\right|^2,\left|h_{l2}\right|^2,\cdots\left|h_{lM}\right|^2\right)}; \tag{4.9}$$

The relay $\tilde{l}$ that is assigned to the group $\tilde{g}$ will transmit on subcarrier $\tilde{n}$. In (4.9), Γ_N is the set of available subcarriers. After getting $\tilde{g},\tilde{l},$ and $\tilde{n}$, the algorithm determines the power of the selected relay. In Table 4.2, there is a sub-routine '*Evaluate'* that jointly performs the power allocation and interference calculation.

We denote by p_l^{Sum}, the total power allocated for the *l*th relay, I_m^{sum} is the cumulative interference on the *m*th primary user. The algorithm is initialized as $p_l^{Sum}=0,\ I_m^{sum}=0,\forall m,p_l^n=0,\ \varepsilon(g,l,n)=0\ \forall g,l,n$ and $C(g,k)=0,\forall(g,k)$.

The power of the selected relay is calculated using the expression

$$p_{\tilde{l}}^{\tilde{n}}=min\left\{\left(p_{\tilde{l}}^{\max}-p_{\tilde{l}}^{sum}\right),\left(\frac{I_m^{max}-I_m^{sum}}{\left|h_{\tilde{l}m}^{\tilde{n}}\right|^2\int_{f_L}^{f_U}\phi^{\tilde{n}}(f)df}\right),\forall m\right\}; \tag{4.10}$$

where p_l^{Sum} is the total power allocated for the *l*th relay and I_m^{sum} is the cumulative interference on the mth primary user. Initially, the values of p_l^{Sum},I_m^{sum}, and p_l^n are set to zero. The expression in (4.10) jointly ensures that the allocated power satisfy the interference and power constraints.

[5] Worst primary user is the primary user that has best channel with the relay.

After getting the power level of the relay $\tilde{l}$ at the *n*th subcarrier, the proposed algorithm updates the capacity of all users in the group $\tilde{g}$. The algorithm terminates when all the subcarriers are assigned.

Table 4.2 Iterative greedy algorithm for JPSARA sum-rate maximization

INITIALIZATION:

$p_l^{Sum}=0, p_l^n=0\,\forall(l,n), I_m^{sum}=0, \forall m, \Gamma_N=\{1,2,...,N\}$, $\varepsilon(g,l,n)=0\ \forall g,l,n$

while $\Gamma_N \neq \varnothing$

1: $\left[\tilde{g},\tilde{l},\tilde{n}\right]=\underset{g\in\{1,2,...,G\},l\in\{1,2,...,L\},n\in\Gamma_N}{\arg\max}\ \dfrac{\left|h_{sl}^n\right|^2\left(\left|\tilde{h}_{g,l}^n\right|^2\right)}{max\left(\left|h_{l1}\right|^2,\left|h_{l2}\right|^2,\cdots\left|h_{lM}\right|^2\right)}$;

2: $(C,I_m^{sum},\varepsilon)$ **=Evaluate** $(\tilde{g},\tilde{l},\tilde{n},C,I_m^{sum},\varepsilon)$

3: $\Gamma_N := \Gamma_N \setminus \tilde{n}$;

End

$(C,I_m^{sum},\varepsilon)$ **=Evaluate** $(\tilde{g},\tilde{l},\tilde{n},C,I_m^{sum},\varepsilon)$

1: $p_{\tilde{l}}^{\tilde{n}}=min\left\{\left(p_{\tilde{l}}^{\max}-p_{\tilde{l}}^{sum}\right),\left(\dfrac{I_m^{max}-I_m^{sum}}{\left|h_{\tilde{l}m}^{\tilde{n}}\right|^2\int_{f_L}^{f_U}\phi^{\tilde{n}}(f)df}\right),\forall m\right\}$;

2: $I_m^{sum}:=I_m^{sum}+p_{\tilde{l}}^{\tilde{n}}\left|h_{\tilde{l}}^{\tilde{n}}\right|^2\int_{f_L}^{f_U}\phi^{\tilde{n}}(f)df \qquad \forall m$

3: $\varepsilon\left(\tilde{g},\tilde{l},\tilde{n}\right)=1$;

4: $p_{\tilde{l}}^{sum}:=p_{\tilde{l}}^{sum}+p_{\tilde{l}}^{\tilde{n}}$;

5: Update Capacity

Output: $\boldsymbol{p,\varepsilon}$

Calculation of computational complexity of IJPSARA is very straightforward. The step 1 of the proposed IJPSARA algorithm requires *GLN* flops, and the *Evaluate* routine require approximately 6*MN*+15*N* flops. The total number of flops require by the proposed greedy algorithm is *GLN+6MN+15N* which is much less than the complexity of dual decomposition approach.

4.1.5 Numerical Results

For performance comparison, we present the simulation results of the proposed iterative greedy algorithm. In our simulations, the channel gains between source, relays and destinations have independent complex Gaussian distribution.

In Figs. 4.3, 4.4 and 4.5, we present the plot for sum-capacity versus interference threshold, $I_m^{\max}$. For these three scenarios, we use ($p_l^{\max}$, *L, N, G,* |*K*|*,B, T*$_s$) = (0.1w, 2, 8, 2, 200, 1MHz, 1*μ* Sec), (0.1w, 2, 128, 4, 150, 1MHz, 1*μ* Sec) and (0.1w, 2, 64, 4, 100, 1MHz, 1*μ* sec). In all these Figs., *w*e observe that as $I_m^{\max}$ increases the capacity increases. This is because at smaller values of $I_m^{\max}$ certain relays and subcarriers, which yield higher capacity, are not optimal because they violate the interference constraint at primary users but at larger values of $I_m^{\max}$ these relays satisfy the interference constraint. We can also observe that proposed IJPSARA is close to the dual. In Fig. 4.6, we present the plot for sum-capacity versus number of primary users. We use ($p_l^{\max}$, *L, N, G,* |*K*|*,B, T*$_s$) = (0.1w, 2, 32, 4, 200, 1MHz, 1*μ* Sec). The interference threshold is set to $I_m^{\max}$ = {100uw, 1mw, 10mw}.From the result, we observe that the sum-capacity decreases with the increase in number of primary users. This is because by increasing the number of primary users, the secondary users need to satisfy more interference constraints. From the numerical results, Fig 4.7 and Table 4.3, we can see that IJPSARA converges to with in 70-85 percent of that obtained by the dual decomposition algorithm.

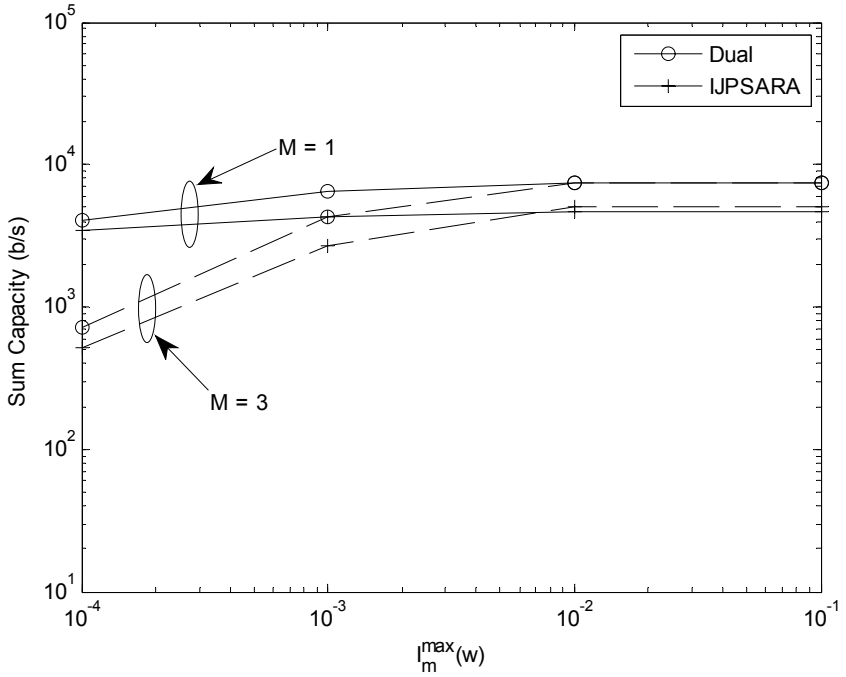

Fig. 4.3 Performance of IJPSARA with $p_l^{\max} = 0.1\text{w},$, *L* = 2, *N* = 8, *G* = 2, $|K_g|$ =*200* , g = 1, 2,…,*G* ,*B* = 1M Hz, and T_s = 1μ sec

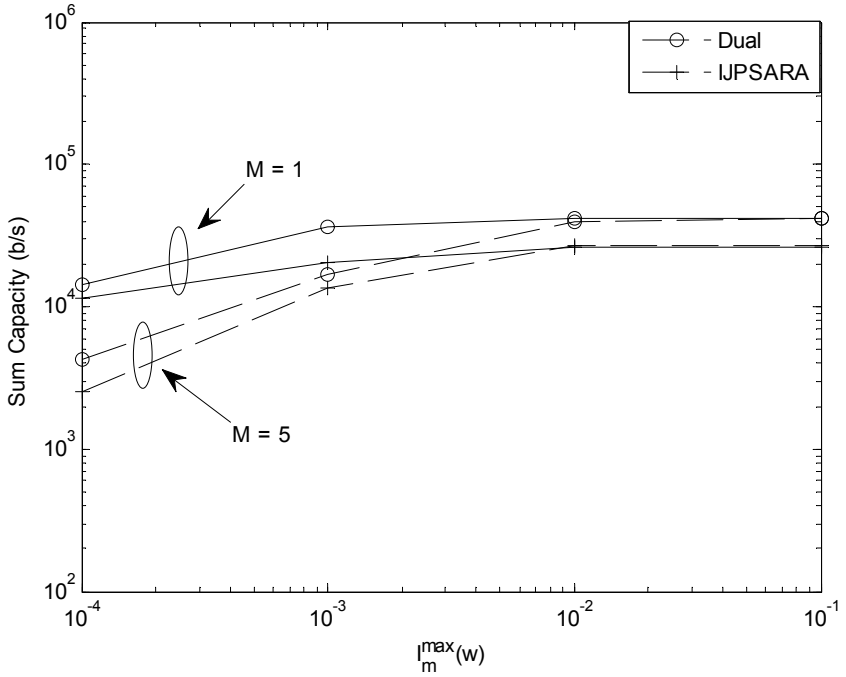

Fig. 4.4 Performance of IJPSARA with $p_l^{\max} = 0.1\text{w},$, *L* = 2, *G* = 4, *N* = 128, $|K_g|$ =*150* , g = 1, 2,…,*G* ,*B* = 1M Hz, and T_s = 1μ sec

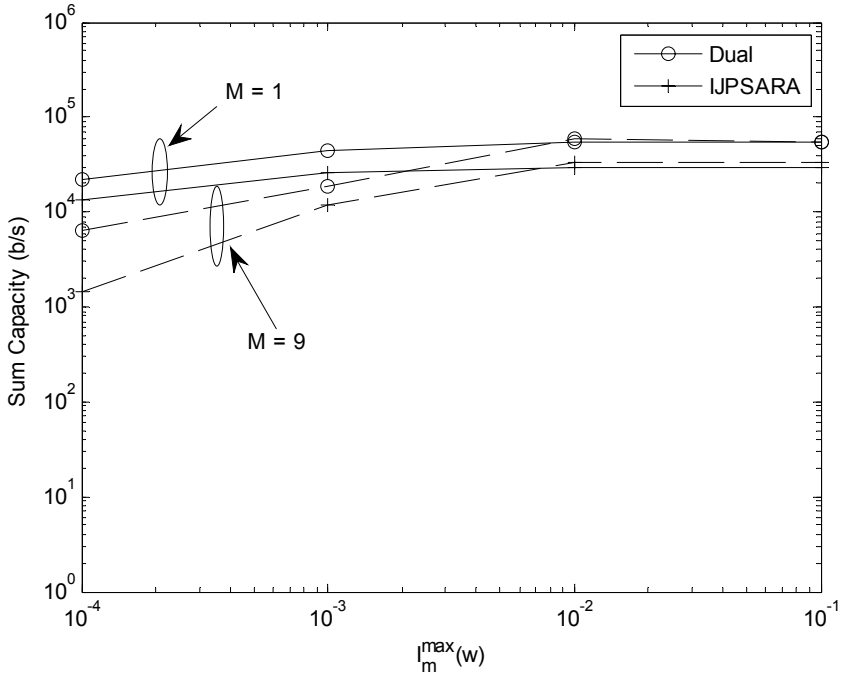

Fig. 4.5 Performance of IJPSARA with $p_l^{\max} = 0.1\text{w},$, *L* = 2, *G* = 4, *N* = 64, $|K_g|$ =*100* , g = 1, 2,…,*G* ,*B* = 1M Hz, and T_s = *1*μ sec

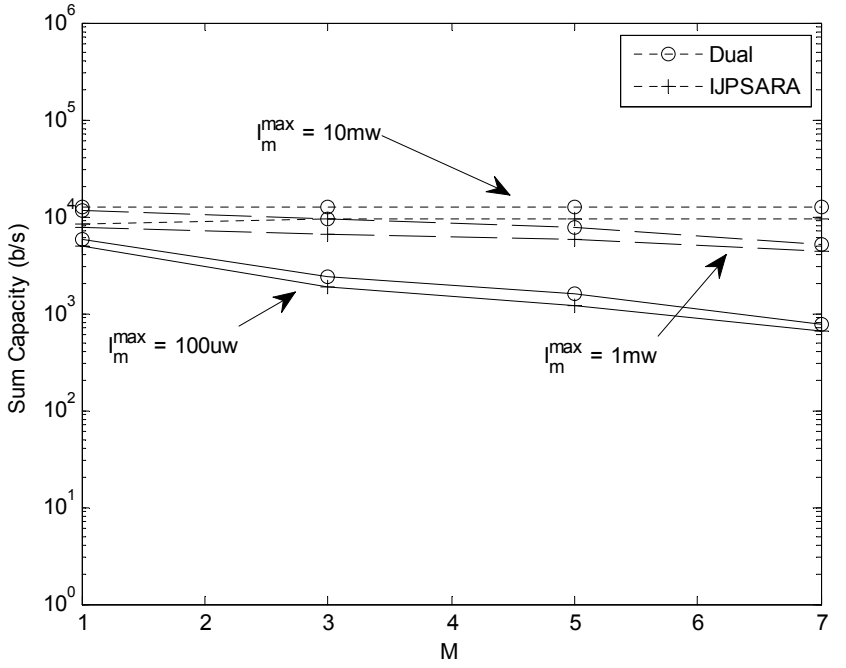

Fig. 4.6 Performance of IJPSARA with $p_l^{\max} = 0.1\text{w},$, *L* = 2, *G* = 4, *N* = 32, $|K_g|$ =*100* , g = 1, 2,…,*G* ,*B* = 1M Hz, and T_s = 1μ sec

Table 4.3 Percentage IJPSARA performance to Dual algorithm

Parameters [L,G,N,M, $I_m^{\max}$]	**M = 1**	**M = 3**	**M = 5**	**M = 7**
[2,4,32,1,10mw]	70.81%	73.98%	73.93%	74.28%
[2,4,32,1,1mw]	85.57%	78.12%	74.29%	84.88%

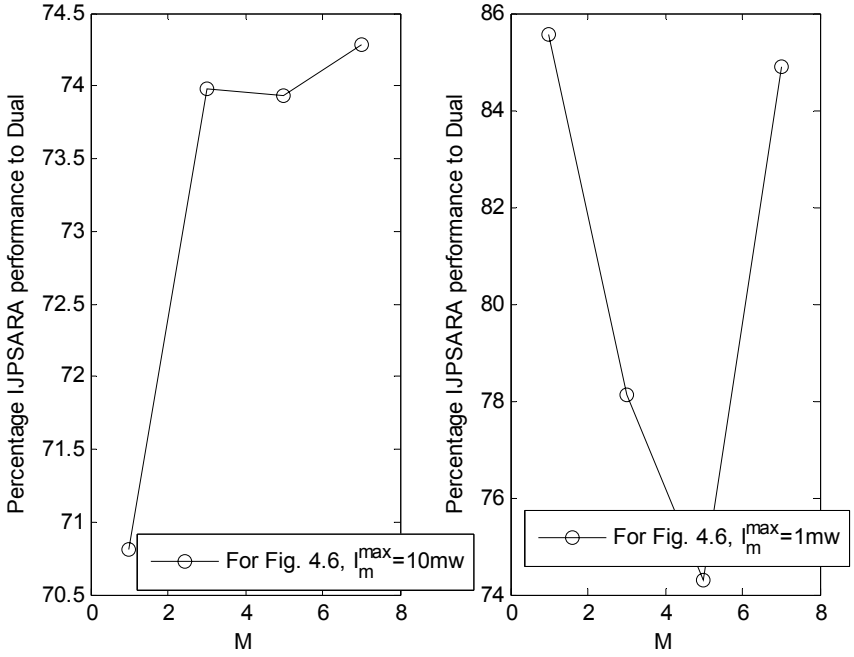

Fig. 4.7 Percentage IJPSARA performance to the Dual algorithm

4.2 Max-Min Resource Allocation in Multicast CRS

In max-min multicast CRS (MMCRS), we define the capacity of each multicast group as the capacity of its worst user. The mismatch of data rate among users in a group occurs because different users in the group can have different channel conditions. The main objective of JPSARA is to maximize the rate of the worst group of users under the constraint of acceptable interference to the primary users. Mathematically:

$$\max_{\varepsilon_{l,g}^{n}\in\{0,1\},p}\ \min_{g=1,2,\ldots,G}\ \sum_{n=1}^{N}\sum_{l=1}^{L}\varepsilon_{l,g}^{n}C_{g,l}^{n}$$

$$C1:\sum_{n=1}^{N}p_{l}^{n}\le p_{l}^{max}\ \ \forall l$$

$$C2:\ \sum_{l=1}^{L}\sum_{n=1}^{N}p_{l}^{n}\left|h_{lm}^{n}\right|^{2}\int_{f_L}^{f_U}\phi_{l}^{n}(f)df\ \le I_{m}^{max}\quad \forall m \tag{4.11}$$

$$C3:\sum_{g=1}^{G}\sum_{l=1}^{L}\varepsilon_{l,g}^{n}\le 1,\ \forall n,$$

$$C4:\ p_{l}^{n}\ge 0,\ \ \forall l,n$$

Constraint *C*1 is the constraint on total transmission power of the relay. Constraint *C*2 is the interference constraint. Constraint *C*3 ensures that no two relay transmit on a subcarrier. It means that relays' transmissions occur on orthogonal subcarriers. Sharing of a subcarrier among multiple relays is possible but it requires coherent combining of the signals transmitted from the different relays, which may be quite challenging in practical systems [8].

An obvious way to solve the non-linear optimization problem in (4.11) is to exhaustively try all the combinations of assignment variables and solve the subsequent nonlinear convex optimization problem using standard convex optimization methods (e.g., interior point method [6] etc.). However, enumeration of all the combinations of assignment variables requires intense computation due to the combinatorial nature of the problem. Therefore, there is a need of low-complexity algorithms for JSPARA. In the next section, we will present low-complexity approach for JSPARA.

4.2.1 Proposed Algorithm and Complexity Analysis

For efficient subcarrier, power allocation and relay assignment in MMCRS, we present a low-complexity iterative greedy max-min algorithm for joint power, subcarrier allocation and relay assignment (IJSPARA). The pseudo code of the proposed algorithm is shown in Table 4.4. The algorithm is similar to the algorithm described in section 4.1.2.

The algorithm considers the channel gain between the relays and the secondary users as a profit (throughput) and the channel gain between the relays and the primary users as a loss (interference). At the start of the algorithm, equations (4.9) and (4.10) are used to select the multicast group $\tilde{g}$, relay $\tilde{l}$, subcarrier $\tilde{n}$ and power $p_{\tilde{l}}^{\tilde{n}}$. The power determined by (4.10) greedily allocates the power to the selected group of users.

To introduce max-min fairness in the system, we introduced a factor $\delta \geq 1$ (we call as greediness control factor) to control the greediness in the power allocation. If we set greediness control factor near to one ($\delta \approx 1$) then the multicast group with best channel condition will always get the maximum benefit and the multicast group with bad channel will always get least benefit. Less value of greediness control factor is useful when one want to maximize the total profit (i.e. sum-rate capacity). In the present scenario, we want to maximize the minimum profit (i.e. worst multicast group capacity). For max-min optimization problem, the value of δ is selected so that there is always a win-win situation for every multicast group. In the numerical results (section 4.2.2), we show the effect of different values of δ on the performance of the system. In the simulation results, we show that a proper value of δ improves the performance of the proposed algorithm.

After getting the power level of the relay $\tilde{l}$ using controlled greediness, the proposed algorithm updates the capacity of all users in the group $\tilde{g}$. In the next step, the algorithm iterates over the remaining subcarriers. In each iteration, the algorithm selects that multicast group that has the lowest capacity using the expression

$$[\tilde{g}] = \arg\min_{g}(C)$$

Then the relay and subcarrier that has the maximum ratio of channel gain with the group $\tilde{g}$ to the worst channel gain with primary user is determined as

$$\left[\tilde{l},\tilde{n}\right]=\underset{l\in\{1,2,\ldots,L\},n\in\Gamma_N}{\arg\max}\ \frac{\left|h_{sl}^{n}\right|^2\left(\left|\tilde{h}_{\tilde{g},l}^{n}\right|^2\right)}{max\left(\left|h_{l1}\right|^2,\left|h_{l2}\right|^2,\cdots\left|h_{lM}\right|^2\right)};$$

again the *Evaluate* subroutine is used to determine the power of the $\tilde{l}th$ relay on the $\tilde{n}th$ subcarrier. The algorithm terminates when all the relays powers are determined.

The main advantage of the proposed algorithm is its low implementation complexity. Complexity is measured in terms of flops Υ. The Table 4.4 shows the flop of each operation. From Table 4.4, we can determine the total number of flops require by the proposed greedy algorithm. The total numbers of flops are

$$\begin{aligned}\Upsilon &\approx 2LM+N\left(3M+LN+GL+G+12\right)\\ &\approx O\left(GLN^2\right)\end{aligned}$$

Table 4.4 IJPSARA for MMCRS

IJPSARA	Flops
INITIALIZATION: $p_l^{Sum}=0, p_l^n=0\,\forall(l,n), I_m^{sum}=0, \forall m, \Gamma_N=\{1,2,...,N\},$ $\varepsilon(g,l,n)=0\ \forall g,l,n$	
1: $\left[\tilde{g},\tilde{l},\tilde{n}\right]=\underset{g\in\{1,2,...,G\},l\in\{1,2,...,L\},n\in\Gamma_N}{\arg\max}\ \frac{\left\|h_{sl}^n\right\|^2\left(\left\|\tilde{h}_{g,l}^n\right\|^2\right)}{max\left(\left\|h_{l1}\right\|^2,\left\|h_{l2}\right\|^2,\cdots\left\|h_{lM}\right\|^2\right)};$ **2:** $(C,I_m^{sum},\varepsilon)$ **=Evaluate** $(\tilde{g},\tilde{l},\tilde{n},C,I_m^{sum},\varepsilon)$ ***While*** $\Gamma_N\neq\varnothing$ **3:** $\left[\tilde{g}\right]=\arg\min_g(C);$ **4:** $\left[\tilde{l},\tilde{n}\right]=\underset{l\in\{1,2,...,L\},n\in\Gamma_N}{\arg\max}\ \frac{\left\|h_{sl}^n\right\|^2\left(\left\|\tilde{h}_{g,l}^n\right\|^2\right)}{max\left(\left\|h_{l1}\right\|^2,\left\|h_{l2}\right\|^2,\cdots\left\|h_{lM}\right\|^2\right)};$ **5:** $(C,I_m^{sum},\varepsilon)$ **=Evaluate** $(\tilde{g},\tilde{l},\tilde{n},C,I_m^{sum},\varepsilon)$ **6:** $\Gamma_N:=\Gamma_N\setminus\{\tilde{n}\};$ ***End***	1:LM+GLN 2: 3M+12 3:GN 4:LM+LN^2 6:*N*
$(C,I_m^{sum},\varepsilon)$ **=Evaluate** $(\tilde{g},\tilde{l},\tilde{n},C,I_m^{sum},\varepsilon)$ **1:** $p_{\tilde{l}}^{\tilde{n}}=min\left\{\left(p_{\tilde{l}}^{\max}-p_{\tilde{l}}^{sum}\right),\left(\frac{I_m^{max}-I_m^{sum}}{\left\|h_{\tilde{l}m}^{\tilde{n}}\right\|^2\int_{f_L}^{f_U}\phi^{\tilde{n}}(f)df}\right),\forall m\right\};$ **2:** $p_{\tilde{l}}^{\tilde{n}}:=p_{\tilde{l}}^{\tilde{n}}/\delta$ **3:** $I_m^{sum}:=I_m^{sum}+p_{\tilde{l}}^{\tilde{n}}\left\|h_{\tilde{l}}^{\tilde{n}}\right\|^2\int_{f_L}^{f_U}\phi^{\tilde{n}}(f)df\qquad\forall m$ **4:** $\varepsilon\left(\tilde{g},\tilde{l},\tilde{n}\right)=1;$ **5:** $p_{\tilde{l}}^{sum}:=p_{\tilde{l}}^{sum}+p_{\tilde{l}}^{\tilde{n}};$ **6***: Update* capacity	1:M 2:1 3: 2M 4:1 5:1 6:8
Output: $\boldsymbol{p,\varepsilon}$	

4.2.2 Numerical Results

For performance comparison, we present the simulation results of the proposed iterative algorithm. In our simulations, the channel gains between source, relays and destinations have independent complex Gaussian distribution. For a comparison, we suggest an upper bound on the JPSARA by relaxing the integer constraint $\varepsilon_{l,g}^{n}$ and solve this optimization problem using non-linear programming techniques.

In Fig. 4.8, we present the plot for minimum group capacity versus interference threshold, $I_m^{\max}$. We use $p_l^{\max} = 5\text{w}$, *L* = 3, *N* = 10, *B* = 1M Hz, and T_s = 1*μ* sec. The greediness control factor δ is set to two and four. We observe that as $I_m^{\max}$ increases the capacity increases. This is because at smaller values of $I_m^{\max}$ certain relays and subcarriers, which yield higher capacity, are not optimal because they violate the interference constraint at primary users but at larger values of $I_m^{\max}$ these relays satisfy the interference constraint. In Figs 4.9 and 4.10, we present the effect of greediness control factor δ δ on the performance of proposed iterative greedy algorithm. We used two different scenarios (*K, M, L, G, N, B,* T_s, $p_l^{\max}$) = (2, 1, 3, 8, 16, 1MHz, 1μ sec, 5w) and (3, 4, 3, 8, 16, 1MHz, 1μ sec, 5w). In both scenarios, the interference threshold is set to $I_m^{\max}$ = {10μw, 100μw, 1mw, 10mw}. From Figs. 4.9 and 4.10, we observe that if greediness control factor is set to one, the worst group capacity will be close to zero. This is because the maximum power will be given to the selected relay and subcarrier. It will be difficult for the remaining subcarriers and relays to allocate any power because of constraint C2 of equation (4.9). On the other hand, if the value of greediness control factor is high, the worst group capacity will be low because available power may not be fully utilized. In Fig 4.10, we present the plot for minimum group capacity versus number of primary users. We use, $p_l^{\max} = 5\text{w}$, *L* = 3, *N* = 10, *B* = 1M Hz, and T_s = 1μ sec. The greediness control factor δ is set to two and four. The interference threshold is set to $I_m^{\max}$ = {1μw, 10μw,

100uw}.From the result, we observe that the minimum group capacity decreases with the increase in number of primary users. This is because by increasing the number of primary users, the secondary users need to satisfy more interference constraints.

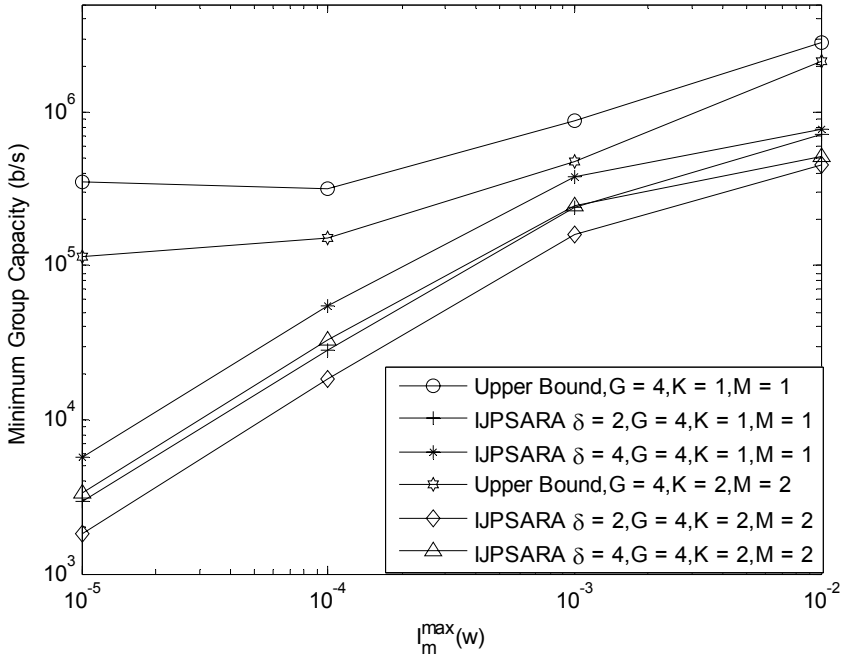

Fig. 4.8 Performance comparison of the multiuser multicast relay network with, $p_l^{\max} = 5\text{w},$, L = 3, N = 10, B = 1M Hz, and T_s = 1μ sec

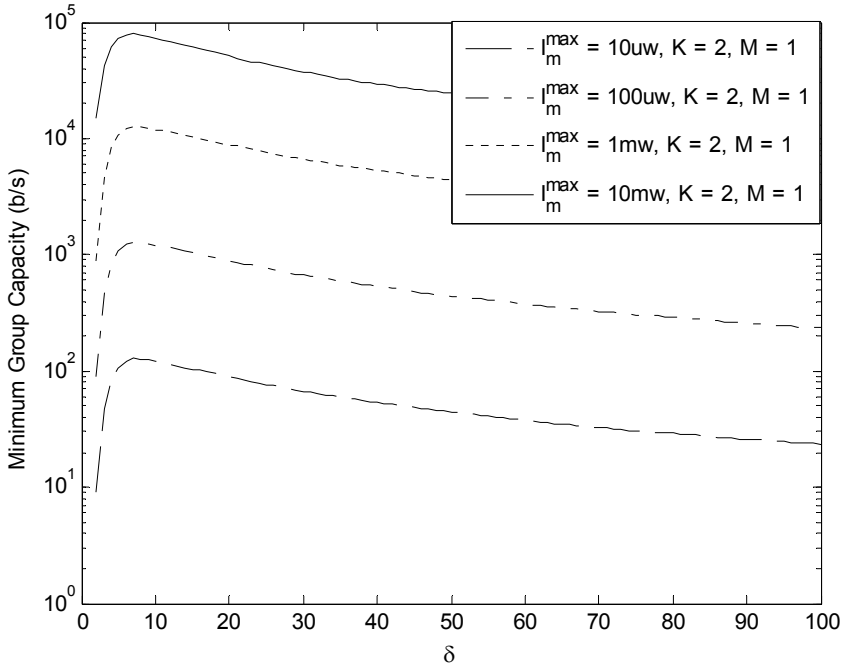

Fig. 4.9 Effect of greediness control factor on the performance of proposed algorithm with $p_l^{\max} = 5\text{w}$, L = 3, N = 16, G = 8, B = 1M Hz, and T_s = 1μ sec

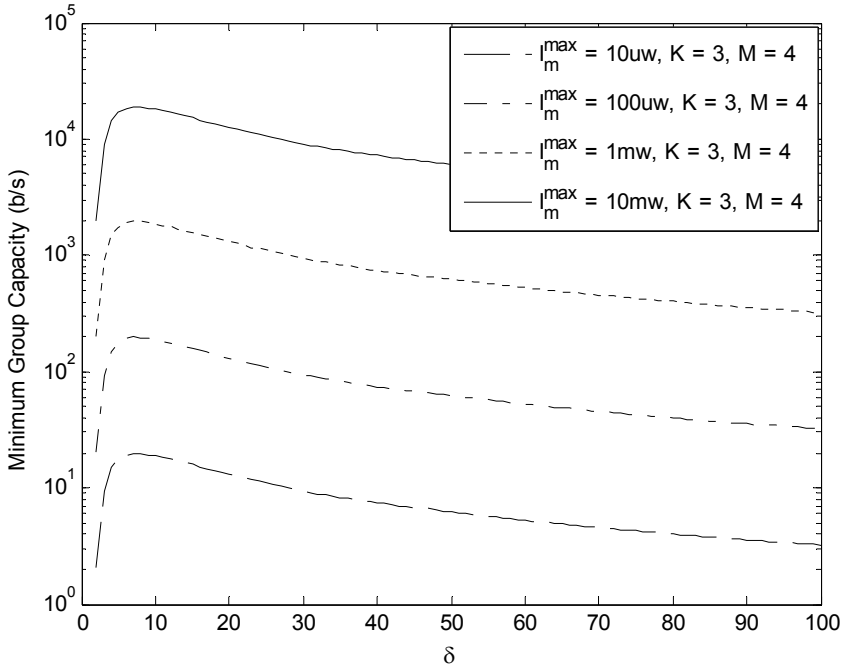

Fig. 4.10 Effect of greediness control factor on the performance of proposed algorithm with $p_l^{\max} = 5\text{w}$, L = 3, N = 16, G = 8, B = 1M Hz, and T_s = 1μ sec

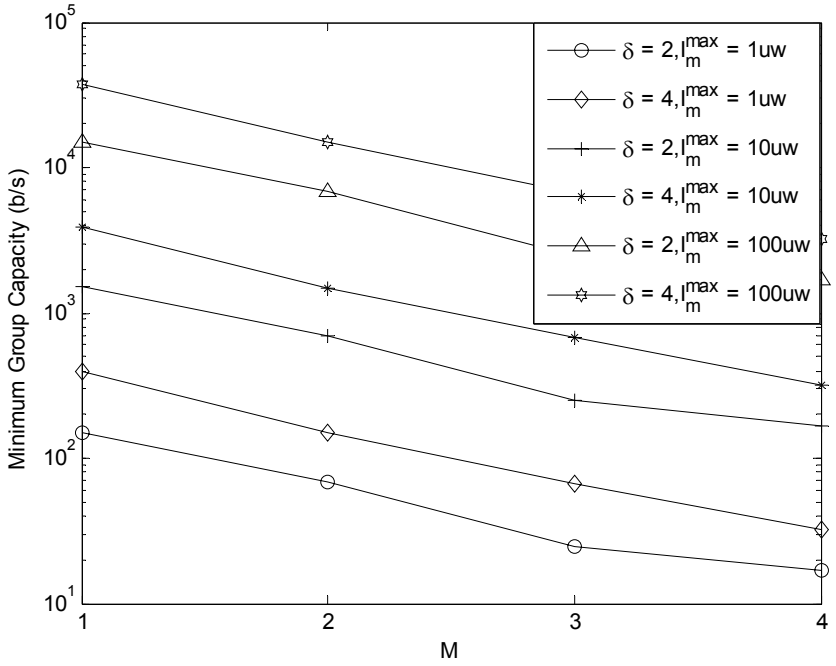

Fig. 4.11 Minimum group capacity vs. the number of primary users with $p_l^{\max} = 5\mathrm{w},$, L = 3, N = 10, G = 4, K = *3,B* = 1M Hz, and T_s = 1μ sec.

To check the feasibility of the proposed algorithms for practical implementation, in Table 4.5, we present the number of flops required by ESA, Dual, and IJPSARA for different parameter settings (i.e., different search space size). The comparison shows that the number of flops required by IJPSARA and Dual algorithms is much less than that of ESA.

Table 4.5 Number of flops required by ESA, Dual and IJPSARA

Parameters [G,L,M,N,I_{sub}]	ESA	Dual	IJPSARA
[2,5,1,8,25]	1.0737e+009	8450	248
[2,5,1,32,25]	1.1259e+015	32450	992
[2,5,1,64,25]	1.1529e+018	64450	1984
[5,10,10,8,25]	1.4272e+045	221500	1000
[5,10,10,32,25]	1.8093e+075	881500	4000
[5,10,10,64,25]	2.0370e+090	1761500	8000
[10,10,10,8,25]	2.030e+090	441500	1400
[10,10,10,32,25]	3.2734e+150	1761500	5600
[10,10,10,64,25]	4.1495e+180	3521500	11200

4.3 Summary

In this chapter, we presented two iterative algorithms for joint power, subcarrier allocation and relay assignment (JPSARA) scheme for MMCRS. The proposed algorithms have low computational complexity. The simple model and low implementation complexity make the proposed algorithms suitable candidates for solving JPSARA problems.

4.4 Chapter References

[1] T. Weiss, A. Krohn, J. Hillenbrand, and F. Jondral, " Mutual Interference in OFDM-based Spectrum Pooling Systems," In Proceedings of IEEE Vehicular Technology Conference *VTC-Spring* Milan, Italy, May 17-19, 2004.

[2] J. N. Laneman, D. N. C. Tse, and G. W. Wornell, "Cooperative Diversity in Wireless Networks: Efficient Protocols and Outage Behavior," *IEEE Trans. Inform. Theory*, vol. 50, no. 12, pp. 3062-3080, Dec. 2004.

[3] Y. Jing and H. Jafarkhani, “Single and multiple relay selection schemes and their achievable diversity orders,” *IEEE Transactions on Wireless Communications*, vol. 8, no. 3, pp. 1414 - 1423, Mar. 2009.

[4] W. Yu and R. Lui, “Dual Methods for Non-convex Spectrum Optimization of Multicarrier Systems,” IEEE Transactions on Communications, vol. 54, no. 7, pp.1310-1322, July 2006.

[5] G. H. Golub and C. F. Van Loan, *Matrix Computations*, the Johns Hopkins Univ. Press, 1983.

[6] S. Boyd and L. Vandenberghe, *Convex Optimization,* Cambridge Univ. Press, 2004.

[7] H. Kellerer, Ulrich Pferschy, David Pisinger, *knapsack Problems*, Springer Verlag. 2005.

[8] I. Maric and R. D. Yates, “Bandwidth and Power Allocation for Cooperative Strategies in Gaussian Relay Networks,” IEEE Trans. Inform. Theory, vol. 56, no. 4, pp. 1880-1889, Apr. 2010.

PART 3: USER SCHEDULING

CHAPTER 5: USER SCHEDULING AND POWER ALLOCATION IN CRS

Generally, in wireless communications, the multiple-input-multiple-output (MIMO) system can achieve higher channel capacity than the single-input-single-output (SISO) system for the same total transmission power and bandwidth [1]. We consider a network of cognitive radio communication systems in which the secondary users and their base station are equipped with multiple antennas and MIMO processing capabilities. We address user scheduling and power control in the uplink multiuser MIMO CRS. We consider the system in which a node's transmission power can be chosen from only a finite set of values; reducing the number of possible power levels reduces the number of bits in the power control message and the complexity of the transmitting node. For each time-frame (block, or slot), the base station ought to select the best group of users and their transmission power levels under the constraint that the interference to the primary users is below a specified level. We consider the sum-rate capacity of the multiuser MIMO multiple access channels as the performance measure to maximize with the assumption that the base station has the full knowledge of the channel conditions. We will refer to this problem as joint secondary user selection/scheduling and quantized power control (JSUS-QPC). Discrete power levels make this optimization problem combinatorial in nature.

The exhaustive search algorithm (ESA) is an obvious method of non-linear integer programming problems such as JSUS-QPC problem. Exhaustive search algorithm evaluates all possible ways of user scheduling and power levels. The complexity of exhaustive search for JSUS-QPC increases exponentially with the number of users and power levels. Therefore, the exhaustive search algorithm is not suitable for real-time user selection/scheduling and power control decisions, which should be made at each time slot (frame). In a real-time environment, the channel conditions may vary from slot to slot, and the decision of the uplink

transmission power levels should be made at each time slot. The algorithm for making such decisions should be computationally efficient. Traditional user scheduling schemes in multiuser MIMO systems [2],[3],[4] and [5] are not applicable in cognitive radio networks because the selected subset of users, which maximizes the sum-rate capacity in traditional multiuser MIMO systems, may generate more interference to the primary users than allowed.

For fast user selection and power control, we present three low-complexity algorithms. We introduce 1) Estimation-of-distribution algorithm (EDA) 2) interference aware capacity maximization algorithm (IACMA), and 3) iterative user scheduling with interference minimization algorithm (IUSIM). The IACMA, in each iteration, incrementally selects one secondary user with suitable power level that has the maximum single-user capacity and whose addition in the set of selected users keeps the total interference at the primary users below the specified interference threshold. The IUSIM algorithm, in each iteration, incrementally selects one user that induces the minimum interference to the primary users. The proposed IACMA and IUSIM schemes have quadratic complexity with respect to the number of secondary users K. Our experiments indicate that the sum-rate capacity achieved by the proposed schemes is close to that of the exhaustive search algorithm.

Table 5.1 Notations

Symbol	Definition
K	Number of secondary users
M	Number of primary users
N_T	Number of Transmit Antennas of each secondary user
N_R	Number of Receive Antennas at base station
$H_{k,bs}$	Channel matrix between the base station and the kth secondary user
$H_{k,m}$	Channel matrix between the mth primary user and the kth secondary user
P_k	power of the kth secondary user
I_{N_R}	Identity matrix of dimension $N_R \times N_R$
K_s	Maximum number of secondary user that can be selected to transmit at the given time slot
ϕ	Set of selected secondary users
$I_m^{\max}$	Maximum tolerable interference threshold for the mth primary user
λ	Number of power levels
$P_k^{\max}$	Maximum allowed transmission power of the kth secondary user
P_L	Set of discrete power levels
Ψ_{FS}	Set of final selected secondary users
Ψ_{PS}	Set of current partially selected secondary users
$\Gamma_{k,C}$	Capacity of the kth secondary user
$\Gamma_{k,m,I}$	Interference from the kth secondary user to the mth primary user
I_m^{sum}	Cumulative interference induced at mth primary user from the selected secondary users
$\Gamma_{k,I}^{Sum}$	Total interference induced by the kth secondary user

5.1 System Model

We consider information flow through uplinks of K secondary mobile users each equipped for MIMO communication. Each secondary user has N_T transmit antennas, and the central controller/base station of secondary users has N_R receive antennas. There are M primary users with single receive antenna. We assume that the secondary users do not have their uplink channel side information (CSI), but the base station has the channel state information (CSI) for

both secondary and primary users. Since the secondary users do not have the uplink CSI, it is reasonable for each of them to allocate equal transmission power to each of their transmission antennas. We denote by $H_{k,bs} \in \mathbb{C}^{N_R \times N_T}$ the channel matrix specifying the gains from the *k*th secondary user's transmission antennas to the base station's receiver antennas and $H_{k,m} \in \mathbb{C}^{1 \times N_T}$ the gain of the channel from the *k*th secondary user's transmission antennas to the *m*th primary user. We assume that the base station (central controller) of the secondary users has knowledge of the primary users and secondary users locations and their channel gains $H_{k,bs}, H_{k,m}$. On the basis of channel information of both secondary and primary users, $H_{k,bs}, H_{k,m}$, the base station will select the best subset of secondary users at each time block/slot that will satisfy the interference constraint to the primary users. The mobile radio channel is assumed to be quasi-static; that is, the channel gain remains constant during each time block. The achievable sum-rate capacity for all users in MIMO multiple access channel without regard to interference to primary users is [11]

$$C_{sum}(H_1^{bs},...,H_K^{bs}) = \log_2 \det\left(I_{N_R} + \frac{1}{N}\sum_{k=1}^{K} H_k^{bs} \Omega_k H_k^{bs\dagger} \right) \tag{5.1}$$

where $H_k^{bs\dagger}$ denotes Hermitian of channel matrix H_k^{bs}, *N* is the noise power, $\Omega_k = \left(P_k I_{N_T}\right)/N_T$, P_k is the power of the *k*th mobile users, and I_{N_R} is the identity matrix.

In this chapter, we will consider imposing a restriction on the system that it cannot schedule more than K_s secondary users to transmit together. This is because the spatial degree of freedom is limited by the number of base station's receive antennas [12]. Therefore, the sum-rate capacity does not increase significantly by adding more secondary users above a certain limit. Having an additional constraint K_s reduces search space and therefore helps reducing computational time of user selection (scheduling). In our system model, we

assume that $K_s \cong \lceil N_R / N_T \rceil$. Although more than $\lceil N_R / N_T \rceil$ can transmit simultaneously, the sum-rate capacity will not increase significantly as the number of transmitting users increase beyond $\lceil N_R / N_T \rceil$.

We denote by ϕ the set of secondary users selected for transmission in one time block. The main objective of this work is to select a subset of secondary users ϕ from *K* secondary users in such a manner that the sum-rate capacity is maximized under the interference constraint to the primary users. We denote by $C_{sum}(\phi, H_{1,bs}, ..., H_{K,bs}) = \log_2 \det\left(I_{N_R} + \frac{1}{N_T N} \sum_{k \in \phi} P_k H_{k,bs} H_{k,bs}^{\dagger} \right)$ as the sum-rate capacity of the selected $|\phi|$ users. Mathematically we can model user selection/scheduling problem in MIMO CRS as a mixed integer non-linear programming problem

$$\begin{aligned} &\max_{P_k, \phi} \quad \log_2 \det\left(I_{N_R} + \frac{1}{N_T N} \sum_{k \in \phi} P_k H_{k,bs} H_{k,bs}^{\dagger} \right) \\ &\text{subject to} \\ &\quad C1: \quad \frac{1}{N_T} \sum_{k \in \phi} P_k H_{k,m} H_{k,m}^{\dagger} \le I_m^{\max} \qquad \forall m = 1, \cdots, M \\ &\quad C2: \quad |\phi| \le K_s \\ &\quad C3: \quad \phi \in \Phi, 0 \le P_k \le P_k^{\max} \quad \forall k \end{aligned} \tag{5.2}$$

where $\frac{1}{N_T} \sum_{k \in \phi} P_k H_{k,m} H_{k,m}^{\dagger}$ is the interference contributed by the $|\phi|$ secondary users on the *m*th primary user, and $I_m^{\max}$ is the maximum tolerable interference threshold for the *m*th primary user. The constraint *C*1 assures that interference to the primary users is less than some acceptable interference threshold $I_m^{\max}$. The constraint *C*2 ensures that at most K_s secondary users can be selected at any time simultaneously. The constraint *C*3 is the power constraints on each secondary user.

In this work, we assume that secondary users' transmission power is discretized into finite levels, which help in reducing the transmission frame overhead as fewer bits are required to describe the user's transmission power. In our formulation P_k is discrete and takes on the values in the set P_L comprising $\lambda+1$ discrete power levels, $P_L = \left\{0, \frac{P_k^{\max}}{\lambda}, \frac{2P_k^{\max}}{\lambda}, ..., P_k^{\max}\right\}$ [13], where $P_k^{\max}$ is the maximum allowed transmission power of the *k*th secondary user. The fewer choices of secondary users' transmission power mean the fewer bits in a control message. Mathematically:

$$\begin{aligned} &\max_{P_k,\phi} \quad \log_2 \det\left(I_{N_R} + \frac{1}{N_T N}\sum_{k\in\phi} P_k H_{k,bs} H_{k,bs}^{\dagger}\right) \\ &\text{subject to} \\ &\quad C1: \quad \frac{1}{N_T}\sum_{k\in\phi} P_k H_{k,m} H_{k,m}^{\dagger} \le I_m^{\max} \qquad \forall m = 1,\cdots,M \\ &\quad C2: \quad |\phi| \le K_s \\ &\quad C3: \quad \phi \in \Phi, P_k \in P_L, \forall k \end{aligned} \tag{5.3}$$

We denote by Φ the collection of all possible secondary user selections. Then, the number of possible ways of selecting the users is $|\Phi| = \sum_{i=1}^{K_s}\binom{K}{i}$. We show that the JSUS-QPC is NP-Hard problem (Appendix E). Exhaustive Search Algorithm (ESA) evaluates all possible |Φ| selections. Enumerating over all possible combinations and finding the one that maximizes $C_{sum}(\phi, H_{1,bs}, ..., H_{K,bs})$ under the interference constraint is computationally inefficient. Computational complexity of exhaustive search increases exponentially with the number of secondary users. High-speed communications require user selection/scheduling schemes with lower complexity. In the next section, we will describe EDA, IACMA and IUSIM schemes MIMO CRS.

5.2 Proposed algorithms

In this section, we proposed low-complexity user selection schemes for cognitive radio MIMO system.

5.2.1 Estimation-of-distribution Algorithm

Now, we will present an evolutionary Estimation-of-distribution Algorithm (EDA) for JSUS-QPC [20]. Evolutionary algorithms (EAs) in general have been often used to solve difficult optimization problems. Candidate solutions to an optimization problem are represented as individuals in the population. Evolutionary Algorithms (EAs) are inspired by the theory of biological evolution. In EAs, the objective function value of a candidate solution indicates the fitness of the individual in the concept of natural selection [19]. Unlike other evolutionary algorithms such as the genetic algorithm, in EDA, the individuals are generated without the crossover and mutation operators. Instead, in EDA, a new population is generated based on a probability distribution, which is estimated from the best-selected individuals of the previous iterations [20].

In general, conventional EDAs can be characterized and described by parameters and notations $(I_s, F, \Delta_l, \eta_l, p_s, \Gamma, I_{Ter})$, where

1. *I_s denotes the space of all potential solutions (entire search space of individuals).*
2. *F denotes the fitness function.*
3. *Δ_l denotes the population (the set of individuals) at the l_{th} iteration and $|\Delta_l|$ denotes its cardinality.*
4. *η_l denotes the set of best candidate solutions selected from set Δ_l at the l_{th} iteration.*
5. *p_s is the selection probability. The EDA selects $p_s|\Delta_l|$ individuals from set Δ_l to make up the set η_l.*

6. *We denote by* Γ_l *the distribution estimated from* η_l *(the set of selected candidate solutions) at the* l_{th} *iteration.*

7. I_{Ter} *is the maximum number of iterations.*

In conventional EDAs each individual can be designated by a binary string of length *n* (*n*-dimensional binary vector). We denote by a binary row vector $\boldsymbol{X} = (x_1, x_2, \cdots, x_n)$, $x_i \in \{0,1\}$ as an individual. In each iteration, an EDA maintains a population of individuals. We denote by $|\Delta_l|$ the number of individuals in population Δ_l. Population Δ_l can be specified by the following $|\Delta_l| \times n$ matrix

$$\Lambda = \begin{pmatrix} \boldsymbol{X}^1 \\ \boldsymbol{X}^2 \\ \vdots \\ \boldsymbol{X}^{|\Delta_l|} \end{pmatrix} = \begin{pmatrix} x_1^1 & x_2^1 & \vdots & x_n^1 \\ x_1^2 & x_2^2 & \vdots & x_n^2 \\ \cdots & \cdots & \cdots & \cdots \\ x_1^{|\Delta_l|} & x_2^{|\Delta_l|} & \vdots & x_n^{|\Delta_l|} \end{pmatrix}, \tag{5.4}$$

where superscript $j \in \{1, 2, ..., |\Delta_l|\}$ in the row vector $\boldsymbol{X}^j = \left(x_1^j, x_2^j, x_3^j, ..., x_n^j\right)$ indexes an individual in the population. We first consider applying the conventional EDA to the JSUS-QPC problem discussed in section II. A typical EDA applied to the JSUS-QPC problem can be described in the following steps:

Step 0*: Generate an initial population* Δ_0*. The initial population (*$|\Delta_0|$ *individuals) is typically obtained by sampling according the uniform (equally likely) distribution* [20]*:*

$$\begin{aligned} p(\theta_1, \theta_2, \cdots, \theta_n) &= \prod_{i=1}^{n} p_i(\theta_i), \\ p_i(\theta_i = 1) &= p_i(\theta_i = 0) = 0.5,\ i = 1, 2, ..., n. \end{aligned} \tag{5.5}$$

(In accordance with Eqn. (5.5)*, in a typical EDA the joint probability distribution from which the individuals are sampled is factorized as a product of n univariate marginal probability distributions, each following a Bernoulli distribution with parameter value equal to 0.5.*

For iterations l = 1,2, ..., follow Step 1 through Step 6:

Step 1*: Evaluate the individuals in the current population* Δ_{l-1} *according to the fitness function F. Sort the candidate solutions (individuals in the current population) according to their fitness orders.*

Step 2*: If the best candidate solution satisfies the convergence criterion*[6] *or if the number of iterations exceeds its limit* I_{Ter} *, then terminate; otherwise go to next step.*

Step 3*: Select the best* $p_s|\Delta_{l-1}| = |\eta_{l-1}|$ *candidate solutions (individuals) from the current population* Δ_{l-1}*. This selection is accomplished according to the sorted candidate solutions.*

Step 4*: Estimate the probability distribution* $p(\theta_1, \theta_2, \cdots, \theta_n)$ *on the basis of* $|\eta_{l-1}|$ *best candidate solutions. We denote this estimation by*

$$\Gamma_{l-1} \equiv P(\theta_1, \theta_2, \cdots, \theta_n \,|\, \eta_{l-1}) \tag{5.6}$$

Step 5*: Generate new* $|\Delta_l| - |\eta_{l-1}|$ *individuals on the basis of this new estimated probability distribution* Γ_{l-1}*. (In randomly generating the new individuals, if an individual drawn from distribution (5.6),* $(x_1, x_2, x_3, ..., x_n)$ *has more than* K_s *1's in its components, then* $\sum_{i=1}^{n} x_i - K_s$ *of those 1's are randomly selected and are replaced with 0 so that the total number of 1's in each individual may not exceed* K_s*.) Combine these newly generated* $|\Delta_l| - |\eta_{l-1}|$ *individuals with members of* η_{l-1} *to form a new population* Δ_l*.*

Step 6*: Go to step 1 and repeat the steps.*

[6] A simple example of the convergence criterion would be to terminate the algorithm if there is no improvement of the fitness value in the iteration.

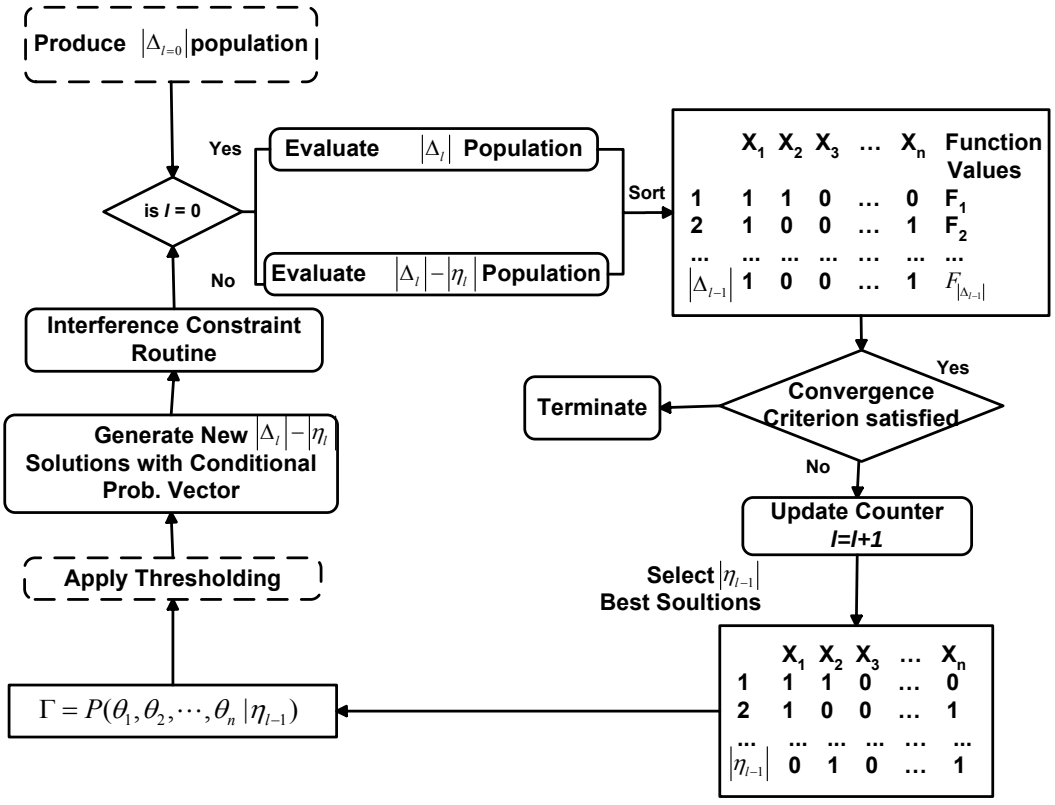

Fig. 5.1 EDA Flow Diagram

	x_1	x_2	x_3	x_4	x_5	x_6	x_7
1	1	0	1	0	1	0	0
2	0	1	1	0	0	1	0
3	0	0	1	0	1	0	0
4	1	0	1	1	0	0	0
5	0	1	1	0	1	0	0
6	1	0	1	0	0	1	0
7	0	1	1	1	0	0	0

Fig. 5.2 Biased Random Population

For the user-scheduling problem, the fitness function of our EDA is the objective function in (5.3). The dimension, *n*, of the vector that represents each

individual is equal to the total number of users *K*. We followed the steps of the above pseudo code for our EDA implementation for the user-scheduling problem. In our experimentation, for estimation, we used the simple scheme of estimating the marginal distributions separately and using the product form

$$\Gamma_{l-1} = p(\theta_1, \theta_2, \cdots, \theta_n \,|\eta_{l-1}) = \prod_{i=1}^{n} p_i(\theta_i \,|\eta_{l-1}) = \prod_{i=1}^{n} \left(\frac{\sum_{j=1}^{|\eta_{l-1}|} \delta\left(x_i^j = \theta_i \,|\eta_{l-1}\right)}{|\eta_{l-1}|} \right) \tag{5.7}$$

In order to generate the samples in the next iteration (generation), where δ is an indicator function for the individual indexed by *j* in the set η_{l-1}.

$$\delta\left(x_i^j = \theta \,|\eta_{l-1}\right) = \begin{cases} 1 & if\ x_i^j = \theta \\ 0 & otherwise \end{cases} \tag{5.8}$$

Even with this simple application of EDA, the simulation results show that its performance is better than previously proposed algorithms. In addition, we were able to modify this basic EDA algorithm and even further improve the algorithm's performance. In this thesis, we propose one modification to the typical EDA in solving the JSUS-QPC problem. The modification is applying thresholds in estimating the distribution.

5.2.1.1 Method of Applying Threshold

A typical EDA can get stuck in a local optimum due to premature convergence of the probability distributions, or can be slowed down due to no-convergence of the probability distributions. During the execution of a typical EDA, some of the estimated probabilities $P(\theta_i = 1 \,|\eta_{l-1}), i = 1, 2, \cdots, n$ may become 0 or become very close to 0 at an early stage of the execution (at a small value of iteration count *l*). In that case, the algorithm is not likely to explore the candidate solutions with $x_i = 1$ during the rest of the execution. For example, suppose that

every individual, represented by row vector X = (x_1, x_2,· · ·,x_n), in the set η_l happens to have value $x_i = 0$. Then, in accordance with (5.7), empirical distribution Γ_l gives 0-probability of drawing a candidate solution with $x_i = 1$ in population Δ_{l+1}, and this in turn provides no chance of drawing any candidate solution with $x_i = 1$ in the future generations. In this scenario, the value of $x_i = 0$, the *i*th component, is stuck with value 0 at iteration *l*, and solutions with $x_i = 1$ are never explored thereafter by the algorithm. More specifically, we take an example system that has seven users (K=7) and allows up to three users (K_s=3) to transmit simultaneously. Let the population size be 7. We consider a scenario illustrated in Fig. 5.2. In this figure, we can observe that the each individual of the population has element x_3 = 1. This causes the probability of selection of third user to one. Now the user 3 will be selected in all candidate solutions in the population at every future iteration of EDA. A similar situation occurs with x_7, where the probability of selection of seventh user is zero. We present a method of avoiding these problems.

Our approach is to apply a threshold on estimated parameters of the distributions. In order to thwart premature convergence, we present an idea of adjusting the estimated probabilities $P(\theta_i = 1 | \eta_{l-1}), i = 1, 2, \cdots, n$ after estimating these at each iteration. The adjustment in general can be regarded as a mapping from set of *n*-tuples

$$\Pi \equiv \left\{ \left(P(\theta_1 = 1 | \eta_{l-1}), P(\theta_2 = 1 | \eta_{l-1}), ..., P(\theta_n = 1 | \eta_{l-1}) \right) \;\middle|\; \begin{matrix} 0 \le P(\theta_i = 1 | \eta_{l-1}) \\ \le 1, i = 1, 2, ..., n \end{matrix} \right\}$$

to set Π itself. First, we address the problem that a marginal probability value, in the estimated distribution, prematurely converges to 1. To avoid this, we set some thresholds $0.5 < \gamma_1, \gamma_2, ..., \gamma_n < 1$. At any iteration, if the probability value $P(\theta_i = 1 | \eta_{l-1}), i = 1, 2, \cdots, n$ is greater than γ_i, we set that value to γ_i −i.e., we set $P(\theta_i = 1 | \eta_{l-1}) = \gamma_i$. This way, some degree of randomness remains in the algorithm until the termination criterion is satisfied. A simpler application of this

idea is to set the same threshold $\gamma = \gamma_1 = \gamma_2 = ... = \gamma_n$. We can similarly address the problem that a probability value prematurely converges to 0. We define thresholds $0 < \tilde{\gamma}_1, \tilde{\gamma}_2, ..., \tilde{\gamma}_n < 0.5$. At any iteration, if the estimated probability value $P(\theta_i = 1 | \eta_{l-1})$, *i* = 1, 2, .., *n*, is less than $\tilde{\gamma}_i$, we set $P(\theta_i = 1 | \eta_{l-1}) = \tilde{\gamma}_i$ so that some degree of randomness remains in the algorithm until the termination criterion is satisfied. A simpler application of this idea is to set the same threshold $\tilde{\gamma} = \tilde{\gamma}_1 = \tilde{\gamma}_2 = ... = \tilde{\gamma}_n$.

5.2.2 Interference Aware capacity maximization algorithm

In this subsection, we describe interference aware capacity maximization algorithm. The proposed IACMA greedily select a user with appropriate power level that gives maximum single-user capacity among all the unselected users, and whose addition in the set of selected users keeps the total interference to the primary users under the interference constraint. The IACMA is a two-stage algorithm. At the first stage , the algorithm determines the transmission power, P_k, of each secondary user and computes some other quantities for second stage. In stage 1, the algorithm sets the transmission power, P_k, of each secondary user *k* to $p_k^* = \max\left\{p_k \in P_L \,|\, (1/N_T) P_k H_{k,m} H_{k,m}^{\dagger} \le I_m^{max} \forall(m)\right\}$; Note that $\Gamma_{k,m,I} = (1/N_T) P_k H_{k,m} H_{k,m}^{\dagger}$ can be interpreted as the interference that user *k* individually contribute to the interference on primary user *m* −that is, the interference user *k* would cause on primary user *m* if no other secondary users were transmitting. In words, the algorithm at stage 1 sets the transmission power of each secondary user as high as possible with the constraint that the interference it individually causes on each primary user is within its interference constraint (interference tolerance level). Note that such a transmission power level for some secondary user can be 0 if every positive power value in set P_L individually causes interference on some primary user above its tolerance level. The secondary users with power level set to 0 are removed from consideration; it means at the end of stage one, the algorithm selects the secondary users that

individually satisfy the interference constraints at all the primary users. At stage one, algorithm also computes the individual capacity of each selected user and store in $\Gamma_{k,C}$. The pseudo code of IACMA is described in Table 5.2.

To obtain the final selected secondary users that maximize the sum-rate capacity under the interference constraint, the IACMA, in the second stage, incrementally selects one user, with non-zero transmission power, in each iteration. The algorithm first selects the user $\Lambda := \arg\max_{k}\left(\Gamma_{k,C}\right)$ that gives maximum single user capacity. Then, the interference induced by this selected user is added to the sum-interference $I_m^{sum} + \Gamma_{\Lambda,m,I},\ \forall(m)$. If the interference $I_m^{sum} + \Gamma_{\Lambda,m,I},\ \forall(m)$ satisfies the interference constraint I_m^{max} then that user is included into the set Ψ_{FS} and its corresponding index/data is removed from $\Gamma_{k,m,I}$ and $\Gamma_{k,C}$. The second stage steps are repeated for the remaining users with non-zero transmission power.

5.2.3 Iterative User scheduling with interference minimization

Although the interference aware capacity maximization algorithm performs very well, there are certain situations where performance of IACMA is not good. An exemplary situation is shown in the Table 5.3. In this example, we have four secondary users with their respective individual capacities $\Gamma_{k,C}$, interference $\Gamma_{k,m,I}$ induced by these users on the primary users' m_1 and m_2, and interference thresholds $I_m^{\max}$ on primary users' m_1 and m_2. Let K_s = 2. If we apply IACMA on Table 5.3 to select the users then greedily it will select first user 2 and store in set Ψ_{FS}. The interference $\Gamma_{k,m,I}$ induced by the user 2 on primary users' m_1 and m_2 is 4.5 and 3.8 respectively. Since K_s = 2, the algorithm can select one more user but by adding any other user to user 2 will violate the interference constraint. One good solution to the above example is to select users 1 and 3. In this subsection, we describe iterative user scheduling with interference

minimization (IUSIM). The IUSIM algorithm, in each iteration, incrementally selects one user that induces the minimum interference to the primary users.

Table 5.2 IACMA

IACMA	**Flops**
INPUT: $K,M,N_T,N_R,P,\ I_m^{\max}\ H_{k,m},\ H_{k,bs},P_k,\ \forall(k,m),\ \lambda$	
INITIALIZATION: $\Psi_{FS}=\{\ \},\ \Gamma_{k,m,I}=0\ \forall(k,m)$, $I_m=0\,\forall m,\ I_m^{sum}=0,\forall m,\ \Gamma_{k,C}=0\ \forall k$	
STAGE 1: 1: ***For*** *k=1 to K* 2: $p_k^*=\max\left\{p_k\in P_L\mid\frac{P_kH_{k,m}H_{k,m}^{\dagger}}{N_T}\le I_m^{max}\forall(m)\right\}$ 3: ***If*** $p_k^*\neq 0$ 4: $\Gamma_{k,C}=GetCapacity\left(p_k^*,H_{k,bs},k\right);$ 5: $\Gamma_{k,m,I}=\frac{p_k^*H_{k,m}H_{k,m}^{\dagger}}{N_T}\ \forall m;$ 6: ***End if*** 7: ***End for***	2: $2M\lambda N_T$ 3: 1 4: $2N_R^2N_T$ 5: *1* 6: MN_T
STAGE 2: 9: ***while*** $\left\lvert\Psi_{FS}\right\rvert\le K_s$ 10: $\Lambda=\arg\max_k\left(\Gamma_{k,C}\right);$ 11: ***If*** $I_m^{sum}+\Gamma_{\Lambda,m,I}\le I_m^{max}\ \ \forall(m)$ 12: $\Psi_{FS}:=\Psi_{FS}\cup\{\Lambda\};$ 13: $I_m^{sum}:=I_m^{sum}+\Gamma_{\Lambda,m,I}\ \ \forall(m)$ 14: ***End if*** 16: $\Gamma_{\Lambda,C}=0$ 17: $\Gamma_{\Lambda,m,I}=0\ \ \forall m$ 18: ***End While***	10: $\left\lvert\Psi_{PS}\right\rvert$ 11: *2M* 12: *1* 13: *2M* 15: *1* 16: *1* 17: *M*
OUTPUT: Ψ_{FS}	

We denote by Ψ_{FS} the set of final selected secondary users, $\Gamma_{k,m,I}$ the interference from the *k*th user to the *m*th primary user, I_m^{sum} the sum-interference from the selected secondary users, and $\Gamma_{k,I}^{Sum}$ the total interference induced by the *k*th user.

The IUSIM is also a two-stage algorithm. At stage 1, the algorithm determines the transmission power, p_k, of each secondary user and computes some other quantities for stage 2. The determination of transmission power p_k, is identical to the IACMA. The secondary users with power level set to 0 are removed from consideration; it means at the end of stage one, the algorithm selects the secondary users that individually satisfy the interference constraints at all the primary users. For the users with non zero transmission power levels, the algorithm then calculates the aggregated or sum-interference, $\Gamma_{k,I}^{Sum} = \sum_m \Gamma_{k,m,I}$ where $\Gamma_{k,m,I} = (1/N_T) P_k H_{k,m} H_{k,m}^{\dagger}$ is the interference that user *k* individually contribute to the interference on primary user *m*, from each secondary user to the primary users. The pseudo code of IUSIM is described in Table 5.4.

Table 5.3 Example

K	$\Gamma_{k,C}$	$\Gamma_{k,m,I}$		$I_m^{\max}$	
		m_1	m_2	m_1	m_2
1	10	2.5	4.0	5	5
2	17	4.5	3.8	5	5
3	15	2.3	1.0	5	5
4	3	3.5	1.1	5	5

To obtain the final selected secondary users that minimize the sum-interference, the IUSIM, in the second stage, incrementally selects a user with non-zero transmission power in each iteration. The algorithm first selects the user which gives minimum sum interference $\Gamma_{k,I}^{Sum}$. Then, the interference induced by this selected user is added to the sum-interference I_m^{sum}. If the sum-interference satisfies the interference constraint then that user is included in Ψ_{FS} and the selected user data is removed from $\Gamma_{k,m,I}$ and $\Gamma_{k,I}^{Sum}$. The second stage

steps are repeated for the remaining users with non-zero transmission powers. The IUSIM algorithm is described in Table 5.4.

Table 5.4 IUSIM

Iterative User Scheduling with interference minimization (IUSIM)	**Flops for IUSIM**
INPUT: $K,M,N_T,N_R,P,\ I_{\max}^{m}\ H_m^k,\ H_k^{bs},P_k,\ \forall(k,m),\ \lambda$	
INITIALIZATION: $\Psi_{FS}=\{\ \},\ \Gamma_{k,m,I}=0\ \forall(k,m)$, $\Gamma_{k,I}^{Sum}=\infty\ \forall k$, $I_m=0\forall m,\ I_m^{Sum}=0\forall m$,	
STAGE 1:	
For *k=1 to K*	
2: $p_k^*=\max\left\{p_k\in P_L\mid\frac{P_kH_{k,m}H_{k,m}^{\dagger}}{N_T}\le I_m^{max}\forall(m)\right\}$	2: $2M\lambda N_T$
3: ***If*** $p_k^*\neq 0$	3: *1* 4: $2MN_T$ 5: *M*
4: $\Gamma_{k,m,I}=\frac{p_k^*H_{k,m}H_{k,m}^{\dagger}}{N_T}\ \forall m;$	
5: $\Gamma_{k,I}^{Sum}=\sum_m\Gamma_{k,m,I};$	
6: ***End if***	
7: ***End for***	
STAGE 2:	
8: ***while*** $\left\lvert\Psi_{FS}\right\rvert\le K_s$	10: $\lvert\Psi_{PS}\rvert$
9: $\Theta=\arg\min_k\Gamma_{k,I}^{Sum};$	11: $2M$
10: ***If*** $I_m^{sum}+\Gamma_{\Theta,m,I}\le I_m^{max}\ \forall(m)$	12: *M* 13: $2M$
11: $\Psi_{FS}:=\Psi_{FS}\cup\{\Theta\};$	15: *1*
12: $I_m^{sum}:=I_m^{sum}+\Gamma_{\Theta,m,I}\ \forall(m)$	16: *M*
13: ***End if***	
14: $\Gamma_{k,I}^{Sum}=\infty$	
15: $\Gamma_{\Theta,m,I}=0\ \forall m$	
16: ***End while***	
OUTPUT: Ψ_{FS}	

5.3 Complexity Analysis

The main motivation of the proposed algorithms is low implementation complexity. In this section, we will compare the complexity of the proposed

algorithms with optimal (ESA) algorithm. Complexity is measured in terms of flops Υ.

5.3.1 Complexity of IACMA and IUSIM

Table 5.2 and 5.4 describe the complexity of IACMA and IUSIM operations. The IACMA takes approximately $K\left(2M\lambda N_T + 2 + MN_T + 2N_R^2 N_T\right) + K_s\left(|\Psi_{PS}| + 5M\right)$ flops. To get the flop count Υ_{IACMA}, we set $|\Psi_{PS}| = K$, and $K_s = K$. The flop count Υ_{IACMA} is

$$\begin{aligned}\Upsilon_{IACMA} &\approx K\left(2M\lambda N_T + 2 + MN_T + 2N_R^2 N_T\right) + K\left(K + 5M\right) \\ &\approx O\left(KM\lambda N_T + K^2 + KN_R^2 N_T\right)\end{aligned} \tag{5.9}$$

The IUSIM requires approximately $K\left(2M\lambda N_T + K + MK + 2MN_T\right) + K_s\left(|\Psi_{PS}| + 5M\right)$ flops. To get the flop count Υ_{IUSIM}, we set $|\Psi_{PS}| = K$ and $K_s = K$. The flop count Υ_{IUSIM}

$$\begin{aligned}\Upsilon_{IUSIM} &\approx K\left(2M\lambda N_T + K + MK + 2MN_T\right) + K_s\left(|\Psi_{PS}| + 5M\right) \\ &\approx O\left(K^2 M + KM\lambda N_T\right)\end{aligned} \tag{5.10}$$

5.3.2 Exhaustive Search Algorithm

The number of floating point operations for computing the term inside the determinant in (5.3), $I_{N_R} + \frac{1}{N_T N}\sum_{k\in\phi} P^k H_k^{bs} H_k^{bs\dagger}$ can be expressed as $O\left(K_s N_R^2 N_T + N_R\right) = O\left(K_s N_R^2 N_T\right)$ for the worst case of $|\phi| = K_s$[7]. Computing the determinant requires $N_R^3/3$ complex operations. Thus, computational complexity of evaluating $\det\left(I_{N_R} + \frac{1}{N_T N}\sum_{k\in\phi} P^k H_k^{bs} H_k^{bs\dagger}\right)$ can be expressed as

[7] It may take much less if the number of selected users is less than K_s.

$O\left(K_s N_R^2 N_T + N_R^3\right)$. The exhaustive search algorithm (ESA) needs to compute $\sum_{i=1}^{Ks}\binom{K}{i}$ determinants. The interference constraint takes $2MN_T$ flops. The computation of power level requires $\left(K_s\right)^{\lambda}$ flops. Finally, the computational complexity of exhaustive search algorithm with discrete/quantize power (ESA-D)is

$$\Upsilon_{ESA-D} \approx O\left(\left(K_s N_R^2 N_T + N_R^3\right)\times\left(K_s\right)^{\lambda}\times\sum_{i=1}^{Ks}\binom{K}{i}\right) \tag{5.11}$$

The complexity analysis shows that the proposed IACMA and IUSIM have quadratic complexity with respect to the number of users *K.* The complexity of exhaustive search for user scheduling increases exponentially with the number of users.

5.4 Numerical results

For performance comparison, we present the simulation results of the proposed EDA, IACMA and IUSIM-based user selection. We use the objective function of optimization problem (5.3) as the fitness function. For evaluating sum-rate capacities for different user scheduling methods in our experiments, we randomly generate channel gain H_k^{bs} under the assumption that elements of the channel matrix have independent complex Gaussian distributions. In all simulations noise variance is assumed to be one. The system parameters used for simulations are selected such that we can examine the effect of different system parameters (e.g., interference threshold level, number of primary users, number of secondary users, quantize power levels etc.) on the performance of the proposed schemes. From the results we compare EDA, IACMA, IUSIM, exhaustive search algorithm with continuous power control (ESA-C), and the exhaustive search algorithm with discrete (or quantized) power control (ESA-D).

In Figs. 5.3−5.6, we used four different scenarios $\left[K, K_s, N_T, N_R, \lambda, I_m^{\max}\right]$ = [8, 3, 2, 6, 8, 1mw], $\left[K, K_s, N_T, N_R, \lambda, I_m^{\max}\right]$ = [12, 3, 2, 6, 8, 1mw], $\left[K, K_s, N_T, N_R, \lambda, M\right]$ = [12, 3, 2, 6, 8, 4], and $\left[K, K_s, N_T, N_R, \lambda, M\right]$ = [8, 3, 2, 6, 8, 4], The performance is shown in terms of average sum-rate capacity SNR power plots. The results show that average sum-rate capacities achieved by the proposed EDA, IACMA and IUSIM are close to the ESA-D. From these figures, we observe that for a given interference tolerance and power level by increasing the user's individual transmit power level (or increase in SNR) we can only increase the sum-rate capacity up to a certain level. After that, further increase of users' individual transmit power will decrease the sum-rate capacity. The decrease in the sum-rate capacity with the uniform increase of the users' transmit power can be explained by the fact that above some threshold further increase in transmit power will also increase the interference to the primary users, so the users are required to transmit at lower discrete power level which may not be the optimum power level. In case of continuous power control the capacity will always be non-decreasing because even by increasing the maximum transmit power level, the users' can still transmit on optimum transmit power level.

In Figs. 5.7 and 5.8, we show the sum-rate capacity versus number of power levels. The result illustrates that increase in the power levels satisfy more primary users' interference constraint and increase the system capacity. There is always trade-off between number of power levels and control channel traffic. More power levels per user mean increase in the control channel traffic and vice versa.

In Figs. 5.9 and 5.10, we present performance of the proposed algorithms against number of primary users. We set $\left[K, K_s, N_T, N_R, SNR\right]$ = [8, 3, 2, 6, 8dB, 4] and $\left[K, K_s, N_T, N_R, I_m^{\max}\right]$ = [8, 3, 2, 6, 10mw, 4]. The result shows that average sum-rate capacity achieved by the proposed IACMA and IUSIM is close to the ESA-D for a wide range of *M*. From Figs. 5.9 and 5.10, we observe that we achieve low sum-rate capacity by increasing the number of primary users. This is

because by increasing the number of primary users, the secondary users need to satisfy more interference constraints. In Figs. 5.11 and 5.12, we plot the sum-rate capacity versus number of secondary users. For thses scenario, we set $\left[K_s, N_T, N_R, I_m^{\max}, M\right]$ = [3, 2, 6, 1mw, 4] and $\left[K_s, N_T, N_R, SNR, M\right]$ = [3, 2, 6, 8dB, 4] The result shows that average sum-rate capacity achieved by the proposed EDA, IACMA and IUSIM is close to the ESA-D for a wide range of *K*. The results also show that the performance of IUSIM improves with more number of primary users.

Fig. 5.13 focuses on the method of applying thresholds. This figure reports the results of applying different threshold values in shaping the distribution that generates the population. We ran an EDA-R with parameters $\left[K, K_s, N_T, N_R, SNR, M\right]$ = [12, 3, 2, 6, 8dB, 1] for threshold values γ = {0.7, 0.8, 0.9, 1.0.} and $\tilde{\gamma} = 1 - \gamma$. Note that setting $\gamma = 1$ is equivalent to not applying the threshold at all. Setting γ close to 0.5 means that the algorithm generates the population from an almost identical distribution in each iteration− that is, the algorithm does not take advantage of the natural selection. An interesting issue is what values of the threshold facilitates the computation. From Fig. 5.13, we can observe that the performance of EDA-R is poor at γ = 0.7. We can interpret that at the threshold value γ =0.7, which is close to 0.5, the algorithm does not evolve significantly. We can see from Fig. 5.13 that threshold value γ = 1.0 results in better performance than all other threshold values (0.7, 0.8, and 0.9) at early stage of the algorithm (up to iteration 4). However, for the case of γ = 1.0 the fitness value (average sum-capacity) does not improve much as we run more iterations beyond the seventh iteration. On the other hand, in the case of γ = 0.8 and 0.9, the fitness value continues to improve beyond iteration 5, and produced the best solution if we terminate the algorithm at iteration 5,6,7,8 etc. From the numerical results, we can see that IACMA and EDA converge to with in 97 percent of that obtained by the exhaustive search. The IUSIM converges to with in 92 percent of that obtained by the exhaustive search.

To check the feasibility of the proposed algorithms for practical implementation, in Table 5.5, we present the number of flops required by ESA, EDA, IACMA and IUSIM for different parameter settings (i.e., different search space size). The comparison shows that the number of flops required by IACMA and IUSIM is much less than that of EDA and ESA.

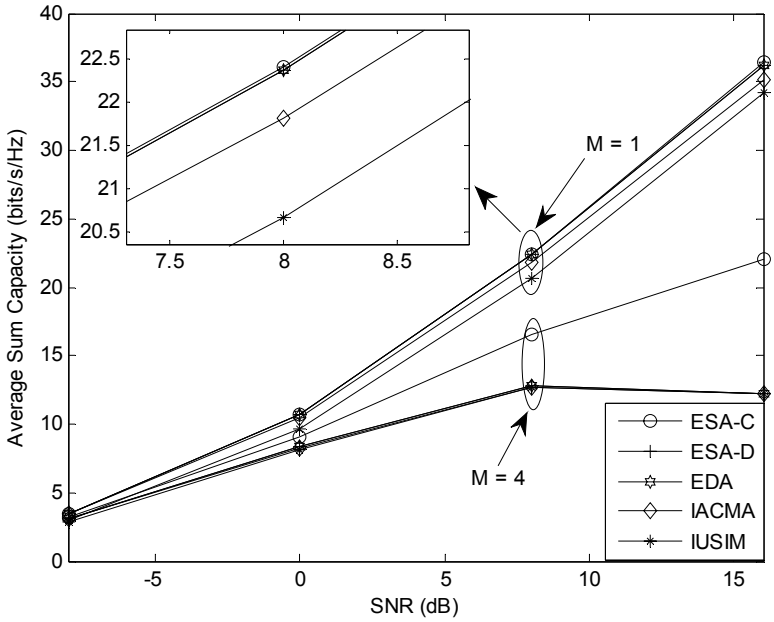

Fig. 5.3 Sum-rate capacity comparison. The parameters are $\left[K, K_s, N_T, N_R, \lambda, I_m^{\max}\right]$ = [8, 3, 2, 6, 8, 1mw].

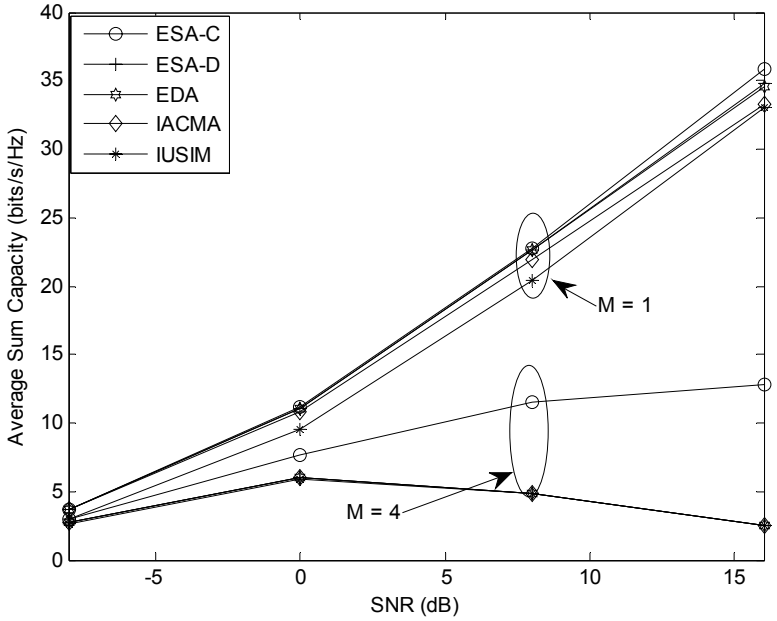

Fig. 5.4 Sum-rate capacity comparison .The parameters are $\left[K, K_s, N_T, N_R, \lambda, I_m^{\max}\right]$ = [12, 3, 2, 6, 8, 1mw].

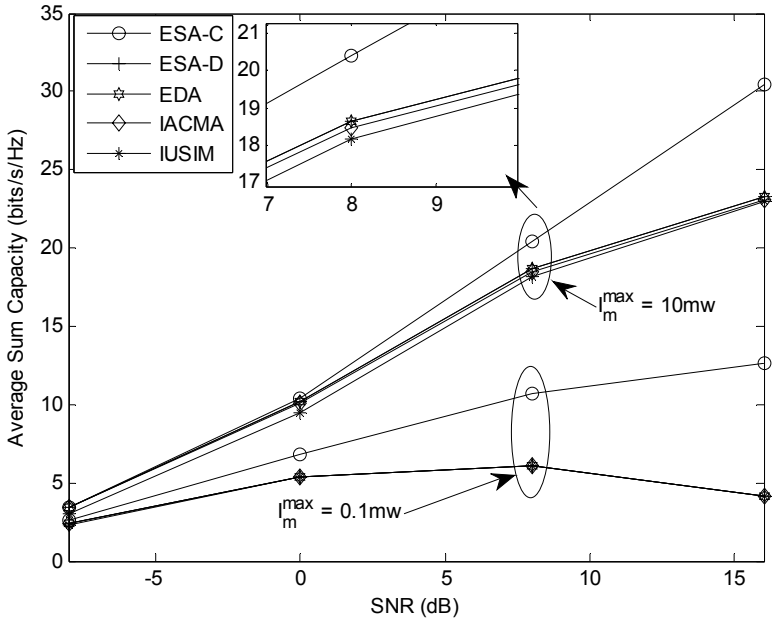

Fig. 5.5 Sum-rate capacity comparison .The parameters are $\left[K, K_s, N_T, N_R, \lambda, M\right]$ = [8, 3, 2, 6, 8, 4].

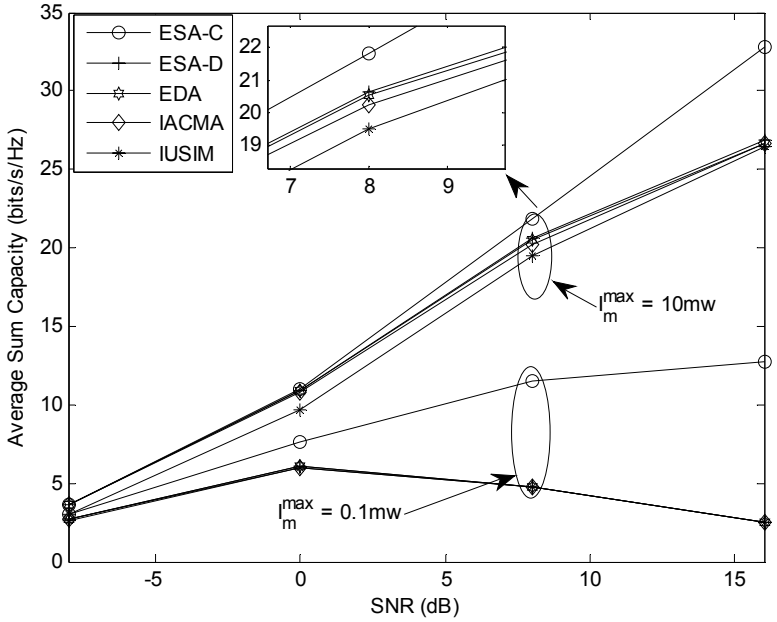

Fig. 5.6 Sum-rate capacity comparison .The parameters are $[K, K_s, N_T, N_R, \lambda, M]$ = [12, 3, 2, 6, 8, 4].

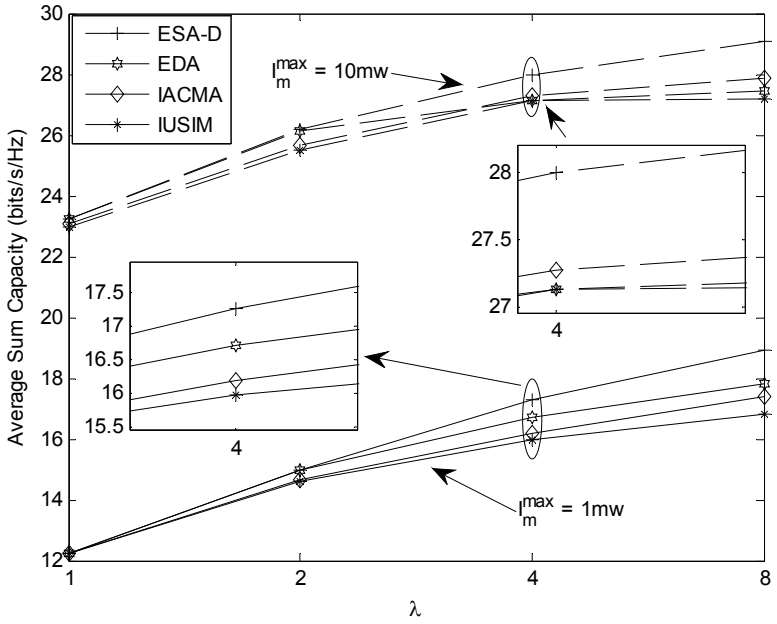

Fig. 5.7 Sum-rate capacity comparison for different power levels .The parameters are $[K, K_s, N_T, N_R, SNR, M]$ = [8, 3, 2, 6, 8dB, 4].

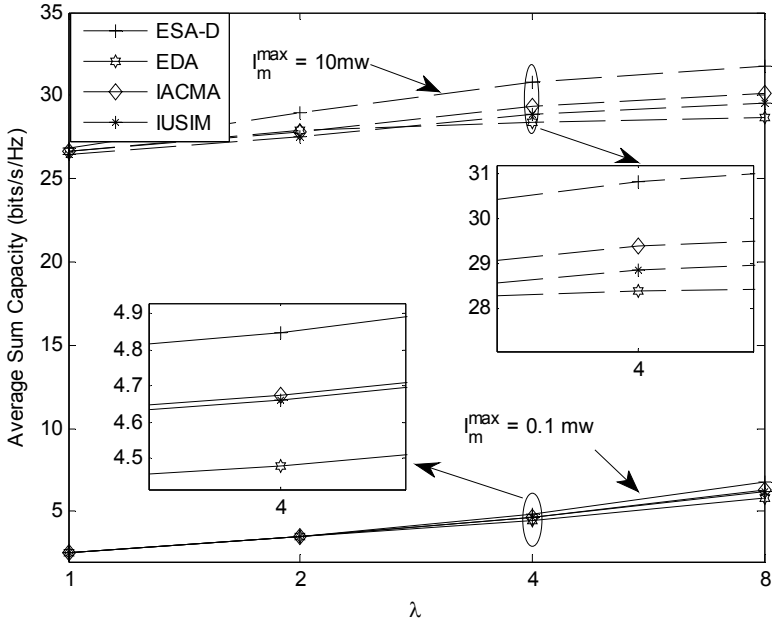

Fig. 5.8 Sum-rate capacity comparison for different power levels .The parameters are $[K, K_s, N_T, N_R, SNR, M]$ = [12, 3, 2, 6, 16dB, 4].

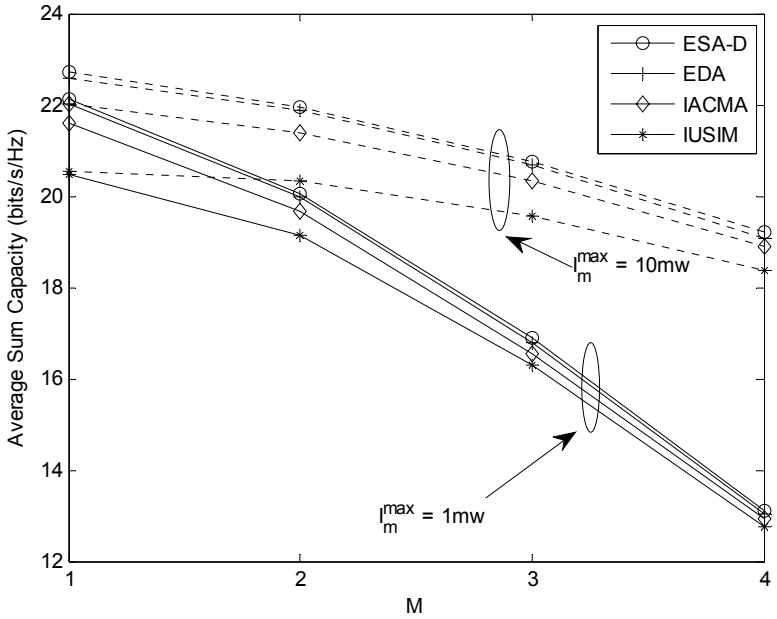

Fig. 5.9 Sum-rate capacity vs. number of primary users. The parameters are $[K, K_s, N_T, N_R, SNR]$ = [8, 3, 2, 6, 8dB].

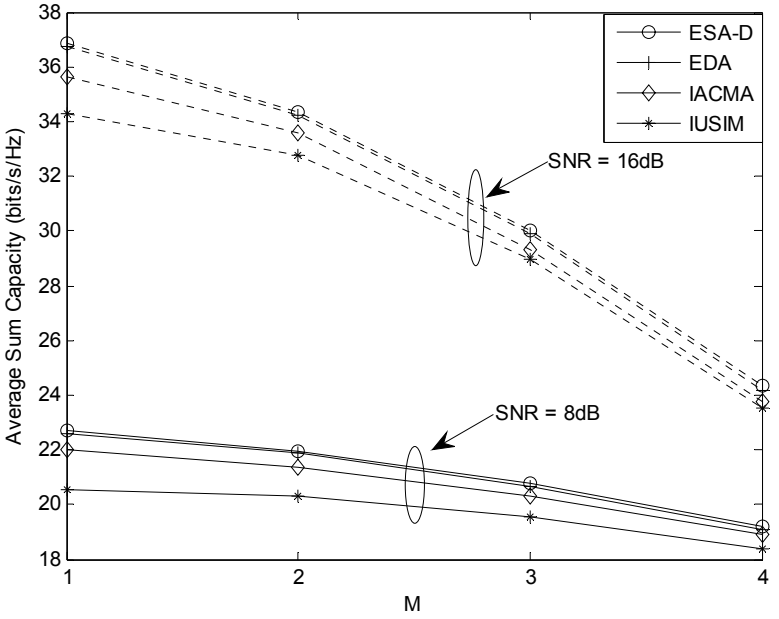

Fig. 5.10 Sum-rate capacity vs. number of primary users. The parameters are $\left[K, K_s, N_T, N_R, I_m^{\max}\right]$ = [8, 3, 2, 6, 10mw].

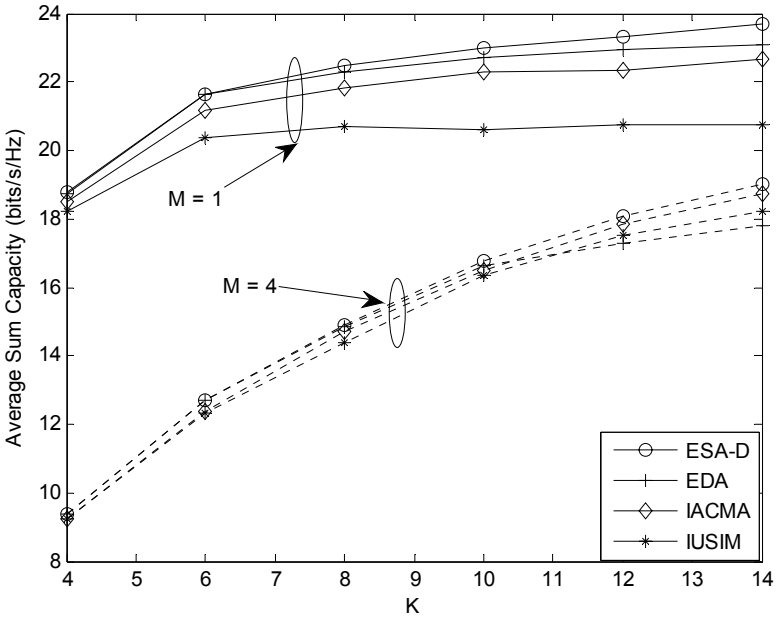

Fig. 5.11 Sum-rate capacity vs. number of secondary users. The parameters are $\left[K_s, N_T, N_R, I_m^{\max}, M\right]$ = [3, 2, 6, 1mw, 4].

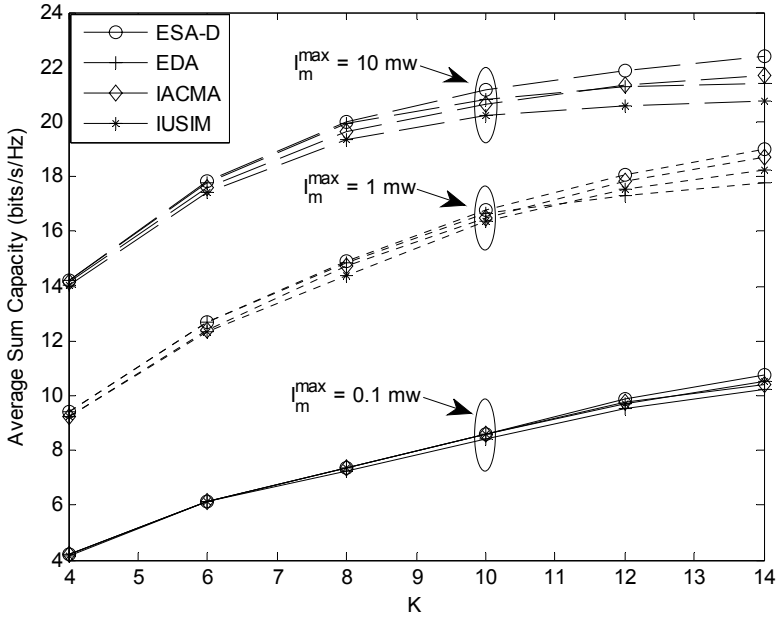

Fig. 5.12 Sum-rate capacity vs. number of secondary users. The parameters are $\left[K_s, N_T, N_R, SNR, M\right]$ = [3, 2, 6, 8dB, 4].

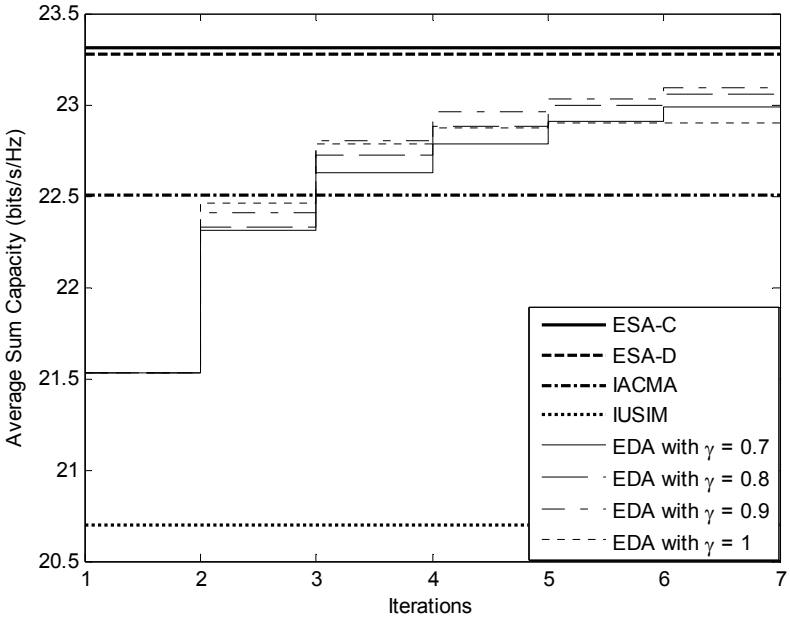

Fig. 5.13 Effect of threshold on the performance of EDA. $\left[K, K_s, N_T, N_R, SNR, M\right]$ = [12, 3, 2, 6, 8dB, 1].

Table 5.5 Number of flops required by ESA, EDA, IACMA and IUSIM

Parameters $\left[K, K_s, M, N_T, N_R, \lvert\Delta\rvert, I_{Ter}\right]$	**ESA**	**EDA**	**IACMA**	**IUSIM**
[20,3,1,4,2,2,20,10]	2954880	518400	1100	1224
[15,3,10,4,2,2,20,10]	1179360	518400	3855	5634
[10,5,1,2,2,10,10]	302400	120000	370	370
[30,2,1,2,2,10,10]	41760	9600	1710	2174
[25,4,4,2,2,10,10,10]	364320000	2880000	6100	1586
[18,8,1,2,2,16,18,10]	2.2942e+010	94371840	9882	968
[12,6,1,2,2,16,12,10]	238436352	30965760	6516	498

5.5 Summary

In this chapter, we presented three low-complexity user scheduling schemes in cognitive MIMO systems. The proposed interference aware capacity maximization algorithm and iterative user scheduling with interference minimization have low computational complexities, and their performance is close to that of the exhaustive search algorithm with discrete power control (ESA-D). Simple underlying concept and ease of implementation with low-complexity make the proposed schemes suitable candidates for the joint user selection/scheduling and power control problem discussed in this chapter.

5.6 Chapter References

[1] E. Telatar, “Capacity of Multi-antenna Gaussian Channels,” European Trans. on Telecomm. vol. 10, pp 569-709, Nov. 1999.

[2] Y. Zhang, C. Ji, W. Q. Malik, Y. Liu, D. C. O'Brien, and D. J. Edwards, “Joint antenna and user selection algorithm for uplink multiuser MIMO systems using sequential Monte Carlo optimization,” IEEE Statistical Sig. Proc. Workshop (SSP). WI. USA, pp. 493−496, Aug. 2007.

[3] Z. Shen, J. G. Andrews, R. W. Heath, Jr., and B. L. Evans, “Low-complexity User Selection Algorithms for Multiuser MIMO Systems with Block

Diagonalization," IEEE Trans. on Signal Processing, vol. 54, no. 9, pp. 3658−3663, Sep. 2006.

[4] Z. Shen, R. Chen, J. G. Andrews, R. W. Heath, Jr., and B. L. Evans, "Sum-capacity of multiuser MIMO broadcast channel with block Diagonalization ," IEEE Transactions on Wireless Communications, vol.6 no. 6, June 2007.

[5] X. Zhang and J. Lee, "Low-complexity MIMO scheduling with channel decomposition using capacity upper bound," IEEE Transactions on Communications vol.56 no. 6, pp. 871−876, June 2008.

[6] E. Hossain, D. Niyato, and Z. Han, Dynamic Spectrum Access and Management in Cognitive Radio Networks, Cambridge University Press, 2009.

[7] Q. Zhao and B.M. Sadler, "A Survey of Dynamic Spectrum Access," IEEE Signal Processing Magazine, vol. 24, no. 3, pp. 79-89, May 2007.

[8] J.H. Snider and Max Vilimpoc, "Reclaiming the vast wasteland: Unlicensed Sharing of Broadcast Spectrum," New America Foundation: Spectrum policy program, Report, July 2003.

[9] M. J. Marcus, P.Kolodzy, and A. Lippman, "Reclaiming the vast wasteland: why unlicensed use of the white space in the TV bands will not cause interference to DTV viewers," New America Foundation: Wireless Future Program, Report, 2005.

[10] J.H. Snider and Max Vilimpoc, "Reclaiming the vast wasteland: Unlicensed Sharing of Broadcast Spectrum," New America Foundation: Spectrum policy program, Report, July 2003.

[11] S. Vishwanath, N. Jindal, and A. Goldsmith, "Duality, achievable rates, and sum-rate capacity of Gaussian MIMO broadcast channels," IEEE Trans. Inform. Theory, vol. 49, pp. 2658–2668, Oct. 2003.

[12] D. Tse and P. Viswanath, Fundamentals of Wireless Communication, Cambridge University Press, May 2005.

[13] Y. Thomas Hou, Yi Shi, and H. D. Sherali, “Spectrum sharing for multi-hop networking with cognitive radios,” IEEE Journal on Selected Areas of Communications, vol. 26, no. 1, pp. 146-155, January 2008.

[14] G. H. Golub and C. F. Van Loan, Matrix Computations, Johns Hopkins Univ. Press, 1983.

[15] A.E. Eiben and J.E. Smith, Introduction to Evolutionary Computing, Springer Verlag, 2003.

[16] P. Larrañaga and J. A Lozano, Estimation-of-distribution Algorithms: A New Tool for Evolutionary Computation. Kluwer Academic Publishers, 2001.

CHAPTER 6: CONTRIBUTIONS AND FUTURE WORK

In this chapter, we present a brief overview of the contributions and discuss open issues that can be addressed in future research.

6.1 Contributions

In this thesis, we have proposed a number of polynomial-time algorithms for resource allocation in cooperative cognitive radio systems. In particular, we have made following major contributions in this thesis:

6.1.1 Relay Assignment

1. We presented an optimization framework for joint multiple relay assignment and power allocation in CRS. The optimal solution of the proposed optimization problem can be obtained by using Exhaustive Search Algorithm. However, its computational complexity increases exponentially with the number of secondary users and the number of relays. We propose iterative algorithms that have very low computational complexity and their performance is close to the exhaustive search algorithm. We also present fairness aware relay assignment schemes in CRS.
2. A multi-objective optimization framework is proposed for joint relay assignment and power allocation in green CRS. We proposed a hybrid estimation-of-distribution algorithm for joint relay assignment and power allocation in green CRS.

6.1.2 Joint subcarrier allocation and relay assignment

We presented resource allocation schemes for cooperative multiuser multicast cognitive radio system (MMCRS). For resource allocation, we proposed schemes that jointly assign subcarriers and relays to the multicast groups and allocate power to the relays in cooperative MMCRS. We considered two separate optimization problems. In one optimization problem, we maximized the total throughput of the cooperative MMCRS under the constraint of acceptable interference to the primary users. In the other optimization problem, we maximized the throughput of the worst multicast group in cooperative MMCRS under the constraint of acceptable interference to the primary users. For each optimization problem, we proposed an iterative algorithm with polynomial time complexity.

6.1.3 User scheduling

We presented three low-complexity user scheduling schemes in cognitive MIMO systems. The proposed schemes have polynomial-time complexity, and their performance is close to that of the exhaustive search algorithm with discrete power control. Simple underlying concept and ease of implementation with low-complexity make the proposed schemes suitable candidates for the joint user selection/scheduling and power control problem.

6.2 Future work

The proposed schemes in this thesis address some aspects of resource allocation in CRS with MIMO and relaying capabilities. However, there are still many open issues. In the following, we list some important future research directions.

6.2.1 Resource allocation in multi-hop CRS

In this thesis, we focused on two-hop cooperative CRS. A natural extension would be to consider multiple relay assignment in multi-hop cooperative CRS. The proposed resource allocation in cooperative CRS is for single antenna systems. This work can also be extended to the multiple antenna system.

6.2.2 Resource allocation in cooperative CRS with imperfect CSI

For resource allocation, we have assumed that the central controller knows the perfect CSI. However, there always exists some uncertainty in the CSI due to unreliable feedback channel. Therefore, a possible extension of the proposed resource allocation formulation is to analyze the relay assignment schemes with imperfect CSI in multi-hop CRS. Another interesting issue to consider is the effect of quantized CSI on the relay assignment in multi-hop cooperative CRS.

6.2.3 Green communication with adaptive weights

For green communication technologies, we proposed a multi-objective optimization framework for relay assignment and power allocation. In this framework, the weights of the objective functions are fixed. An extension of this work would be to consider adaptive weights for each objective functions. The adaptive weights can give better Pareto optimal front for the proposed multi-objective green CRS framework. The adaptive weights will increase the computational complexity thus low complexity algorithms will be needed to address the complexity issues.

APPENDICES

Appendix A

We need to show that for any set of fixed values of integer variables $\varepsilon_{l,k}, l=1,...,L$ and p_l the objective function in (2.2) is monotonically increasing with P_s^k. For a fixed $\varepsilon_{l,k}, l=1,...,L$ and p_l , The objective function is

$$\frac{1}{2}\log_2\left\{1+\frac{P_s^k\left|h_{s,k}\right|^2}{N}+\frac{P_s^k}{N}\frac{\left(\sum_{l=1}^{L}\varepsilon_{l,k}\sqrt{\frac{\left|h_{s,l}h_{l,k}\right|^2 p_l}{P_s^k\left|h_{s,l}\right|^2+N}}\right)^2}{1+\sum_{l=1}^{L}\frac{\left|h_{l,k}\right|^2 p_l}{P_s^k\left|h_{s,l}\right|^2+N}}\right\} \qquad \text{(A.1)}$$

Since log( ) is a monotonically increasing function, proving that its argument is increasing with P_s^k shows that the objective function is monotonically increasing with P_s^k. The first two terms inside the log( ) is obviously monotonically increasing with P_s^k. Then, considering the last term inside the log( ), to establish monotonicity of expression (A.1), we only need to show that the function

$$H_k(P)\equiv P\frac{\left(\sum_{l=1}^{L}\varepsilon_{l,k}\sqrt{\frac{\left|h_{s,l}h_{l,k}\right|^2 p_l}{P\left|h_{s,l}\right|^2+N}}\right)^2}{1+\sum_{l=1}^{L}\frac{\left|h_{l,k}\right|^2 p_l}{P\left|h_{s,l}\right|^2+N}}=\frac{\left(\sum_{l=1}^{L}\varepsilon_{l,k}\sqrt{\frac{\left|h_{s,l}\right|^2\left|h_{l,k}\right|^2 Pp_l}{P_s^k\left|h_{s,l}\right|^2+N}}\right)^2}{1+\sum_{l=1}^{L}\frac{\left|h_{l,k}\right|^2 p_l}{P\left|h_{s,l}\right|^2+N}}$$

is monotonically increasing with P for each *k*. . Denoting $\bar{p}_{l,k}\equiv p_l\left|h_{l,k}\right|^2$, we can express $H_k(P)$ as

$$H_k(P)=\frac{\left(\sum_{l=1}^{L}\varepsilon_{l,k}\sqrt{\frac{P\left|h_{s,l}\right|^2\overline{p}_{l,k}}{P\left|h_{s,l}\right|^2+N}}\right)^2}{1+\sum_{l=1}^{L}\frac{\overline{p}_{l,k}}{P\left|h_{s,l}\right|^2+N}}\equiv\frac{\left(\sum_{l=1}^{L}\varepsilon_{l,k}\sqrt{F_{l,k}(P)}\right)^2}{1+\sum_{l=1}^{L}G_{l,k}(P)}$$

where

$$F_{l,k}(P)=\frac{P\left|h_{s,l}\right|^2\overline{p}_{l,k}}{P\left|h_{s,l}\right|^2+N}=\overline{p}_{l,k}-\frac{\overline{p}_{l,k}N}{P\left|h_{s,l}\right|^2+N} \qquad \text{(A.2)}$$

and

$$G_{l,k}(P)=\frac{\overline{p}_{l,k}}{P\left|h_{s,l}\right|^2+N} \qquad \text{(A.3)}$$

From (A.2), it is obvious that $F_{l,k}(P),\forall l,$ is increasing with P for $P>0$, and from (A.3), it is obvious that $G_{l,k}(P),\forall l,$ is decreasing with P for $P>0$. Thererfore, $H_k(P)$ is increasing with P for $P>0$. Q.E.D.

Appendix B

We need to establish the concavity of function f:$\mathbf{R}^{L}\rightarrow\mathbf{R}$, defined as $f(p_1,p_2,\cdots,p_L)=\dfrac{\sum_{l=1}^{L}\left(\left|h_{l,k}\right|\beta_l\right)^2 p_l}{1+\sum_{l=1}^{L}\left(\left|h_{l,k}\right|\beta_l\right)^2 p_l}=\dfrac{\sum_{l=1}^{L}x_l}{1+\sum_{l=1}^{L}x_l}$, where $x_l=\left(\left|h_{l,k}\right|\beta_l\right)^2 p_l$. From definition, function f is concave if **dom** f is a convex set and if for all $\bar{x},\bar{y}$ ϵ **dom** f, and λ with $0\le\lambda\le 1$, we have

$$f\left(\lambda\bar{x}+(1-\lambda)\bar{y}\right)\ge\lambda f\left(\bar{x}\right)+(1-\lambda)f\left(\bar{y}\right) \qquad \text{(B.1)}$$

Let us define a linear function g:$\mathbf{R}^{L}\rightarrow\mathbf{R}$ as $g(x_1,x_2,..,x_L)=\sum_{l=1}^{L}x_l$ and a concave function h:$\mathbf{R}\rightarrow\mathbf{R}$, as $h(z)=\dfrac{z}{1+z}$. We know that composition of a concave function with an affine mapping is concave− i.e. $h\left(g\left(\bar{x}\right)\right)$ is concave. Therefore,

$$h\left(g\left(\lambda\bar{x}\right)+g\left((1-\lambda)\bar{y}\right)\right)\ge\lambda h\left(g\left(\bar{x}\right)\right)+(1-\lambda)h\left(g\left(\bar{y}\right)\right) \qquad \text{(B.2)}$$

Further, we observe that $h\left(g\left(\lambda\bar{x}\right)+g\left((1-\lambda)\bar{y}\right)\right)=\dfrac{\lambda\sum_l x_l+(1-\lambda)\sum_l y_l}{1+\lambda\sum_l x_l+(1-\lambda)\sum_l y_l}=$ $f\left(\lambda\bar{x}+(1-\lambda)\bar{y}\right)$ and $\lambda h\left(g\left(\bar{x}\right)\right)+(1-\lambda)h\left(g\left(\bar{y}\right)\right)=\lambda f\left(\bar{x}\right)+(1-\lambda)f\left(\bar{y}\right)$. Hence, from (B.2), we conclude that $f\left(\lambda\bar{x}+(1-\lambda)\bar{y}\right)\ge\lambda f\left(\bar{x}\right)+(1-\lambda)f\left(\bar{y}\right)$, which establishes that function f is concave.

Appendix C

Let us denote function

$$f\left(p_1, p_2, \cdots, p_L\right) \equiv \frac{\left(\sum_l \left|h_{s,l}\right|\left|h_{l,k}\right|\beta_l \sqrt{p_l}\right)^2}{1+\sum_l \left(\beta_l \left|h_{l,k}\right|\right)^2 p_l}.$$

The, the partial derivative with respect to p_j is

$$\frac{\partial f}{\partial p_j} = \frac{\left[\begin{array}{l} \left|h_{s,j}\right|\left|h_{j,k}\right|\beta_j \, p_j^{-1/2}\left(\sum_l \left|h_{s,l}\right|\left|h_{l,k}\right|\beta_l \sqrt{p_l}\right)\left(1+\sum_l \left(\beta_l \left|h_{l,k}\right|\right)^2 p_l\right) \\ -\left(\beta_j \left|h_{j,k}\right|\right)^2\left(\sum_l \left|h_{s,l}\right|\left|h_{l,k}\right|\beta_l \sqrt{p_l}\right)^2 \end{array}\right]}{\left(1+\sum_l \left(\beta_l \left|h_{l,k}\right|\right)^2 p_l\right)^2}$$

$$= \frac{\sum_l \left|h_{s,l}\right|\left|h_{l,k}\right|\beta_l \sqrt{p_l}}{\left(1+\sum_l \left(\beta_l \left|h_{l,k}\right|\right)^2 p_l\right)^2} \times \left[\begin{array}{l} \left|h_{s,j}\right|\left|h_{j,k}\right|\beta_j \, p_j^{-1/2}\left(1+\sum_l \left(\beta_l \left|h_{l,k}\right|\right)^2 p_l\right) \\ -\left(\beta_j \left|h_{j,k}\right|\right)^2\left(\sum_l \left|h_{s,l}\right|\left|h_{l,k}\right|\beta_l \sqrt{p_l}\right) \end{array}\right]$$

we observe that for any fixed set of values of $p_1, p_2, \cdots, p_{j-1}, p_{j+1}, \cdots, p_L$ $f\left(p_1, p_2, \cdots, p_L\right)$ is nondecreasing w.r.t p_j for the values of p_{j+1} that have

$$\left|h_{s,j}\right|\left|h_{j,k}\right|\beta_j \, p_j^{-1/2}\left\{1+\sum_l \left(\beta_l \left|h_{l,k}\right|\right)^2 p_l\right\} - \left(\beta_j \left|h_{j,k}\right|\right)^2\left\{\sum_l \left|h_{s,l}\right|\left|h_{l,k}\right|\beta_l \sqrt{p_l}\right\} \geq 0, \quad \text{(C.1)}$$

which is equivalent to

$$\left|h_{s,j}\right|\left|h_{j,k}\right|\beta_j \left\{1+\sum_l \left(\beta_l \left|h_{l,k}\right|\right)^2 p_l\right\} - \sqrt{p_j}\left(\beta_j \left|h_{j,k}\right|\right)^2\left\{\sum_l \left|h_{s,l}\right|\left|h_{l,k}\right|\beta_l \sqrt{p_l}\right\} \geq 0 \quad \text{(C.2)}$$

Inequality (C.2) is equivalent to

$$\left|h_{s,j}\right|\left\{1+\sum_{l}\left(\beta_l\left|h_{l,k}\right|\right)^2 p_l\right\}-\sqrt{p_j}\beta_j\left|h_{j,k}\right|\left\{\sum_{l}\left|h_{s,l}\right|\left|h_{l,k}\right|\beta_l\sqrt{p_l}\right\}\geq 0$$

(C.3)

Inequality (C.3) can be written as

$$\left|h_{s,j}\right|\left\{1+\left(\beta_j\left|h_{j,k}\right|\right)^2 p_j+\sum_{l\neq j}\left(\beta_l\left|h_{l,k}\right|\right)^2 p_l\right\}$$
$$\geq\sqrt{p_j}\beta_j\left|h_{j,k}\right|\left\{\left|h_{s,j}\right|\left|h_{j,k}\right|\beta_j\sqrt{p_j}+\sum_{l\neq j}\left|h_{s,l}\right|\left|h_{l,k}\right|\beta_l\sqrt{p_l}\right\}$$

or

$$\left|h_{s,j}\right|\left(\beta_j\left|h_{j,k}\right|\right)^2 p_j+\left|h_{s,j}\right|\left\{1+\sum_{l\neq j}\left(\beta_l\left|h_{l,k}\right|\right)^2 p_l\right\}$$
$$\geq\left|h_{s,j}\right|\left(\beta_j\left|h_{j,k}\right|\right)^2 p_j+\sqrt{p_j}\beta_j\left|h_{j,k}\right|\left\{\sum_{l\neq j}\left|h_{s,l}\right|\left|h_{l,k}\right|\beta_l\sqrt{p_l}\right\},$$

which is equivalent to

$$\left|h_{s,j}\right|\left\{1+\sum_{l\neq j}\left(\beta_l\left|h_{l,k}\right|\right)^2 p_l\right\}\geq\sqrt{p_j}\beta_j\left|h_{j,k}\right|\left\{\sum_{l\neq j}\left|h_{s,l}\right|\left|h_{l,k}\right|\beta_l\sqrt{p_l}\right\}\qquad\text{(C.4)}$$

Finally, after rearranging the terms in (C.4) we obtain

$$p_j\leq\left[\frac{\left|h_{s,j}\right|\left\{1+\sum_{l\neq j}\left(\beta_l\left|h_{l,k}\right|\right)^2 p_l\right\}}{\beta_j\left|h_{j,k}\right|\left\{\sum_{l\neq j}\left|h_{s,l}\right|\left|h_{l,k}\right|\beta_l\sqrt{p_l}\right\}}\right]^2$$

Appendix D

The flow diagram of IAGA.

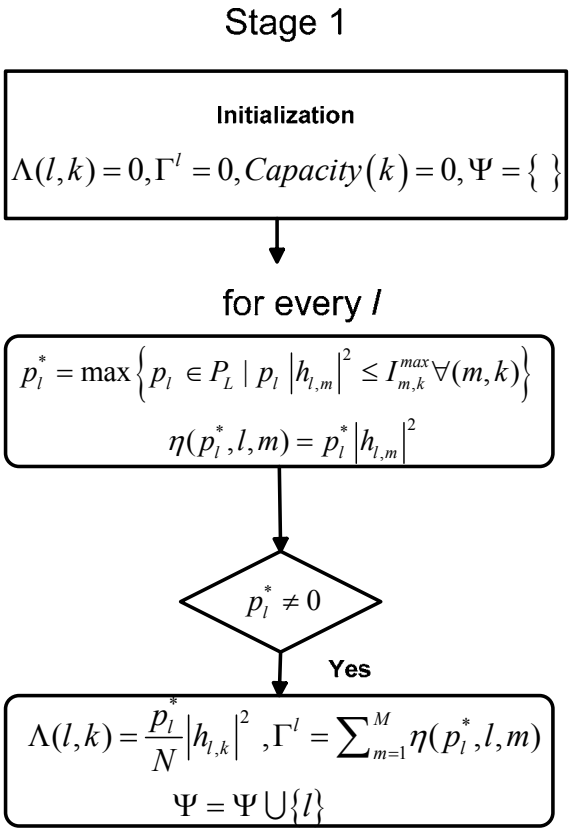

Fig. D.1 Stage 1 of IAGA

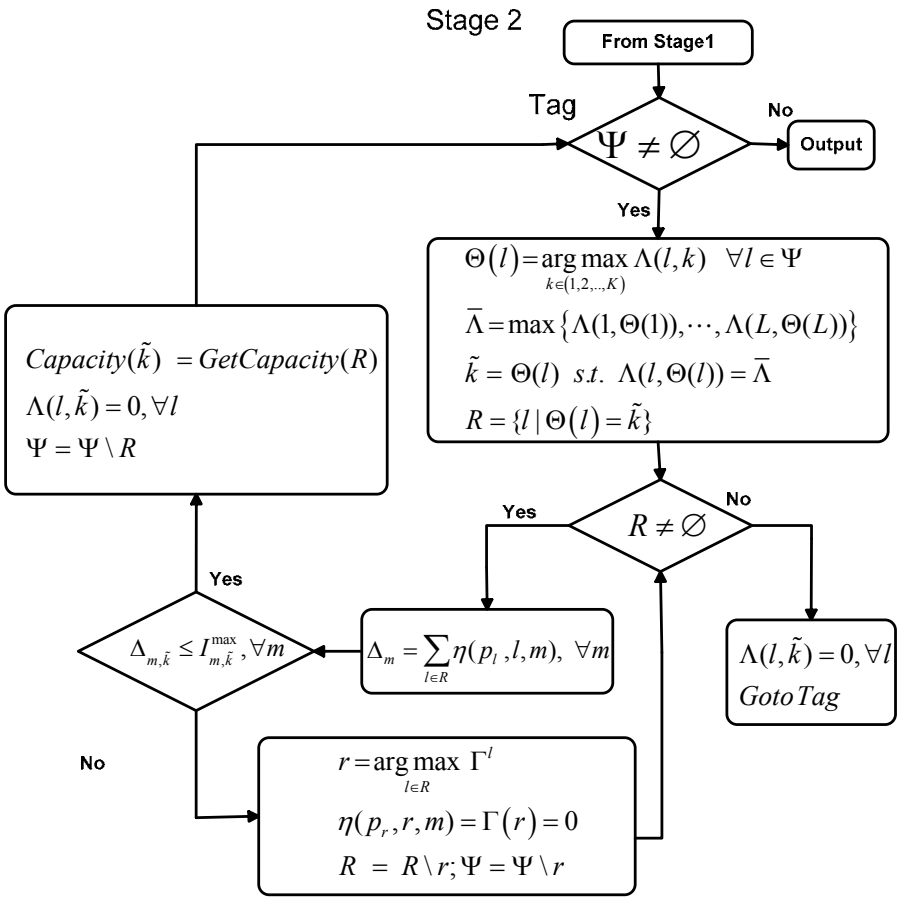

Fig. D.2 Stage 2 of IAGA

Appendix E

The optimization problem is

$$\begin{aligned} &\max_{P_k,\phi} \quad \log_2 \det\left(I_{N_R} + \frac{1}{N_T N}\sum_{k\in\phi} P_k H_{k,bs} H_{k,bs}^{\dagger} \right) \\ &\text{subject to} \quad C1: \quad \frac{1}{N_T}\sum_{k\in\phi} P_k H_{k,m} H_{k,m}^{\dagger} \le I_m^{\max} \qquad \forall m \\ &\qquad\qquad C2: \ |\phi| \le K_s \\ &\qquad\qquad C3: \ P_k \in P_L, \forall k \end{aligned} \tag{E.1}$$

Let there are *K* secondary users and M primary users in the system. Each secondary/primary user and central controller is equipped with a single antenna. The noise variance is assumed to be one. With these assumptions, we can rewrite (E.1) as

$$\begin{aligned} &\max_{P_k,\phi} \quad \log_2 \det\left(1 + \sum_{k\in\phi} P_k \left| h_{k,bs} \right|^2 \right) \\ &\text{subject to} \quad C1: \sum_{k\in\phi} P_k \left| h_{k,m} \right|^2 \le I_m^{\max} \quad \forall m \\ &\qquad\qquad C2: |\phi| \le K_s \\ &\qquad\qquad C3: P_k \in P_L, \forall k \end{aligned} \tag{E.2}$$

We define a binary indicator x_k

$$x_k = \begin{cases} 1 & \textit{if the kth secondary user is selected for transmission} \\ 0 & \textit{otherwise} \end{cases}$$

Let us define $P_L = \{P\}$. We can write (E.2) as

$$\begin{aligned} &\max_{x_k} \quad \log_2 \det\left(1 + \sum_{k=1}^{K} x_k P \left| h_{k,bs} \right|^2 \right) \\ &\text{subject to} \quad C1: \sum_{k=1}^{K} P x_k \left| h_{k,m} \right|^2 \le I_m^{\max} \quad \forall m \\ &\qquad\qquad C2: \sum_{k=1}^{K} x_k \le K_s \\ &\qquad\qquad C3: x_k \in \{0,1\}, \forall k \end{aligned} \tag{E.3}$$

Since log is monotonically increasing function, we can also write (E.3) as

$$\begin{aligned} &\max_{x_k} \quad \sum_{k=1}^{K} x_k \alpha_k \\ &\text{subject to } C1: \sum_{k=1}^{K} x_k \beta_k \le I_m^{\max} \quad \forall m \\ &\qquad C2: \sum_{k=1}^{K} x_k \le K_s \\ &\qquad C3: x_k \in \{0,1\}, \forall k \end{aligned} \tag{E.4}$$

Where $\alpha_k = P\left|h_{k,bs}\right|^2$ and $\beta_k = P\left|h_{k,m}\right|^2$. The multidimensional cardinality constraint knapsack problem (MCCKP) is

$$\begin{aligned} &\max_{x_k} \quad \sum_{k=1}^{K} x_k A_k \\ &\text{subject to } \quad C1: \sum_{k=1}^{K} x_k W_k \le C_i \quad \forall i \\ &\qquad C2: \sum_{k=1}^{K} x_k \le N \\ &\qquad C3: x_k \in \{0,1\}, \forall k \end{aligned}$$

We can see that the user-scheduling problem is identical to MCCKP. Since MCCKP is NP-Hard, it means that user-scheduling problem is also NP-Hard.